MicroRNAs as Predictors and Therapy for Prostate Cancer

By

Melania Montes Pérez

To obtain the degree of Doctor of Biology for the UAB

Department of Biomedicine and Translational Oncology

Vall d'Hebron Research Institute

September 2015

MicroRNAs as Predictors and Therapy for Prostate Cancer

By Melania Montes Pérez

To obtain the degree of

Doctor of Biology for the UAB

PhD thesis done in the Research Unit in Biomedicine and Translational Oncology Department in Vall d'Hebron Research Institute, under the supervision of

Drs.

Jaume Reventós I Puigjaner, Joan Morote Robles and Mireia Olivan Riera

Universitat Autònoma de Barcelona, Faculty of Bioscience, Department of Cellular Biology, under the supervision of

Dr. Joan Blanco

Dr. Jaume Reventós Dr. Joan Morote Dra. Mireia Olivan

September 2015

This thesis has been supported by the pre-doctoral grant AGAUR 2012 from “Generalitat de Catalunya”.

Moreover, this work was supported in part with a grant for a short stay fellowship from “Ministerio de Ciencia e Innovación, Red Temática de Investigación Cooperativa en Cáncer” (RTICC), in National Cancer Center Research Institute, Tokyo. Finally, the financial support for the projects presented was granted by “Instituto de Salud Carlos III, Ministerio de Ciencia e Innovación” (FIS PI11/02486; FIS PI13/00173), by “Asociación Española Contra el Cáncer” (AECC-JB-2011-03; AECC-JB-2013), by “Fundación para la Investigación en Urología” (2011), and by the “Global Action on Urine-Based Detection of Biomarkers for Distinguishing Aggressive from Non-Aggressive Prostate Cancers” from Movember Foundation.

AGRADECIMIENTOS

Los cuatro años que he pasado en el Insitut de Recerca Vall d'Hebron no solo han sido importantes para mi carrera profesional como bióloga, sino que también han constituido un periodo de tiempo muy importante para mi vida personal, que me ha influenciado profundamente.

En primer lugar, quisiera dar las gracias a mis directores de tesis, a Jaume Reventós, Joan Morote y Mireia Olivan por haberme dado la oportunidad de estar aquí y por el apoyo continuo a mi investigación. Estoy muy agradecida con todos mis compañeros, especialmente con las ¡prostáticas! Tamara, Marina, Marta G., Yolanda y las personas de prácticas Meritxell, Aida y Jorge. Por supuesto, muchísimas gracias a toda la unidad, Aroa, Miquel, Luz, Anna Santamaría, Rosana… y a aquellas personas que han colaborado con nosotros, Ochiya san, Takeshita san, Mónica Vázquez-Levin, Viki, Inés de Torres, Cinta, los miembros de la UEB… ¡Todos vosotros me habéis inspirado y enseñado!

Mi más sincera gratitud a Andrés, papas y tatas por toda vuestra confianza y amor incondicional, ¡sacáis siempre lo mejor de mí!

Por último, ¡gracias Dios! por darme la pasión e inspiración a mi vida, mostrarme el camino, dándome siempre la fuerzas para seguir y enseñarme en cada momento a confiar en ti.

¡Muchísimas gracias a todos!

“I always felt that a scientist owes the world only one thing, and that is the truth as he sees it”

Hans Eysenck

INDEX

ABBREVIATIONS

ADT: Androgen Deprivation Therapy

Ago: Argonaute

AR: Androgen Receptor

ASO: Antisense Oligonucleotides

AUC: Area Under the Curve

BPH: Benign Prostate Hyperplasia

CDK: Cyclin-dependent Kinase

CK: Cytokeratin

CM: Conditioned Medium

CRPC: Castration Resistance Prostate Cancer

CSC: Cancer Stem Cells

CV: Coefficient of Variation

CZ: Central Zone

DGCR8: DiGeorge Syndrome Chromosomal Region 8

DRE: Digital Rectal Exam

DTT: Dithiothreitol

E-cadh: E-cadherin

ECM: Extracellular Matrix

EMT: Epithelial-mesenchymal Transition

ERG: V-Ets avian erythroblastosis virus E2G oncogene homolog

FDA: Food and Drug Administration

FFPE: Formalin Fixed Paraffin Embedded

H&E: Haematoxylin and Eosin

KLK3: Kallikrein-3

MiRNA, miR: microRNA

MV: Microvesicle

NC: Negative Control

N-cadh: N-cadherin

NcDNA: non-coding DNA

NcRNA: non-coding RNA

NTA: Nanoparticle Tracking Analysis

PB: Prostate Biopsy

PC: Prostate Cancer

PCA3: Prostate Cancer Antigen 3

p-Erk: phospho-Erk

PI: Propidium Iodide

PM: Prostate Massage

Pre-miRNA: Precursor microRNA

PSA: Prostate-specific Antigen

PZ: Peripheral Zone

RG: Reference Gene

RISC: RNA-induced Silencing Complex

ROC: Receiver Operating Characteristic

RP: Radical Prostatectomy

rRNA: Ribosomal RNA

RT-qPCR: Real Time Quantitative PCR

SCR: Scramble

SnoRNA: Small Nuclear RNA

TMPRSS2: Transmembrane Protease, Serine 2

TNM: Tumour, Node, and Metastasis

TRUS: Transrectal Ultrasound

TZ: Transition Zone

WB: Western Blotting

GENERAL INTRODUCTION

1. PROSTATE GLAND

1.1. Anatomy and Histology

Herophilus of Alexandria first used the term “prostate” in 335 B.C. to refer to the organ situated in front of the bladder. In male it is the largest accessory reproductive gland that surrounds the first part of urethra, and produces important components of the seminal fluid, secreting an alkaline fluid that forms 50-70% of the total ejaculate that aids in motility and nourishment of the sperm (1).

The prostate anatomy has been the subject of controversy for 200 years. It is a walnut-sized tissue, partly glandular and muscular, limited with the prostate capsule. Its average anatomic size, which may vary with age, is around 28-47 cm^2 (2). Since 1968 and for the next 25 years, McNeal presented his view of prostate anatomy in terms of 4 anatomic zones on the bases of biological and histological concepts. The term “zone” was chosen because there was no external lobation. Each zone originates from prostatic urethra and has specific architectural features. These major glandular regions of the prostate are labelled as the peripheral zone (PZ), the central zone (CZ), the transitional zone (TZ) and the periurethral glandular zone (PGR). In 1981, McNeal introduced yet another anatomic region, the anterior fibromuscular stroma (AFS) **(Fig.1)** (3).

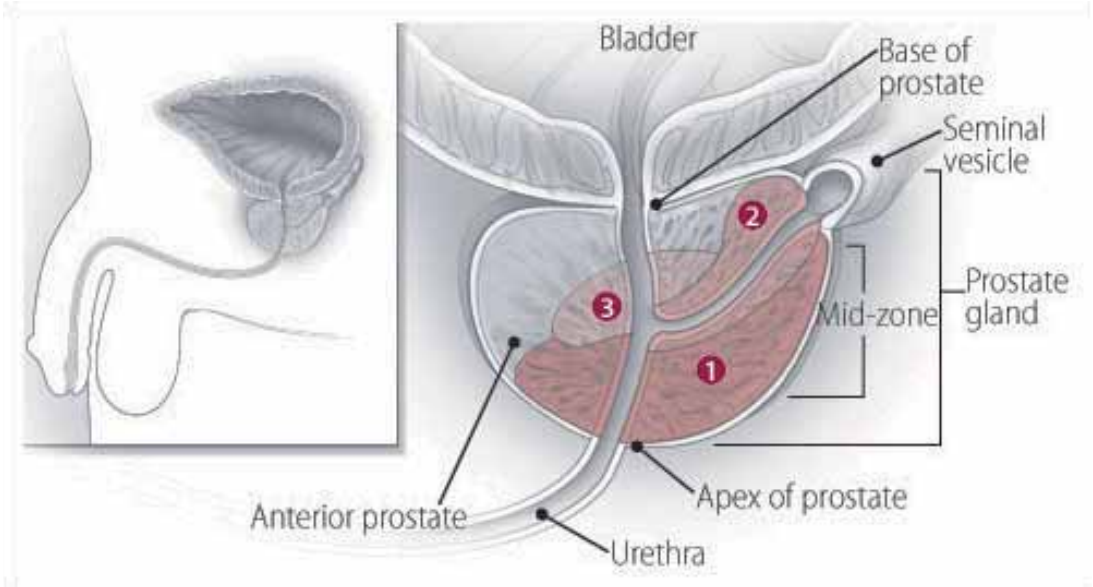

Figure 1. Prostate location and anatomy (image obtained from http://www.harvardprostateknowledge.org/prostate-basics)

The PZ constitutes the bulk of the apical, posterior, and lateral prostatic tissue and accounts the most of the glandular tissue (70%). It is the zone in which 70% of prostate cancers (PCs) emerge. The TZ accounts for 5-10% of the glandular tissue of the prostate. Cellular proliferation in the TZ results in benign prostatic hyperplasia (BPH), a common non-malignant condition found in old men. In addition, 20% of the cases of PC arise in this zone. The CZ surrounds the ejaculatory ducts. Only 2,5% of the reported cases of PC appears in this zone, but these cancers tends to be more aggressive and more likely to invade the seminal vesicles (4,5).

At the histological level, the architecture of the prostate is that of a branched duct gland. The glands are tubuloalveolar, extend out to the prostatic capsule, and have a relatively simple branching pattern, with acini distributed uniformly along the course of the main duct. Prostate epithelium is organized in bilayer of basal and luminal cells along with a few rare embedded neuroendocrine cells **(Fig.2)** (3).

A B

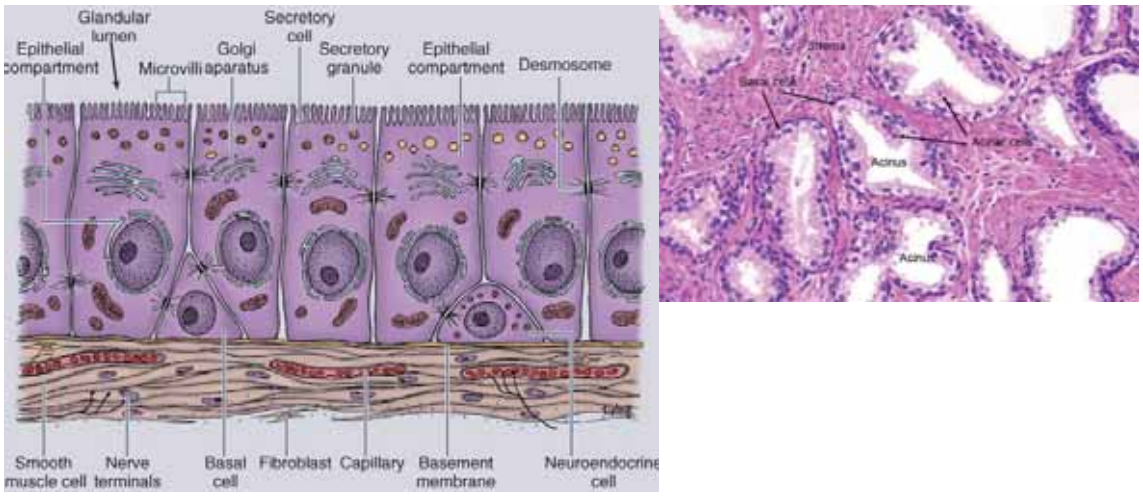

Figure 2. A) Schematic description of prostate epithelium cell types (image obtained from https://www.studyblue.com/notes/note/n/too-many-sleepless-nights-haem-and-neoplasia/deck/1079655). **B)** Haematoxylin and eosin stain of a normal prostate (image obtained from https://www.auanet.org/education/modules/pathology/normal-histology/prostate.cfm)

These cells are pathologically distinguishable based on various cellular markers. For example, luminal epithelial cells, the predominant cell type, are polarized, columnar cells that line prostate lumen, which express high levels of androgen receptor (AR) and are positive for prostate cytokeratin (CK) 8 and 18, cytokine CD57, and homeobox protein NKX3.1. These cells

also secrete PSA and prostate acid phosphatase (PAP) into the glandular lumen. Basal cells, the second major epithelial cell type, are elongated cells that separate from stroma, and express low levels of AR, and stain positive for CK 5 and 14, tumour protein p63 (TP63), cell-surface glycoprotein CD44, and glutathione S-transferase P1-1 (GSTP1). These cells are relatively undifferentiated and conform to the proliferative compartment. Finally, neuroendocrine cells that comprise only a small percentage of the epithelium, are AR-negative, post-mitotic, and secrete neuropeptides and growth factors for luminal cell growth. The neuroendocrine peptides support the growth or differentiation of the surrounding epithelial cells (6).

Furthermore, prostate epithelium is surrounded by laminin (LM5, LM10) and collagen matrix (COL IV, COL VII), and fibromuscular stroma that include fibroblasts, myofibroblasts, and smooth muscle cells that transmit signals to guide the growth and differentiation of the epithelium (7).

2. PROSTATE CANCER

2.1. Epidemiology and Etiology

Cancer is one of the most critical health problems in our society, both in terms of morbidity and social impact. In North American, PC is the most common malignant neoplasia diagnosed among males, and the second leading cause of cancer related death, with an estimation of 220,800 new cases and 27,540 deaths in 2015 (8). Incidence rates vary by more than 25-fold worldwide, with the highest rates recorded primarily in the developed countries of Oceania, Europe, and North America, largely because of the wide utilization of prostate-specific antigen (PSA) testing. In contrast, African descents in the Caribbean region have the highest PC mortality rates in the world, which is through to reflect in part a difference in genetic susceptibility (9).

Although the exact causes of PC development and progression are not yet known, substantial evidence suggests that both genetics and environment play a role in the origin and evolution of prostatic neoplasia, as some risk factors. PC is a disease that primarily affects elderly men at an average age of 69 years at first diagnosis; therefore, it is a greater concern for developed

countries (10). Additionally, family history of PC increases 2-fold for men who have a first degree relative with PC, and the risk is further increased if the relative diagnosed at an age younger than 60 and if more than one first degree relative have been diagnosed. Other risk factors in PC include race, diet, inflammation or sex hormone levels (2).

The rate of PC diagnosis increased over the past decades due to an aging population, increased awareness, and the use of PSA in serum for screening and diagnosis since the late 1980s **(Fig.3)** (11). This epidemic of PC was quickly followed by a sharp decline due to a smaller pool of prevalent cases. In other high-income countries with a low and gradual increase in the prevalence of PSA testing, such as Japan and the United Kingdom, PC rates continue to increase slightly (9,12).

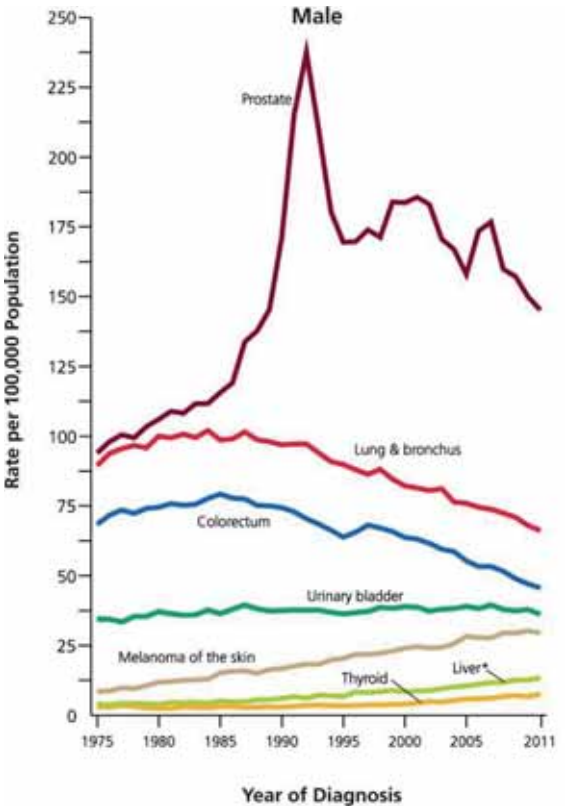

Figure 3. Trends in incidence rates for selected cancers (including PC) in the United States male population, 1975 to 2011. Adapted from (8)

On the other hand, PC mortality decreases in most western countries since the introduction of PSA test. It is estimated that screening and early detection account for at least 50% of this important mortality reduction (13). In contrast to these trends, incidence of metastatic PC and mortality rates in most native Asian populations have gradually increased, and is substantially higher than in migratory Asian populations residing in Western countries. Lower exposure to PSA screening in Asian individuals might be a major contributing factor to this effect (9,14).

2.2. Screening and Diagnosis

Usually PC is found by testing men with no sign or symptoms. The current screening method to detect PC is based on the measurement of serum PSA levels and digital rectal exam (DRE), whereas the decisive diagnosis is by a histologic evaluation of prostate tissue sampled from a prostate biopsy (PB). Transrectal ultrasound (TRUS) guided needle biopsy is the most widely used method for obtaining prostatic tissue (2). However, this procedure is limited by false-negative biopsies and over-diagnosis of clinically insignificant malignancies (1).

2.2.1. PSA Blood Test

PSA, also called kallikrein-3, is a glycoprotein formed by the prostate. Its function is to liquefy semen, promote sperm motility and dissolve cervical mucus. Richard Albin discovered PSA in the 1970s, whereas the possibilities for early detection of PC were recognised in 1991, when Catalona and collaborators reported a cohort of 1653 men who underwent PSA testing in addition to DRE (11). Currently, PSA serum level of ≥4.0ng/ml is the established cut-off for recommending biopsy, regardless of findings on DRE (15). However, the decision of perform a PB must be made between the practitioner and patient following a through history and physical, evaluation of current and prior serum PSA values, history of PB, DRE findings, ethnicity, and co-morbidities (2).

2.2.1.1. PSA Dilemma

Screening for PC with PSA results in the identification of potentially lethal PC at a much more curable stage. However, PSA testing has some well-recognized limitations, as it lacks diagnostic specificity and prognostic value. Although PSA is prostate-specific, it is not cancer-specific due to elevated levels of serum PSA under benign conditions, like BPH, urinary retention, prostatitis, trauma, or physical manipulation (16). Approximately, 30% of men with a serum PSA of 5-10ng/ml, and >50% of men with a PSA>10ng/ml will have PC. Moreover, PSA cannot distinguish between PC clinically insignificant and aggressive. By definition, clinically insignificant PC does not contribute to PC mortality and the treatment of indolent PC with

radical treatment can result in side effects that reduce quality of life of the patient for no or little benefit (17,18). Therefore, clinical trials have shown that the PSA testing and screening is associated with an over-diagnosis and as a consequence and over-treatment of patients with indolent disease.

Several modifications to PSA biomarker detection in serum have been suggested to improve its sensitivity and selectivity including PSA density, ratio of free: total PSA, PSA velocity (PSAV) or PSA doubling time (PSADT) and different PSA isoforms, but they all present their own limitations and further research needs to be done to evaluate their performance (19).

On the other hand, the effect of mass PSA screening on PC mortality remains debated (20,21). Still, the current strategy of the European Association of Urology (EAU) recommends that a baseline PSA testing should be offered to men 40 years of age or older who have a life expectancy of at least 10 years (2).

For all of the reasons listed above, approximately two thirds of the 1 million biopsies made annually both in the United States and in Europe are unnecessary (22). PB is an uncomfortable method, time consuming, and invasive. Therefore, the introduction of simple, non-invasive, sufficiently sensitive and specific method for the detection and monitoring of PC patients is needed.

2.2.2. Digital Rectal Exam

DRE was for a long time the primary means of diagnosis of PC, until the popularization of the PSA test in the 1990s. The technique consists in the palpation of the prostatic gland by inserting a lubricated, gloved finger through the rectum. It allows a fairly accurate estimate of the gland volume, as well as a description of the character of the tissue with respect to the known pathologic conditions that can affect the prostate, e.g. a hard, irregular prostate is typical of a PC (23).

The sensitivity of DRE is limited because the cancer might not have a different “feel” from the surrounding benign tissue or may be beyond the reach of the examining finger. The DRE also has limited specificity, producing a large proportion of false-positive results (24). Additionally, it has low accuracy in localizing PC, and it is subject to wide inter-observer variability, even among experienced urologists (24–26).

2.2.3. Prostate Biopsy

Grey scale TRUS-guided needle biopsy using local anaesthesia remains the standard approach to the definitive diagnosis of PC. AIthough there is intense controversy concerning PC screening, when a decision is made to perform a diagnostic PB, based on abnormal DRE or increased PSA level, it is the preferred and standard-of-care technique. TRUS has many advantages over other medical imaging modalities, such as the lack of ionizing radiation, low cost, and the proximity of the prostate to the rectal wall (27).

PB techniques have significantly changed since the original Hodge's “sextant scheme” (six cores, three from each side of the prostate: apical, middle and basal) described in 1989, which should now be considered obsolete. As a result of the great improvement and efficacy of local anaesthesia, nowadays it is feasible to carry out a biopsy scheme with a high number of cores in an outpatient setting (28).

Evidence supports the inclusion of at least four additional laterally directed cores (typically a total of 12 cores) during PB, which significantly improves cancer detection without a demonstrable increase in morbidity. These data indicate that such PB templates, known as extended PB, represent the optimal template in initial PB intended to detect clinically significant PC (29). On the contrary, it has been suggested that repeat PB should be based on saturation biopsies (number of cores ≥20) and should include the TZ, especially in patients with an initial negative biopsy (30).

2.3. Tumour Classification and Treatment

2.3.1. Gleason Grading System

Gleason score grading system, devised by Donald Gleason in the 1970s (31), is based entirely on the histologic pattern of arrangement of carcinoma cells in haematoxylin and eosin (H&E)-stained sections from a PB. The Gleason system assigns a grade to the two largest areas in each biopsy specimen. The two numbers are added together to equal the total Gleason score. Five basic grade patterns are used to generate a histologic score, which can range from 2 to 10, by assigning a grade to the most and second most common tumour pattern and adding these two

numbers up (32). These patterns are illustrated in a standard drawing that can be employed as a guide for recognition of the specific Gleason grades **(Fig.4)**.

Gleason grade of PC is a well-established prognostic indicator that has stood the test of time. Increasing Gleason grade has been linked to a number of clinical end points, including clinical stage, progression to metastatic disease, and survival, and it is routinely used to plan patient management (32). However, one of the major drawbacks of the Gleason grading system is that it is partly subjective, and therefore associated with significant inter-observer variability (33,34).

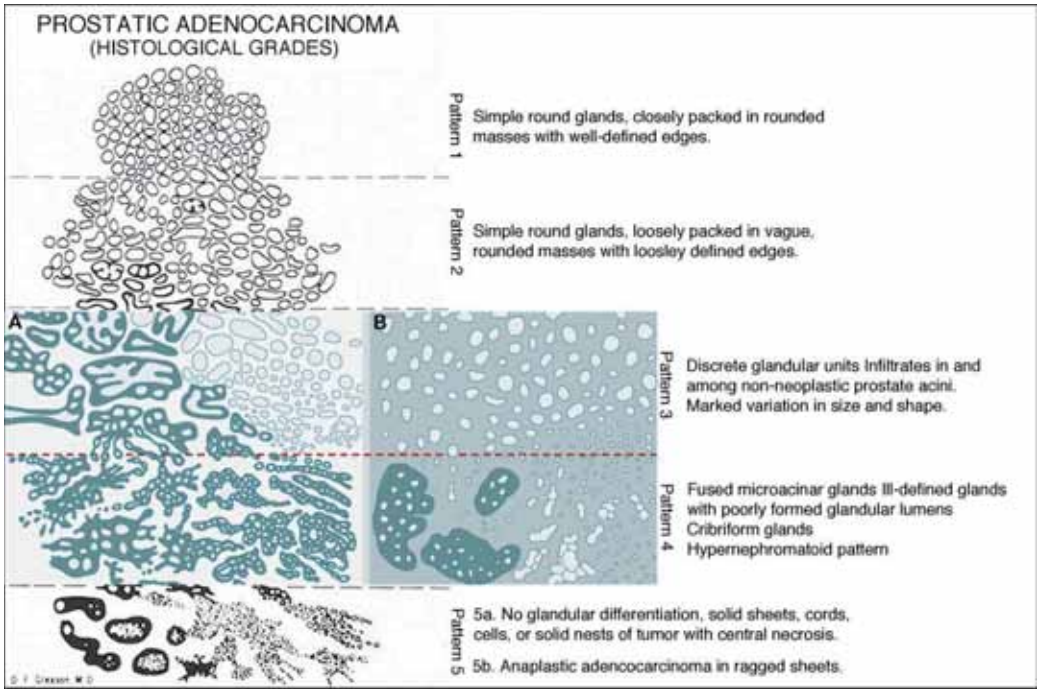

Figure 4. Original simplified drawings of the 5 Gleason grades of PC. Grade 1 appears on the top and grade 5 on the bottom of the drawing. The colour image shows a comparison of the original Gleason and the International Society of Urological Pathology (ISUP) 2005 modified systems for patterns 3 and 4, **(A)** Gleason's original and **(B)** ISUP modified system. Adapted from (36)

2.3.2. TNM Staging System

PC is staged according to the Tumour Node Metastasis (TNM) nomenclature. The American Joint Committee on Cancer (AJCC) and the International Union for Cancer Control (IUCC), the organizations responsible for the TNM cancer staging system, update it periodically. The most recent revision is the 7th edition, effective for cancers diagnosed on or after January 1, 2010 **(Fig.5)** (35).

Once the T, N, and M categories have been determined, this information is combined, along with the Gleason score and PSA levels. The overall stage is expressed in Roman numerals from I (the least advanced) to IV (the most advanced). This is done to help determine the prognosis for the patients, as well as the best treatment options (36).

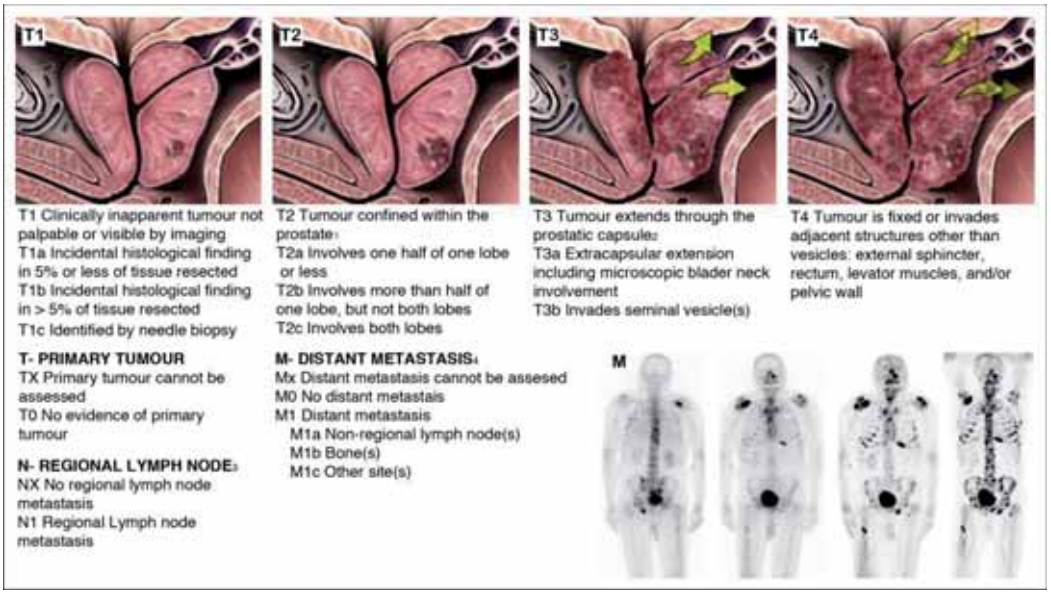

Figure 5. TNM classification of PC. Adapted from (207)

2.3.3. Treatment

Currently, T category, Gleason score, and PSA can accurately stratify populations of men with PC into broad groups with respect to risk of disease progression **(Table 1)**. However, the practitioner should consider the extent of disease, patient age, and competing co-morbidities when choosing a treatment for an individual patient.

Table 1: D'Amico stratification criteria. Adapted from (207)

Groups	Description
Low Risk	cT1-T2a and Gleason score 2-6 and PSA < 10ng/ml
Intermediate Risk	cT2b-T2c or Gleason score =7 or PSA 10-20ng/ml
High Risk	cT3a or Gleason score 8-10 or PSA > 20ng/ml

By nature, PC progresses slowly and in many cases it can be treated effectively by radical prostatectomy (RP) when it is detected early. Excellent cancer-specific survival is seen when specimen-confined PC is found at final histopathology, even for high-risk PC patients (37). Active surveillance rather than immediate treatment is also a reasonable and commonly recommended approach, especially for older men and men with less aggressive tumours and/or more serious comorbid conditions (38). Nonetheless, the best treatment for localized PC remains controversial. This controversy is highlighted by a recent specialist survey on the "optimal" treatment of a hypothetical patient with localized PC: approximately 29% favoured expectant management, 33% favoured radiation therapy (RT) and 39% chose RP (39).

On the other hand, PC depends on androgen receptor activity at all stages. Standard therapy of disseminated PC, presenting lymph node or bone metastases, in hormone-naïve patients is based on an androgen-deprivation therapy (ADT) or androgen receptor antagonists. Current evidence suggests a survival benefit to multimodality therapy, which combines local therapies, such as surgery and RT, with systemic ADT (40).

Most men with advanced PC initially respond to various types of androgen ablation, but a considerable portion of them eventually followed by recurrence of PC, resulting in the so-called castration-resistant PC (CRPC). Among patients with non-metastatic CPRC, about one-third will develop bone metastasis within 2 years (41). Currently, there are no curative treatments for CRPC available. Docetaxel is the first-line chemotherapy for CRPC, providing modest survival benefits (42,43).

3. URINE AS A SOURCE OF BIOMARKERS

In contrast to PB, for physiological and anatomical reasons, post-DRE urine sample may represent the most minimally invasive and valuable source of PC biomarkers (44,45). Because of urine likely to pass through the malignant lesions in the urologic system before discharge, its molecular content often reflects the disease status as presented by tumour tissues. The gentle massage of each side of the prostate gland during DRE stimulates the release and movement of prostatic fluids and detached epithelial cells into the urethra **(Fig.6)**. These fluids can contain both cells and secretions originating in PC (46).

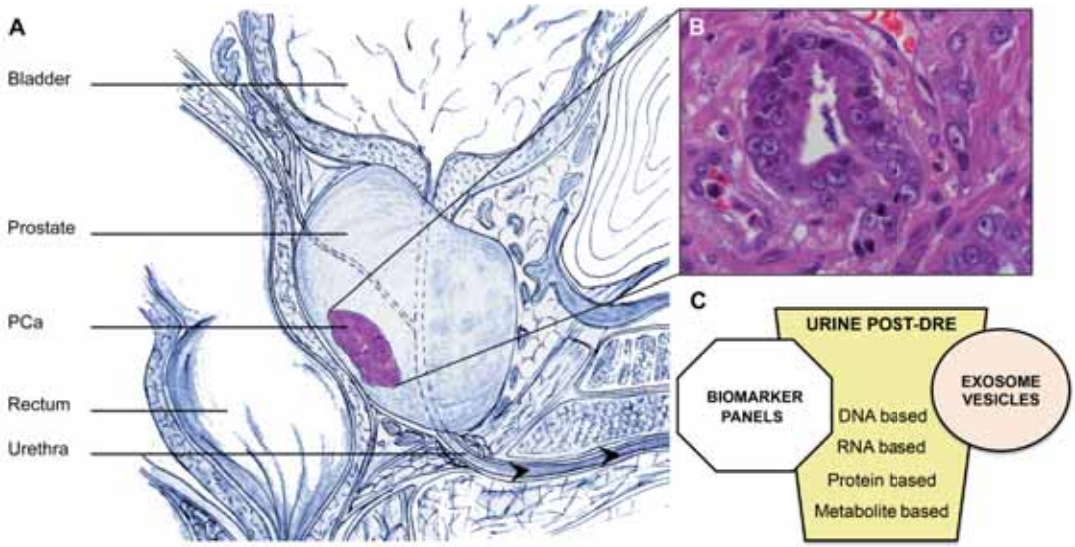

Figure 6. A) Anatomical location of the prostate; **B)** PC cells; C) Biomarkers found in urine. Based on their descriptions, biomarkers can be divided into the following groups; DNA-based, RNA-based, and protein-based. Of late, urinary exosomes, which are secreted vesicles that contain proteins and functional RNA and microRNA molecules, have emerged as a novel approach to acquiring new PC biomarkers. Adapted from (46)

3.1. RNA-based Urine Biomarkers

The search for new PC biomarkers is a challenge that needs to determine which are the molecular pathways that lead to the development and progression of PC. Transcriptomic analysis reveal that prostate tumours can be identified and sub-classified, with some success in predicting aggressive features of disease or impact of prognosis (47–50).

A wide range of promising RNAs-based PC biomarkers, which are not only prostate-specific, but are also differentially expressed in prostate tumours, has been identified. RNA-based biomarkers include coding and non-coding transcripts and regulatory RNAs, such as microRNAs (miRNAs) (51). After PSA, the most promising markers to date are the prostate cancer antigen 3 (PCA3), and the fusion of erythroblast transformation-specific-related gene (ERG) with transmembrane protease, serine 2 (TMPRSS2-ERG) that is found in approximately 50% of PC patients and it is associated with poor prognosis (52). The combination of both markers with serum PSA increased diagnostic accuracy for PC outcome compared to serum PSA. The combination of PCA3 and TMPRSS2-ERG has been seen necessary in order to improve the sensitivity for PC diagnosis, since most of the false-negative results of the PCA3 test are corrected by TMPRSS2-ERG (53). More importantly, in men with persistently elevated total PSA levels and a history of negative biopsies the positive predictive value of TMPRSS2-ERG fusion transcripts was 94%, while PCA3 does not have prognostic value (54).

3.2. MiRNA-based Urine Biomarkers

In last years, several studies have demonstrated the aberrant expression of miRNAs related with the development of several cancers, including PC (55). Some of the previously identified cancer-associated miRNAs in tissues have also been found in body fluids, such as urine.

MiRNAs are certainly more stable than mRNA after being subject to severe conditions such as boiling, extreme pH, extended storage, and several freeze-threw cycles, supporting their possible use as novel and robust biomarkers (56,57). Yun and collaborators (2012) validated stability of miRNA in the supernatant of urine, and in contrast to mRNAs, miRNAs are more resistant against nuclease degradation because of their smaller size, packaging inside microvesicles (MVs), association with RISC or chemical modifications (methylation, adenylation, uridylation) (58,59).

However, the detection and validation of miRNAs as urine biomarker is still at an early stage of research, studies need to be validated in larger cohorts of patients with good controls and comprehensive follow-up data using robust methods and standards for miRNA extraction and detection (60,61).

3.2.1. MiRNA-containing Cells

The first miRNA expression profile (miRNome) evaluated for its potential as PC biomarkers from urine samples was carried out by Bryant and collaborators (2012) who showed that miR-107 and miR-574-3p were up regulated in the urine sediment of cancer patients compared with the controls (62). Interestingly, in this cohort, the diagnostic value of these miRNAs was greater than PCA3 mRNA normalized to PSA that has been incorporated into an Food and Drug Administration (FDA)-approved test (http://www.gen-probe.com/productsservices/progensa-pca3) (63). However, the multivariate analysis of the PSA values and the expression levels of miRNAs showed that neither measure was superior in predicting PC (59). Then, Srivastava and collaborators (2013) analysed significantly deregulated miRNAs of tissue in urine samples, and obtained two miRNAs (miR-205 and miR-214) significantly down regulated in PC patients compared with controls (89% sensitivity and 80% specificity). Although the limitation of this study is the small sample size, it provides proof of concept that deregulated miRNAs in tissues can be explored by non-invasive methods in PC (64). Recently, Stephan and collaborators (2015) also translated the results of their previous tissue-based miRNA profile into a urine-based testing procedure for PC diagnosis. However, they showed that miRNAs failed to detect PC despite of presenting a high deregulation in cancer tissue (65).

3.2.2. Cell-free MiRNA

Urine, as well as other body fluids like blood, consists of cellular and extracellular fractions that can be roughly separated by a conventional centrifugation step into urinary sediment and the corresponding supernatant. Urine supernatant contains cell-free miRNAs as protein-bound or incorporated into MVs. The first description of extracellular miRNAs came in 2008 by Lawrie and collaborators who proposed that these miRNAs might serve as biomarkers of certain cancers (66). Firstly, this idea generated scepticism, since it was believed that miRNAs in the extracellular space were simply a result of cell death. Nowadays, it is known that the secretion of miRNAs is a controlled, active and specific process. Cell-cell communication hypothesis assumes that miRNAs mediate communication among cells. This hypothesis, based on miRNA export, seems to be the most satisfying explanation for the presence of extracellular miRNA **(Fig.7)** (67).

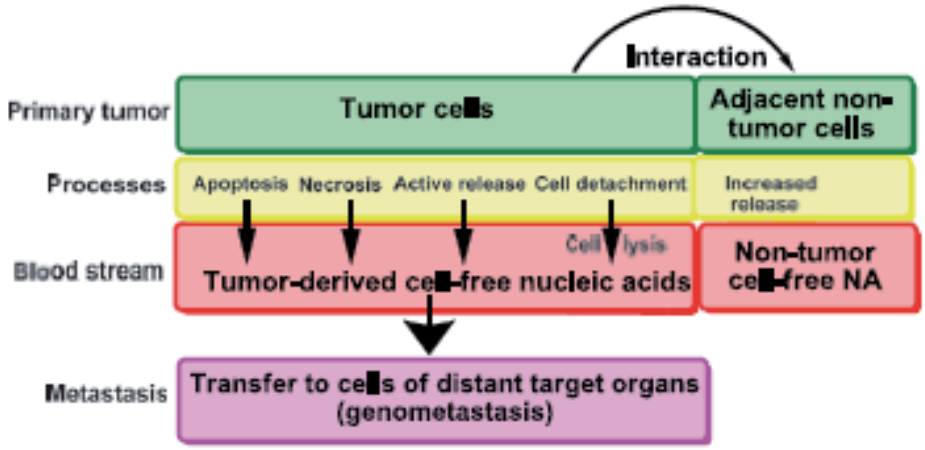

Figure 7. Formation of extracellular/circulating miRNA. Adapted from (68)

MVs are small vesicles that can be detected under both normal and pathological conditions in almost all cell types. Generally, they include microparticles and exosomes that differ in their vesicular structures. Exosomes are 50-150nm-membrane bound MVs to selectively concentrate and transport miRNAs inter-cellularly. They are enriched several hundred fold in miRNAs content compared with the donor cells; therefore, analysing transcriptome in secreted PC exosomes found in urine is more informative than heterogeneous solid tumour biopsy (59).

Lewis and collaborators (2014) analysed the miRNA expression from expressed prostatic secretions (EPS) of urine supernatant because of the presence of exosomes in this fraction. In this work, they demonstrated that miR-888 discriminated high risk PC (69). Another study showed a decreasing trend of miR-34a in PC compared to BPH from urine samples. However, a larger cohort of patients would be necessary to verify this result (70).

Regarding extracellular non-exosome derived miRNA, Korzeniewski and collaborators (2015) were the first who showed that miRNAs could also be detected in the cell-free, non-exosome-enriched fraction of urine collection from patients with PC (71). This is a new advantageous strategy, since the method used does not require exosomes isolation, which is a long and tedious process, and then, it could potentially simplify the future use of miRNAs as urine-based biomarkers.

4. MIRNA: SUITABLE BIOMARKER AND TARGET FOR PROSTATE CANCER

4.1. MiRNA History

The central dogma of molecular biology is based on the transfer of genetic information within cells from DNA to RNA to proteins. Although genetic and epigenetic aberrations that occur in components of the central dogma clearly leads to disease development, non-protein coding regions of the genome have also a prominent role in regulating cell and tissue homeostasis, as well as in contributing to the formation of tumours (57). In fact, the most of the human genome does not code for any protein and, therefore, it is called noncoding DNA (ncDNA). Only about 25,000 protein-coding genes (covering approximately 2% of the human genome) have been recognized by the International Human Genome Sequencing Consortium (72).

Around 60-90% of the ncDNA is transcribed into functional non-coding RNAs (ncRNAs), which, during the last years, have received increased attention from scientific community as they can target multiple signalling pathways related to tumour progression, invasion, metastasis, and chemoresistance. According to their size and function, ncRNAs can be divided into small and long ncRNAs. Small ncRNAs are molecules of 200 nucleotides and can be subdivided based on their size and function into miRNAs that are the best-characterized, piwi-interacting RNAs (piRNAs), ribosomal RNAs (rRNAs), short interfering RNAs (siRNAs), small cajal body-specific RNAs (scaRNAs), small nuclear RNAs (snRNAs), small nucleolar RNAs (snoRNAs), and transfer RNAs (tRNAs) **(Fig.8)** (1).

The family of miRNAs is the best characterized, and most extensively studied class of ncRNAs that play essential functions during embryogenesis and tissue development, and during cell differentiation, proliferation and survival (57). MiRNAs are described as small single stranded ncRNAs that vary in length from 18 to 25 nucleotides that regulated gene expression in metazoans and plants (73). They are reported to regulate more than 50% of all protein-coding genes in mammalian cells (74), and their expression and activity are spatially and temporally controlled (75). MicroRNAs were initially discovered in 1993, when a small RNA encoded by the lin-4 locus was associated to the developmental timing of the nematode *Caenorhabditis elegans* (*C. elegans*) by modulating the protein lin-14, consequently revealed as essential part of the uncoding genome, playing a crucial role through a complex gene regulation in all the most important processes and in different species, including vertebrates (76).

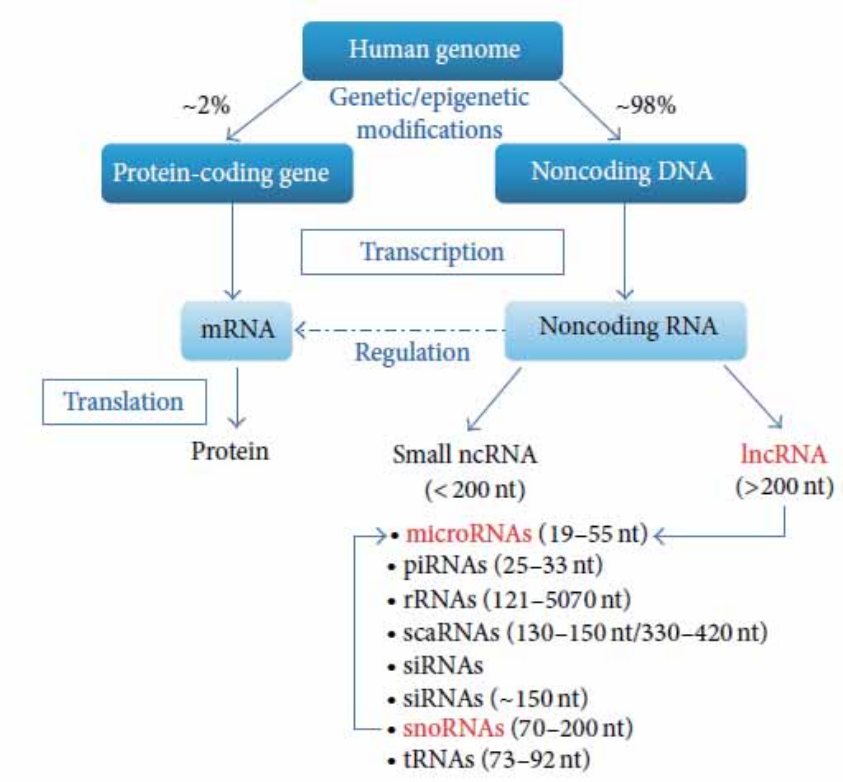

Figure 8. The human genome. Adapted from (1)

4.2. Biogenesis and Genomic Location

MiRNA coding genes are widespread on all chromosomes except chromosome Y and approximately 50% of the described miRNAs are clustered in specific region on chromosomes. When these clustered miRNAs are under control of a single promoter, they are dubbed polycistronic miRNAs. When miRNA coding genes are independent gene units are then called intergenic. In this case, miRNAs are located within the introns and exons of protein-coding or non-coding genes. These homologous and clustered miRNAs have pivotal roles in multiple biological pathways by co-regulating biological processes (77,78).

Most mammalian miRNA genes are first transcribed into long primary miRNAs (pri-miRNAs), which are 5' capped and 3' polyadenylated in the nucleus by RNA polymerase II or III. In the nucleus, pri-miRNA is processed by the Drosha-DiGeorge Syndrome Critical Region gene 8 enzyme complex (DGCR8) to generate stem loop precursor miRNA (pre-miRNA) of 60 to 90 nucleotides. The pre-miRNA is transported to the cytoplasm by Exportin 5, where it is cleaved by the type III RNase Dicer to generate mature double-stranded RNAs (18-25 nt). One strand of

the miRNA duplex can be incorporated into the RNA-Induced Silencing Complex (RISC) composed of Argonaute (Ago) and associated proteins, and the complementary strand (miRNA*) will be degraded based on base-pairing stability at the duplex termini. MiRNA* has been originally considered to have no function; however, recent evidence strongly suggests that they might play significant biological roles **(Fig.9)**(79).

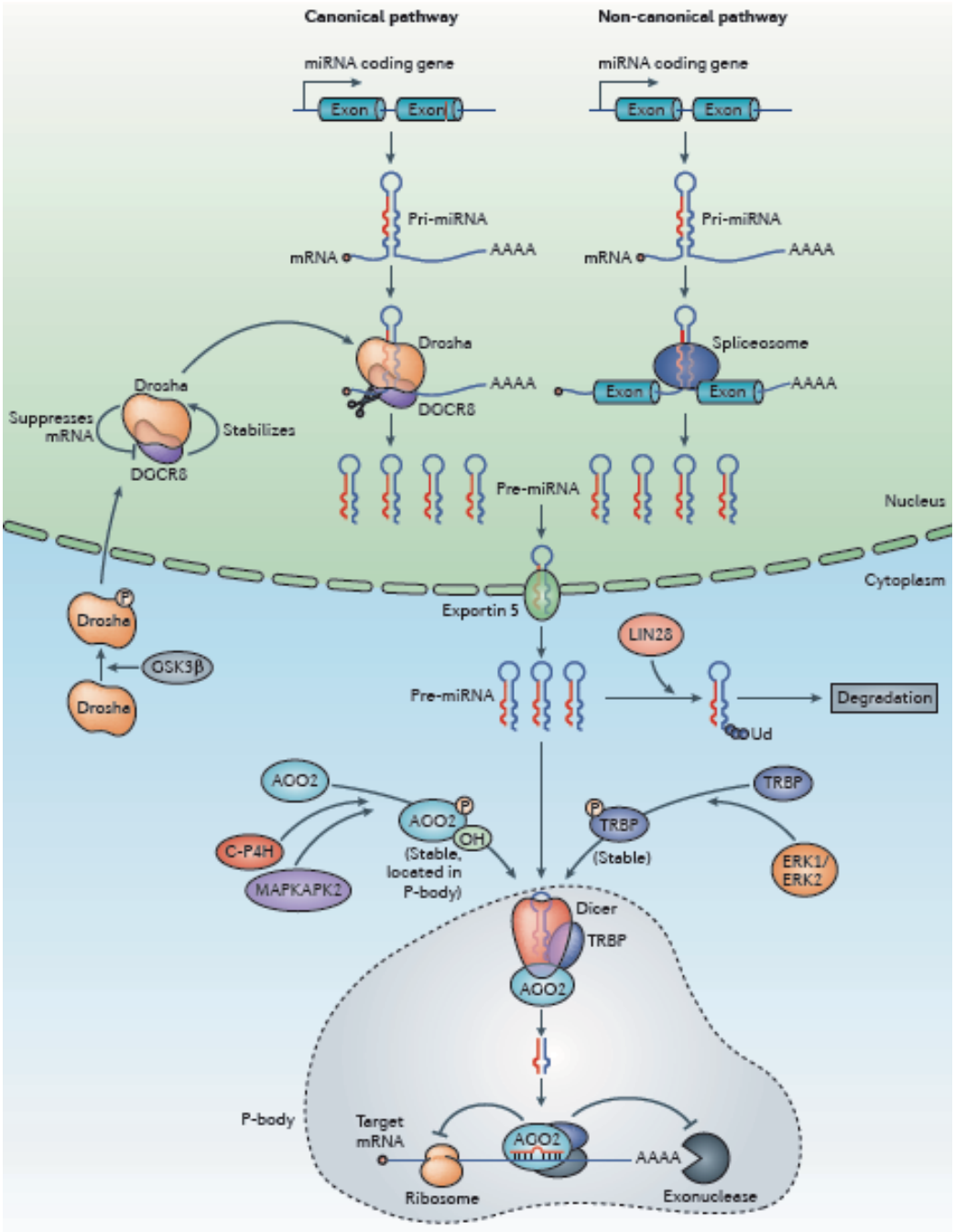

Figure 9. MiRNA location and biogenesis. Adapted from (117)

4.2.1. Nomenclature

While genes or pre-miRNAs are noted "mi**r**-X", mature miRNAs are noted "mi**R**-X" where X is a numeric value. In addition, a three-letter code is added as a prefix to refer to the organism they originate from. One letter stands for the organism genus and the two others for the species, e.g., hsa for *Homo sapiens* or mmu for *Mus musculus*. When mature miRNAs differ by a few bases, a letter is added as a suffix, reflecting the difference, e.g. miR-181a and miR-181b.

When both strands of the stem-loop structure of pre-miRNA are processed as mature miRNAs, an indication is given to specify which arm of the hairpin generates one or the other of these two miRNAs. Several nomenclatures can be used: miR-X and miR-X* (miR-X* is the less abundant of the two mature miRNAs in the cells); miR-X-5p and miR-X-3p (5p and 3p strand for the 5′ and 3′ arms, respectively). This nomenclature is mainly used when the respective abundance of the two miRNAs is still unknown. Finally, miR-X-s (5′ arm) and miR-X-as (3′ arm). Furthermore, a mature miRNA can result from the transcription and maturation of transcripts from separate genomic loci. A numeral suffix is added to the names of all the multiloci miRNAs, e.g. miR-181a-1 and miR-181a-2 (miR-181a-1 originates from a locus on chromosome 1 and miR-181a-2 from a locus on chromosome 9). Nevertheless, some miRNAs, such as hsa-let-7 and cel-lin-4, do not follow the above-described nomenclature.

Currently, all miRNAs named in scientific publications are listed in the well-known miRBase database. MiRBase allows the user to search both hairpin and mature sequences, and entries can also be retrieved by name, keyword, references and annotation (80). There are 2,578 mature human miRNAs listed in the miRBase catalogue of human miRNAs (v20, June 2013) (81,82) and it is still rising. MiRBase is available online at: http://www.mirbase.org/.

4.3. Mechanisms of Action

The canonical mechanism of miRNA-mediated gene regulation is by its binding to the 3' untranslated regions (UTR) of an mRNA and inhibiting protein production by translation inhibition (imperfect match) or degradation of the mRNA (perfect match) (79). In plants, most miRNAs show a perfect complementarity with their mRNA targets and perfect duplex formation is associated with the degradation of the targets by endonucleolytic cleavage. On the

other hand, in metazoans, a perfect complementary between miRNAs and their mRNA targets is no always the rule (76). Nucleotides 2-7 from the 5' end of the miRNA, called seed sequence, are essential to the binding of the mRNA to the target. Seed sequence nucleotides bind perfectly, whereas all the other can bind partially.

Although the majority of published data has focused on mRNAs that act through the canonical pathway, miRNAs can influence gene expression through "non-canonical pathways". For example, miRNAs have also been shown to use 5'UTR and open reading frame (ORF) binding sites to regulate mRNA expression (83). In addition, it has been report that miRNAs influence gene expression by directly binding to DNA (84–86), and some miRNAs can even activate, rather than inhibit gene expression (87).

4.3.1. Databases

Genes can be targeted by multiple miRNAs and each miRNA is able to target hundreds of mRNAs directly or indirectly, sometimes strongly but often weakly, to mediate diverse array of biological functions (88). The exploitation of the interest in miRNAs has stimulated the organization of several databases that facilitate easy and efficient mining of data for miRNAs and their target genes involved in a specific cancer (89). Among all miRNA target prediction tools that have been developed to discover miRNA targets, there are four main characteristics of miRNA: mRNA target interaction that emerge as common features: seed match, conservation, free energy, and site accessibility (90). Unfortunately, different miRNA target prediction algorithms can provide different results, thus researchers have to check across multiple algorithms to get an additional layer of confidence for true positive targets. StarBase was developed to facilitate the comprehensive exploration of miR-target interaction maps from CLIP-Seq and Degra-dome-Seq data. This has allowed researchers to search targets predicted by different algorithms, including TargetScan, PicTar, PITA, miRanda and RNA22 (91).

However, apart from computational algorithms, an experimental validation for target identification is needed. The validation method most commonly used is represented by a reporter assay, but there are more rigorous pull-down assays that can also be used, such as immunoprecipitation of labelled miRNA/mRNA complexes and consequent target identification by RT-qPCR and sequencing, or immunoprecipitation with Ago2 antibody, thus isolating functional miRNA/mRNA/Ago2 complex (56).

4.4. MiRNA Deregulation Mechanisms

Regulation of miRNA expression can be exerted through several mechanisms that result to be altered in cancer. Fifty per cent of miRNA genes are located in cancer-related genomic locations (92). The expression of miRNAs can be influenced by chromosomal rearrangements (deletions, amplifications, and mutations), epigenetic changes (DNA methylation and histone modifications) or by other types of transcriptional control (79). Key transcription factors; including hypoxia-induced factor, the myelocytomatosis oncogene c-*myc*, the tumour suppressor p53, and NF-Kβ have been shown to up- or down-regulate clusters of miRNAs (93). Furthermore, miRNAs themselves can regulate the expression of components of the epigenetic machinery, creating a highly controlled feedback mechanism (89).

MiRNA deregulation can also be due to a failure in miRNA processing. For example, up regulation of Dicer or DGCR8 expression were found in aggressive PC (55).

4.5. MiRNA and Prostate Cancer

Molecular alterations such as chromosomal instability, epigenetic silencing, alteration of tumour suppressor genes and some proteins are associated with the tumorigenesis of PC (94). Furthermore, there are well-established genetic alterations associated with the sporadic PC. Fundamentally, prostate tumours rely on AR signalling. Beyond the AR alterations in advanced tumours, three of its most common genetic alterations are overexpression of Myc, loss of the tumour suppressor p53, phosphatase and tensin Homolog (PTEN), and fusion of erythroblast transformation-specific (ETS) genes with upstream AR regulated promoter sequences (e.g., TMPRSS2-ERG) (7). Interestingly, these genetic alterations in cancer play important roles in the specific activity of miRNA (95).

Some miRNAs have been found to modulate the androgen pathway **(Table 2)** and further classified PC according to castration resistance (96). MiRNAs expression can also be regulated by androgens via androgen response element (ARE) that is harboured in promoted regions, and there are feedback loops between miRNAs and AR (97).

Table 2. MiRNAs regulating AR expression through direct targeting. Adapted from (96)

References	miRs involved in AR regulation
Hagman et al. (2013)	miR-205
Qu et al. (2013)	miR-185
Lin et al. (2013)	miR-31
Sikand et al. (2011)	miR-488*
Östling et al. (2011)	miR-135b, miR-105b, miR-297, miR-299-3p, miR-34a, miR-34c, miR-371-3p, miR-421, miR-499a, miR-499b, miR-634, miR-654-5p, miR-9

The initial studies of miRNA deregulation in PC were performed by miRNA microarray profiling, and since then several studies have analysed PC-specific miRNA profiles by using genome-wide screenings and validation by quantitative PCR technology (98–101). The expression of specific miRNAs could be a classifier to be used to distinguish between normal and cancer tissues **(Table 3)**. However, differences in the expression patterns of miRNAs that have been reported in different studies create controversy in the use of miRNAs on that way (95).

Table 3. MiRNAs associated with PC diagnosis. Adapted from (96)

References	Sample type	miRs deregulated	miRs selected as candidate biomarkers	
Taylor et al. (2010)	113 PCa tissues 28 normal tissues	Large screening study	Taylor et al. 10.1016/j.ccr.2010.05.026	
Volinia et al. (2006)	56 PCa tissues 7 normal tissues	39 upregulated 6 downregulated	Volinia et al. 10.1073/pnas.0510565103;	
Ambs et al. (2008)	60 microdissected tumor tissues 16 normal tissues	21 upregulated 21 downregulated	miR-32, miR-26a, miR-181a, miR-93, miR-196a, miR25, miR-92 and let-7i	↑
Porkka et al. (2007)	5 hormone-naïve PCa tissues 4 HRPC tissues 4 BPH tissues	14 upregulated 37 downregulated	PCa: miR-16, miR-99 and let-7 family HRPC: miR-205, miR-100 and miR-30	↓ ↓
Ozen et al. (2008)	16 PCa tissues and 10 normal tissues	9 upregulated 76 downregulated	Let-7, miR-30, miR-16	↓
Martens-Uzunova et al. (2012)	102 PCa tissues and normal adjacent tissues	54 deregulated	miR-205	↓
Larne et al. (2013)	49 PCa tissues 25 normal tissues	7 deregulated	miR-96-5p, miR-183-5p miR-145-5, miR-221-5p (combined in miQ score)	↑ ↓
Moltzahn et al. (2011)	Serum samples from PCa (n = 36) and HD (n = 12)	6 upregulated 4 downregulated	miR-20b, miR-874, miR-1274a, miR-1207-5p, miR-93, miR-106a miR-223, miR-26b, miR-30c, miR-24	↑ ↓
Bryant et al. (2012)	Plasma samples from PCa (n = 78) and HD (n = 28) Urine samples from PCa (n = 118) and HD (n = 17)	12 deregulated	miR-107, miR-574-3p	↑
Srivastava et al. (2013)	40 PCa tissues and 40 normal adjacent tissues. Urine samples from PCa (n = 36) and HD (n = 12)	2 downregulated	miR-205, miR-214	↓
Haj-Ahmad et al. (2014)	Urine samples from PCa (n = 8) BPH (n = 12) patients and HD (n = 10)	17 deregulated (only 7 selected for further analysis)	miR-1825 (only in PCa) miR-484 (in PCa and BPH)	↑ ↓
Schaefer et al. (2010)	76 PCa and adjacent normal tissues	5 upregulated 10 downregulated	miR-96, miR-182, miR-182* miR-183 and miR-375 miR-16, miR-31, miR-125b, miR-145, miR-149, miR-181b, miR-184, miR-205, miR-221, miR-222	↑ ↓

HRPC: hormone refractory PC; HD: healthy donors; FFPE: formalin-fixed paraffin-embedded

In addition, there are miRNAs that are abnormally expressed in different stages of disease progression and metastasis, and they are hence implicated as prognostic markers of clinical aggressiveness and recurrence **(Table 4)**. In addition, Musumeci and collaborators (2011) found that miRNA could also influence in tumour microenvironment (102).

Table 4. MiRNAs associated with PC prognosis. Adapted from (96)

References	Sample type	Clinical parameters	miRs deregulated	miRs selected as candidate biomarkers	
Taylor et al. (2010)	113 PCa tissues 28 normal tissues	Large screening study		Taylor et al. 10.1016/j.ccr.2010.05.026	
Martens-Uzunova et al. (2012)	102 PCa tissues and normal adjacent tissues	High risk biochemical recurrence	12 upregulated 13 downregulated	miR-19a, miR-130a, miR-20a/106/93 miR-27, miR-143, miR-221/222	↑ ↓
Tong et al. (2009)	40 FFPE prostatectomy Specimens (20 without early BCR 20 with early BCR)	Biochemical recurrence	2 upregulated 4 downregulated	miR-135, miR-194 (40% of case) miR-145, miR-221, miR-222	↑ ↓
Schaefer et al. (2010)	76 PCa and adjacent normal tissues	Biochemical recurrence	5 upregulated 10 downregulated	miR-96	↑
Hulf et al. (2013)	149 PCa and 30 matched normal tissues	Biochemical recurrence	1 downregulated	miR-205	↓
Schubert et al. (2013)	BCR tissues and disease-free tissues	Biochemical recurrence	2 downregulated	let-7b and let-7c	↓
Leite et al. (2011)	21 frozen BCR tissues 28 frozen disease-free tissues	Biochemical recurrence	4 upregulated	miR-100	↑
Karatas et al. (2014)	82 PCa tissues (41 BCR and 41 disease-free)	Biochemical recurrence	3 downregulated	miR-1, miR-133b	↓
Selth et al. (2013)	Serum samples from PCa patients (BCR = 8) disease-free = 8)	Biochemical recurrence	3 upregulated	miR-194 miR-146-3p	↑
Shen et al. (2012)	Plasma samples from PCa (n = 82)	Castration resistance	2 upregulated	miR-21, miR-145	↑
Jalava et al. (2012)	28 primary PCa tissues 14 CRPC tissues 12 BPH tissues	Castration resistance	4 upregulated 3 downregulated	miR-32, miR-148a, miR-590-5p, miR-21 miR-99a, miR-99b, miR-221	↑ ↓
Peng et al. (2011)	6 primary PCa tissues 7 bone metastatic tissues	Metastasis	5 downregulated	miR-508-5p, miR-143, miR-145, miR-33a, miR-100	↓
Saini et al. (2011)	36 PCa tissues 8 metastatic tissues 8 normal tissues	Metastasis	1 downregulated	miR-203	↓
Mitchell et al. (2008)	Serum samples from metastatic PCa (n = 25) and age-matched HD (n = 25)	Metastasis	6 deregulated	miR-141	↑
Brase et al. (2011)	Serum samples from localized PCa (n = 14) and metastatic PCa (n = 7)	Metastasis	5 upregulated	miR-141, miR-375	↑
Bryant et al. (2012)	Serum samples from PCa (n = 72) and metastatic PCa (n = 47) Plasma samples from PCa (n = 55) and metastatic PCa (n = 24)	Metastasis	2 upregulated	miR-141 and miR-375	↑
Nguyen et al. (2013)	Serum samples from localized PCa (n = 58) and metastatic CRPC (n = 26)	Castration resistance	3 upregulated 1 downregulated	miR-141, miR-375, miR-378* miR-409-3p	↑ ↓
Zhang et al. (2011)	Serum samples from localized PCa (n = 20), ADPC (n = 20), CRPC DTX treated (n = 10) and BPH (n = 6)	Castration resistance	1 upregulated	miR-21	↑

BCR: biochemical recurrence

4.6. Role of MiRNA in Prostate Tumorigenesis and Progression

The "Hallmarks of Cancer" were eloquently proposed by Hanahan and Weinberg to describe the essential features ingrained in the physiology of all malignant cells that drives their growth and dissemination (103). Indeed, included amongst the traits displayed by all carcinoma cells is their ability to *(i)* activate proliferative and replicative immortality programs, while simultaneously inactivating antigrowth programs; *(ii)* resist apoptotic programs; and *(iii)* stimulate angiogenic, invasive, and metastatic programs **(Fig.10).** Importantly, miRNAs play active roles in modulating all of these physiological processes in carcinomas, including PC. Especially miRNAs correlate with PC cell epithelial-mesenchymal transition (EMT), cancer stem cells (CSCs), drug sensitivity, cancer microenvironment, energy metabolism, androgen independence transformation, and diagnosis prediction (57).

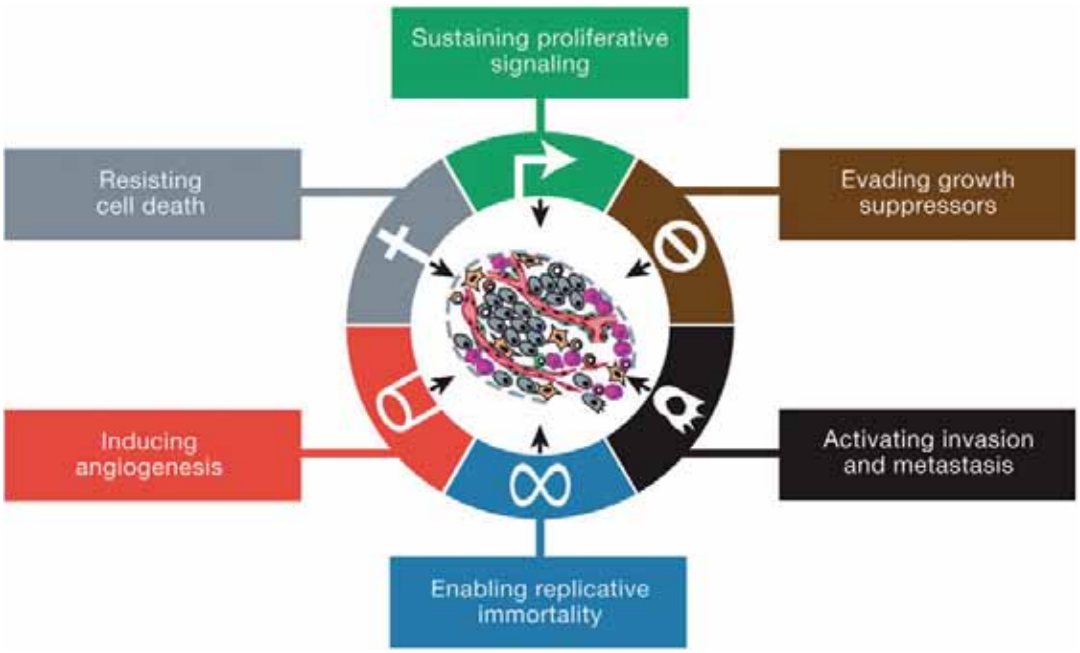

Figure 10. The hallmarks of cancer. Adapted from (103)

Gain- and loss of-function experiments, together with target prediction analyses, have provided insights into the role of miRNAs in carcinogenesis as tumour suppressor genes or oncogenes **(Table 5)**, and provide novel opportunities to design and implement miRNA-directed therapies (96).

Table 5. MiRNAs associated with PC therapy. Adapted from (96)

References	Sample type	Therapy	miRs deregulated	miRs selected as candidates	
Josson et al. (2008)	LnCaP and LnCaP C4-2B	Radiation therapy	6 downregulated	miR-521	↓
Huang et al. (2013)	PC3 radiation resistant cells	Radiation therapy	1 upregulated	miR-95	↑
Ribas et al. (2009)	LNCaP and LAPC-4	Hormone therapy	Overexpressed	miR-21	↑
Ottman et al. (2014)	LnCap CDX sensitive cells LnCap CDX non-sensitive cells	Androgen deprivation-therapy and casodex	21 upregulated 22 downregulated	http://www.molecularcancer.com /content/13/1/1	
Lehmusvaara et al. (2013)	28 tumor tissues ($n = 8$ goserelin-treated patients $n = 9$ bicalutamide-treated patients $n = 11$ no treated-patients)	Endocrine treatment	10 deregulated	miR-9 and miR-17	↑
				miR-218	↓
Zhang et al. (2011)	Serum samples from localized PCa ($n = 20$), ADPC ($n = 20$), CRPC DTX treated ($n = 10$) and BPH ($n = 6$)	Docetaxel	1 upregulated	miR-21 (in CRPC docetaxel resistant)	↑
Puhr et al. (2012)	PC3 docetaxel-resistant cells	Docetaxel	2 downregulated	miR-200c, miR-205	↓
Lin et al. (2014)	Serum and plasma samples from CRPC PCa ($n = 97$) before and after therapy	Docetaxel	46 deregulated	miR-200c, miR-200b, miR-146a, miR-222, miR-301b, miR-20a	
Kojima et al. (2010)	PC3 paclitaxel-resistant cells	Paclitaxel	1 downregulated	miR-34a	↓
Fujita et al. (2010)	PC3 and DU145	Paclitaxel	1 downregulated	miR-148	↓

ADPC: androgen dependent prostate cancer; DTX: docetaxel; CDX: casodex.

4.6.1. Prostate Cancer Stem Cells

The cell of origin for PC is highly relevant, since different cells of origin may generate clinically relevant subtypes with different prognosis and outcome. The PC cell of origin refers to the cancer-initiating cell(s) within the prostate epithelium.

Given that prostate adenocarcinoma has a luminal phenotype, it is characterized by loss of basal cells and reduced matrix diversity. Therefore, the origin for PC should correspond to a luminal cell that has undergone oncogenic transformation, or a basal cell that differentiated and proliferates as luminal progeny following tumorigenesis **(Fig.11)** (104). However, there are evidences that supporting stem/progenitor cell itself within the tumours as potential PC cell of origin in human (105).

The CSC hypothesis postulates that only a subset of cells within the tumour are capable of sustaining tumorigenesis and driving disease progression, while establishing the cellular heterogeneity that constitutes the primary tumour (106). Several studies related them with the cancer development, drug resistance, metastasis and recurrence (107). Thus defining how prostate (PCSCs) contributes to these processes may lead to therapeutic intervention (108).

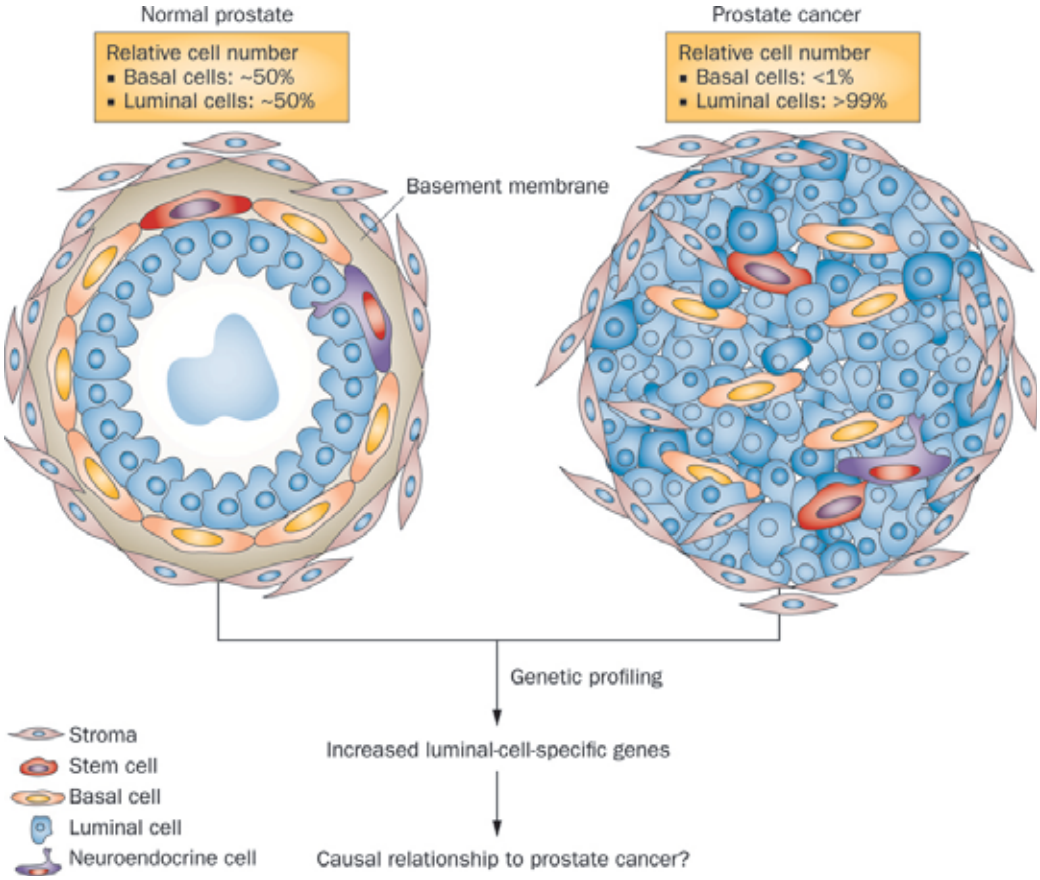

Figure 11. Advanced PC *vs.* normal prostate. Adapted from (104)

CSCs are described as a subset of cancer cells that have self-renewal and tumour-initiating capacity, multi-linage differentiation potential, and high proliferation rate. MiRNAs have emerged as important regulators for the acquisition of these cancer stem-like cell features during tumour progression **(Table 6)**. MiRNAs have been demonstrated to control the self-renewal and differentiation of embryonic stem cells (ESC) (96,109). Furthermore, a variety of studies have shown that miRNA expression is altered in CSC compared to normal tissues or non-CSC tumour tissues (105). One example in PC is the miR-34a, which is down regulated in CD44+ cancer cell. The miR-34a forced expression in CD44+ PC cells resulted in the inhibition of clonogenic growth and inhibition of metastatic behaviour and tumour regeneration (109).

Table 6. MiRNAs associated with stemness properties acquisition. Adapted from (96)

References	miRs associated with stemness properties
Liu et al. (2012)	miR-34a
Saini et al. (2012)	miR-708
Huang et al. (2012)	miR-143 and miR-145
Hsieh et al. (2013)	miR-320

4.6.2. Proliferation

The most fundamental trait of cancer cells involves their ability to sustain chronic proliferation. Normal tissues carefully control the production and release of growth-promoting signals that instruct entry into and progression through the cell growth and division cycle (103).

Several miRNAs, when overexpressed or inhibited in cancer cells have been reported to interfere with cell cycle regulators. Many of these miRNAs modulate cell proliferation pathways through direct interaction with critical regulators such as PTEN, Myc, RA-t-sarcoma (Ras) or Abelson murine leukaemia viral oncogene homolog 1 (ABL), as well as members of the retinoblastoma (Rb) pathway, cyclin-dependence kinase (CDK) complexes or cell cycle inhibitors of INK4 (inhibitors of CDK4) or CDK interacting protein/kinase inhibitory protein (Cip/Kip) families (110).

In PC, abnormalities of the cell cycle are frequently observed, including reduced CDK, inhibitor p21 (Wafl/Cip1) and increased abundance of p27 (Kip1) and cyclin D. MiRNAs interact with E2F transcription factor, cyclins, CDKs, and CDK inhibitors, providing the potential to regulate cellular division and cell cycle progression (79).

4.6.3. Apoptosis

In terms of molecular events occurring in tumours, apoptosis resistance is now considered an important hallmark of tumour progression (103). In contrast to normal cells, cancer cells can break the balance between pro- and anti-apoptotic factors to promote cell survival under conditions of environmental stress (88).

MiRNAs are able to interact in the apoptotic pathway in prostate cells, and their deregulation may promote apoptosis avoidance in PC via a number of mechanisms, targeting transcription factor, e.g. E2F, or signalling pathways at different stages: p53 tumour suppressor gene and B-cell lymphoma 2 (Bcl-2) family members (79).

4.6.4. MiRNA in the Multistep Metastatic Program

Metastatic development from a primary tumour to a distant lesion occurs through a multistep process that must be overcome by tumour cells, and includes: detachment from the primary site, acquisition of cell motility, degradation of the extracellular matrix (ECM) and tissue invasion, intravasation, dissemination and survival through the blood or lymph, extravasation and finally proliferation at a distant site **(Fig.12)** (111).

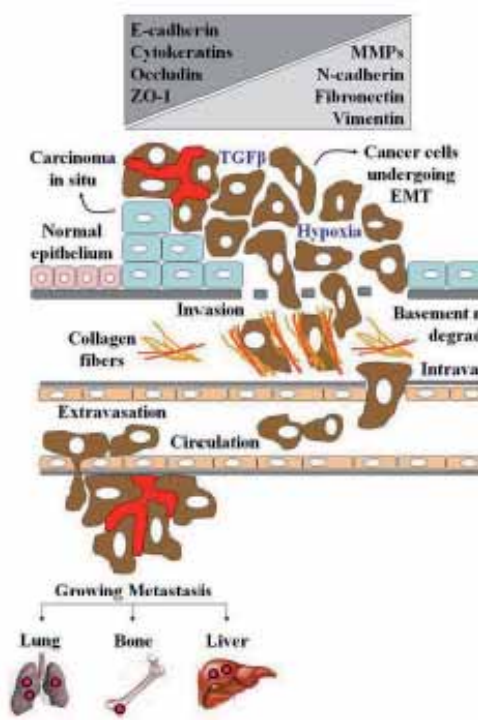

Figure 12. The EMT (Image obtained from http://www.frontiersin.org/files/Articles/76609/fonc-04-00059-HTML/image_m/fonc-04-00059-g003.jpg)

Deregulated miRNAs may function as either tumour suppressors or oncogenes (oncomiR) in cancer. Furthermore, another miRNAs identified as a subclass of these miRNAs are called metastmiRs, which expression is highly associated with the acquisition of metastatic phenotype. MetastmiRs can regulate various steps of the metastatic cascade such as EMT, invasion, migration, angiogenesis, adhesion, and colonization of distant organs (57).

EMT provides mechanisms for epithelial cells to overcome the physical constraints imposed on them by intercellular junctions and allows them to adopt a motile/mesenchymal phenotype. This way, cancer cells can escape the primary tumour, invade surrounding tissues, cross endothelial barriers, enter the circulation through blood and lymphatic vessels, and eventually

colonize remote sites to generate metastases. Once there, metastatic cells can revert through MET (mesenchymal-epithelial transition) to require epithelial characteristics similar to cells in the primary tumour (79). In this multistep program, degradation and invasion of the ECM is also a fundamental passage (111).

MiRNAs have been seen implicated in the EMT process at different levels. In PC, several miRNAs are described to directly target EMT transcription factors or affect the integrity of the epithelial architecture (79). They have also been seen as regulators of the matrix metalloproteinase (MMP) expression and function, and as modulators of the interaction between PC cells and the ECM by intervening in additional pathways, e.g. inhibiting the transmembrane cell adhesion glycoprotein CD44 (112).

4.7. Therapeutic Strategies

Recently, several preclinical studies have illustrated the feasibility of slowing tumour progression by either overexpressing tumour suppressor miRNAs or by neutralizing the activities of oncogenic miRNAs in cell- and animal-based models of cancer.

There are likely distinct advantages in applying miRNAs as therapeutic agents over the current conventional drugs. One of the most appealing properties of miRNAs as therapeutic agents, and probably the most important advantage in comparison with approaches targeting single genes, is their ability to target multiple molecules, frequently in the context of a network, making them extremely efficient in regulating different biological cell processes relevant to normal and malignant cell biology (113). In addition, the combination of several miRNAs that target the same gene would reduce the probability of mutation-induced resistance (114). Another advantage of using miRNAs as drugs is that they are small size, and are therefore less antigenic than protein-coding gene replacement therapies (115).

Accordingly, the pharmacologic delivery of miRNA oligonucleotides or viral-based miRNA expression constructs to tumours seeks limit their growth and dissemination *via* 3 general strategies: *(i)* inactivate the oncogenic activities of oncomiRs; *(ii)* reinstate the expression of tumour suppressive miRNAs; and *(iii)* administer chemotherapeutic agents capable of regulating miRNA transcription or processing (57). These strategies can be accomplished with small RNAs directly delivered or by more conventional gene therapy approaches where plasmids or virus delivered to express the therapeutic molecules (116).

To date, three main anti-oncomiR strategies have been taken: expression vectors (miRNA sponges), small-molecule inhibitors and antisense oligonucleotides (ASO). However, considerably more attention has been paid to ASO technology, particularly to those ASOs that target miRNAs directly (anti-miRs) to specifically inhibit miRNA function. On the other hand, miRNA replacement therapy supplements the lowered level of miRNAs with: double stranded miRNA mimics having identical sequence as the endogenous mature miRNA, synthetic miRNA precursor mimics, and expression vectors (117).

Despite the great potential of miRNAs as anticancer drugs, the broad spectrum of genes targeted by miRNA-based therapeutics might also present a number of challenges, such as the potential for off-targeted miRNA activities that could lead to unwanted toxicities and the limitations that may be overcome by delivery (poor *in vivo* stability, inappropriate biodistribution, disruption and saturation of endogenous RNA machinery, and untoward side effects). Recent chemical modifications of RNA-based structures have greatly improved their stability and lessened their toxicities (113).

Perhaps, the main hurdle in using miRNA-based therapy is delivering the drug to cancer cells, whether locally in the prostate or to metastatic cells disseminated throughout the body. Several delivering strategies are considered plausible, such as incorporation the miRNAs within nanoparticles and liposomes, or conjugating them to peptides that can penetrate the plasma membrane **(Fig.13)** (113,116).

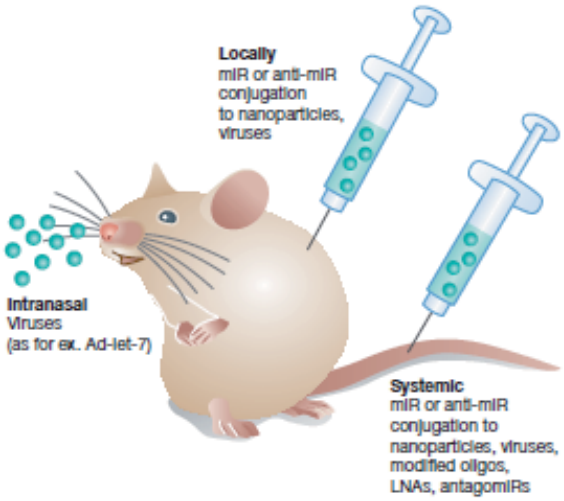

Figure 13. Current approaches to in vivo miRNA targeting. Adapted from (113)

4.7.1. Exosomes as MiRNA Delivery System

Tumour cells have been shown to release exosomes containing miRNAs (118) and miRNAs secreted from donor cells can be taken up and function in recipient cells (119,120). These data indicate that exosomes are natural carriers of miRNA that could be exploited as an RNA drug delivery system, and be called "exocure" **(Fig.14).**

Kosaka and collaborators (2012) assessed the therapeutic application of exosomes in PC. They isolated exosomes from cells over-expressing the tumour-suppressive miR-143. After several intra-tumoral administrations, enriched miR-143 exosomes conditioned medium (CM) led to anti-tumour effect. Furthermore, exogenously transduced miR-143 did not affect the non-cancerous cells, and no overt side effects were observed in exosome-mediated gene delivery in vivo by dendritic cell-derived exosome, suggesting that "exocure" does no have serious side effects (121).

However, the following points are difficulties that arise for their use (122):

- The exosome must be abundant or highly enriched to be use as a therapy. It is necessary to known the precise production mechanism
- The methods to introduce desired tumour suppressive miRNAs into exosomes should be considered. Until now, electroporation and cell transfection to over-express are used
- Methods for the exosomes isolation from CM need to be optimized. The ultracentrifugation, the current most popular isolation method, is time-consuming and complicated, and its recovery rate is poor
- The exosome-producing cells need to be carefully chosen. Because of the tropism against the target cancer cells, we need to understand the mechanism of exosome uptake
- The immunogenicity of exosomes is poorly understood
- The functions and mechanism of tumour-suppressor miRNAs need to be clarified

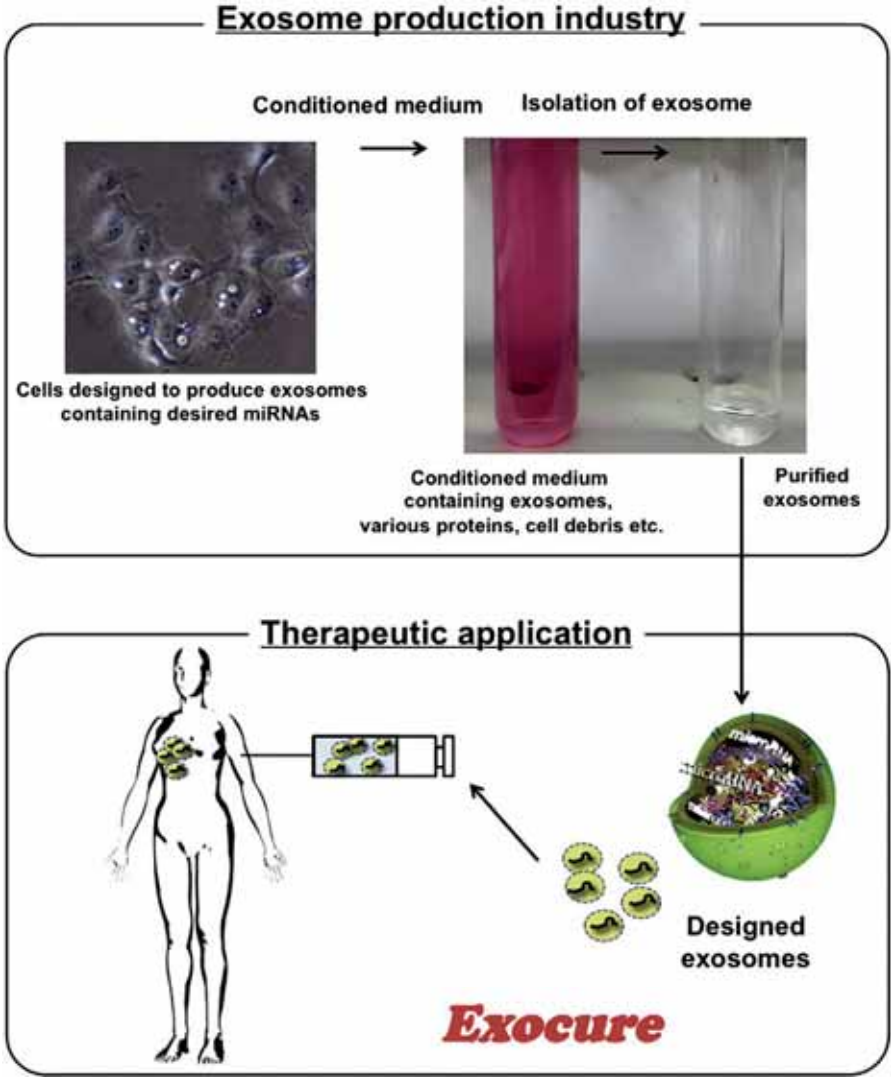

Figure 14. A schematic representation of "exocure". Adapted from (122)

OBJECTIVES

THESIS HYPOTHESIS

A multiplex signature comprised of aberrantly expressed miRNAs in post-prostate massage (PM) urine samples can specifically detect PC from other benign conditions.

GENERAL OBJECTIVE

The main objective of this work is to develop a non/minimally-invasive method, using a miRNAs signature as a biomarker, for the early diagnosis of PC in urine obtained after DRE.

This could, in the future, help to improve the detection and management of PC, avoiding the over-diagnosis and over-treatment associated with the currently used screening methods.

In the long term this will help to reduce the number of unnecessary biopsies practiced (both first and repeat PB) and, therefore, reduce unwanted secondary effects and health care costs.

SPECIFIC OBJECTIVES

Objective 1: Standardization of methods for isolation and quantification of miRNA from different urine fractions (sediment and supernatant).

1.1 Evaluate the effectiveness of different RNA extraction kits to obtain a satisfactory amount of miRNAs to study their expression levels in urine samples

1.2 Compare different RT-qPCR technologies to analyse the miRNAs expression levels

Objective 2: Identification of miRNA profile as urinary diagnostic biomarker for PC.

2.1 Perform a pilot study analysing the expression levels of 22 miRNAs chosen by literature in urine samples by RT-qPCR. The results will show us whether urinary miRNAs could be used to distinguished patients with PC of those with benign diseases (n=40)

2.2 Determine differentially expressed miRNAs profiles for diagnosis of PC by high throughput technologies as Microfluidic Cards, 384-well cards preloaded with TaqMan® gene expression assays that will allow us to measure miRNAs expression using the comparative CT (ΔΔCT) method of relative quantitation of urinary samples obtained after DRE from PC patients and benign controls (n=40)

2.3 Validation of the previously discovered miRNAs by RT-qPCR using customized microfluidic cards in a new cohort of patients who will undergo prostate biopsy (n=154) to establish a diagnostic method able to early detect, by non-invasive methods, the presence of PC reducing the number of unnecessary biopsies practiced

2.4 Validation of deregulated urinary miRNAs in prostatic tissue samples. The most promising deregulated miRNAs in urine will be validated in formalin fixed paraffin embedded tissue (FFPE) of RPs to determine whether the observed changes in this biofluid come from prostate gland

Objective 3: Characterization of the most relevant miRNAs in order to unveil their role in the PC progression and study their potential as new therapeutic targets.

3.2 The most promising miRNAs will be studied by generating loss-of-function or overexpression in the PC cell lines available in our laboratory. The phenotypes of these genetic manipulations will be studied *in vitro* for their effects on cell viability, proliferation, migration, invasion, colony formation capacity, etc...

3.1 Analyse functional miRNAs using bioinformatics and biocomputing approaches to understand if the miRNAs themselves, or their identifiable target genes, belong to networks involved in PC progression, and thus might function as critical targets for future therapies

MATERIALS & METHODS

1. URINE SAMPLES

Urine samples were obtained from males with the suspicion of PC, due to abnormal DRE and/or serum PSA levels higher than 4ng/ml, at the Urology Service of the Vall d'Hebron University Hospital. Written informed consent was obtained from all the study participants, and samples were coded to ensure sample tracking and confidentiality on patient identity.

Urine (30-50ml) was collected in urine collection cups, kept on ice, transported to the laboratory and processed within 2h of their collection. The urine samples were centrifuged at 2500xg for 10min at 4ºC. From this point, pellet and supernatants were processed separately. Cellular pellets were washed twice with cold PBS and finally resuspended 1:5 in RNALater (Ambion, Life Technologies/Thermo Fisher Scientific, Waltham, MA, USA). Supernatant was supplemented with a cocktail of protease inhibitors (Sigma-Aldrich, St Louis, MO, USA). Both urine fractions were stored at -80ºC until their use **(Fig.15)**.

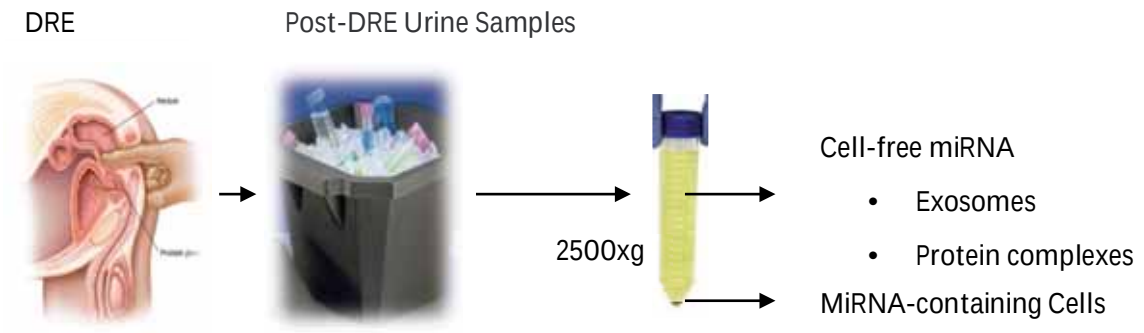

Figure 15. Urine sampling and processing. Supernatant contains cell-free miRNAs inside exosomes or bounded to protein complexes. Whereas, pellet contains intracellular miRNAs

1.1. Standardization of Methods for Isolation and Quantification of MiRNA

To standardize the methods for the isolation of miRNA-containing prostate cells, a urine pool from 12 patients undergoing DRE was used. This pool was aliquoted into 25ml individual samples in order to obtain enough material for all RNA extraction tests and be able to compare them and to avoid the human variability.

For non-vesicle miRNAs assessment, a pool of urine supernatants from patients undergoing DRE and stored at -80ºC was used. Subsequently, the urine pool was divided into individual 3ml samples.

For exosome-derived miRNAs, a pool of 2 PC and another of 2 normal patients undergoing a DRE and stored at -80ºC was used.

1.1.1. Identification of MiRNA as Urinary Diagnostic Biomarker for Prostate Cancer

We selected patients with a diagnosis of PC and age matched controls, including those with benign pathologies of the prostate as BPH, prostatitis, proliferative inflammatory atrophy (PIA), and prostatic intraepithelial neoplasia (PIN). The definitive diagnosis of the patients was achieved after PB. Patients with other known tumours, acute severe illness and/or previous PC therapies were excluded from the study.

The study subjects selected for the pilot study (obj. 2.1) were the same as for the discovery phase (obj. 2.1), a total of 40 urine samples obtained after DRE, and distributed in 2 groups, 20 controls and 20 PC patients **(Table 7)**. However, for the verification phase, we used an independent and larger cohort of 154 patients, 37% of them with PC **(Table 8)**.

Table 7. Clinical and pathological information for the pilot study and discovery phase patients

		All patients average (min, max or %)
Nº of patients		40
Age (yr)		66 (46-83)
PSA level (range)		6,82 (0,7-22,3)
PSA ratio		0,17 (0,06-0,29)
Prostate Cancer		20 (50%)
	GLEASON < 7	6 (30%)
	GLEASON = 7	7 (35%)
	GLEASON >7	7 (35%)
Benign		20 (50%)

Table 8. Clinical and pathological information for the verification phase patients

		All patients average (min, max or %)
Nº of patients		154
Age (yr)		65,5 (44-85)
PSA level (range)		10,9 (2,5-189)
PSA ratio		0,17 (0,00-0,80)
Prostate Cancer		57 (37%)
	GLEASON < 7	7 (12,3%)
	GLEASON = 7	41 (71,9%)
	GLEASON >7	9 (15,8%)
Benign		97 (63%)

2. TISSUE SAMPLES

All FFPE tissue samples from the RP of PC patients without further treatment and their associated information concerning diagnosis, treatment, and outcome were obtained from Pathology Department of the Vall d'Hebron University Hospital. The study was approved by the ethical committee, and samples were coded to ensure sample tracking and confidentiality on patient identity.

Prostate tissue was routinely formalin-fixed promptly after surgery and subsequently paraffin-embedded. The combined FFPE treatment is aimed to histological examination of tissues, and results in highly stable tissue blocks, which can be easily stored for years at RT in form of "biopsy banks". H&E staining was performed to identify malignant and benign areas. FFPE tissue blocks with tumour or normal focus were cut into sections with a microtome, and were placed in 1,5 ml tubes stored at RT during weeks. Paraffin sections were deparaffinised with xylene and rehydrated though ethanol/water dilutions before RNA extraction **(Fig.16)**.

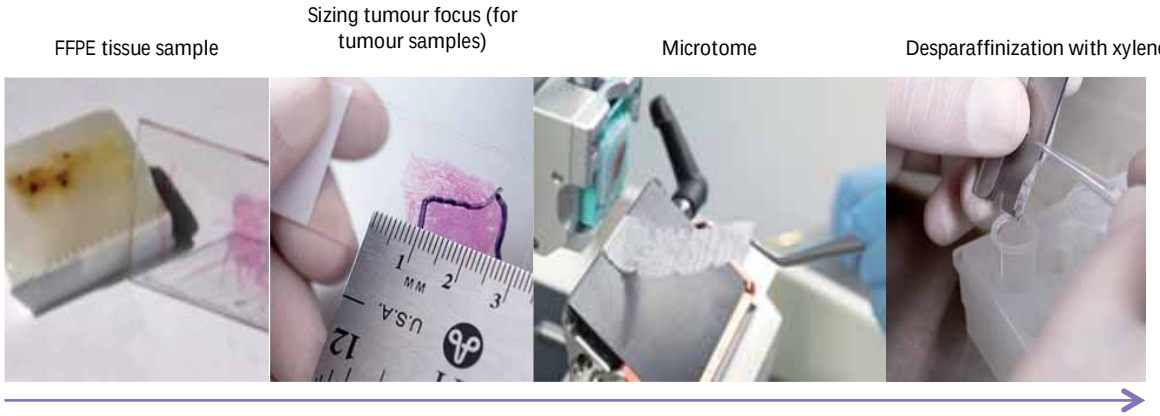

Figure 16. FFPE tissue sampling and processing.

2.1. Standardization of methods for isolation and quantification of miRNA

For the standardization of sampling procedure, we tested to extract and quantify RNA from different paraffin section quantity (number) and thickness (μm). The sample consists of the RP of two PC patients.

2.1.1. Validation of Deregulated Urinary MiRNAs

For the comparative study of the miRNAs expression levels between benign and PC tissue, we selected 2 blocks/patient, containing benign and tumour tissue from 20 patients. Two slides of 20μm were obtained for each block. The tumour focus and grade was histologically reconfirmed to verify a tumour content of at least 60% with a Gleason score ≥7.

3. CELL BIOLOGY

3.1. Human Prostatic Epithelial Cell Lines

The non-tumorigenic human prostatic epithelial cell lines RWPE-1 and PNT-2, and human PC cell lines PC-3, DU-145, LNCaP **(Table 9)** and derivatives PC-3M used in our studies were obtained from the American Type Culture Collection (ATCC).

Table 9. Main features of human PC epithelial cell lines

	Patient	Origin	Tumorigenicity	Androgen-sensitive	PSA
PC-3	62-year-old Caucasian man	Lumbar vertebra metastasis	High	No	No
DU-145	69-year-old Caucasian man	Central nervous system metastasis	Moderate	No	No
LNCaP	50-year-old Caucasian man	Lymph node metastasis	Moderate-low	Yes	Yes

The PC-3M derived-line was established from a PC-3 xenograft and it is more aggressive than the parental line (123).

3.2. Culture Conditions

All prostate cell lines except RWPE-1 were maintained in RPMI medium supplemented with 10% fetal bovine serum (FBS) (PAA Laboratories, Pasching, Austria), penicillin/streptomycin (1:100; Gibco, Life Technologies/Thermo Fisher Scientific, Waltham, MA, USA), and L-glutamine

(Gibco). The base medium for the RWPE-1 is the keratinocyte serum free medium (Gibco), supplied with the two additives: bovine pituitary extract and human recombinant Epidermal Grow Factor (EGF).

Cells were incubated at 37ºC and 5% CO_2 in a humidified incubator. For general maintenance of cells, they were replated two times per week by trypsinization of cell monolayers (0.25% trypsin, 0.02% EDTA). Culture media was changed every 2 days. Only cells under passage number 30 were used in our experiments. Cell concentration was determined using a Neubauer chamber.

3.3. Loss-of-function and Overexpression Studies

3.3.1. Transient Transfection

The transient transfection of PC cell lines was performed using synthetic oligonucleotides, miRIDIAN microRNA Human Inhibitors or Mimics (Dharmacon, Thermo Scientific, Waltham, MA, USA) at a final concentration of 50nM. We used Lipofectamine 2000 (Invitrogen, Life Technologies/Thermo Fisher Scientific, Waltham, MA, USA) as a transfection reagent following manufacturer's instructions.

Furthermore, in all the experiments with mimics and inhibitors a sample treated with a negative control (NC), NC-1 for the mimics and NC-2 for the inhibitors (Dharmacon) were included to confirm that the effects observed with the mimic or inhibitor were specific. NCs are based on *C. elegans* miRNA sequences, and have been confirmed to have minimal sequence identity with miRNAs.

Briefly, miRIDIAN microRNA Mimics and Hairpin inhibitors are designed on known or predicted miRNA sequences in miRBase. MiRNA mimics are double-stranded oligonucleotides designed to mimic function of endogenous mature miRNA. They are chemically enhanced to preferentially program RISC with active miRNA strand. On the other hand, miRNA inhibitors are RNA oligonucleotides with novel secondary structure designed to inhibit the function of endogenous miRNA. They are chemically enhanced to improve efficacy and longevity.

MiRIDIAN microRNA reagents were resuspended in diethylpyrocarbonate (DEPC) water to give a stock concentration of 20μM, and then stored at -20ºC. We always manipulated this

oligonucleotides maintaining nuclease-free conditions. For the transfection complex formation, Lipofectamine and oligonucleotides were diluted in non-supplemented RPMI medium. We mixed them and incubated for 20min at RT. It was added drop-wise to the cell cultures, and kept for 6-15h at 37°C.

The transfected cells percentage was measure with the transfection of a labelled RNA called Block-iT (Invitrogen) for each experiment. The transfection efficiency was monitored by RT-qPCR, but only for the over-expression.

3.3.2. Stable Transfection

The DNA plasmid containing the miRNA or scramble was purchased from System Biosciences (SBI, Mountain View, CA, USA) and shipped in bacterial stock form (*E.coli*) plated on LB-carbenicillin at 50μg/ml.

The human miR-210-3p precursor and scramble molecules have been packaged in a lentiviral-based vector. The miRNA precursor constructs consists of the stem loop structure and 300-500 base pairs of upstream and downstream flanking genomic sequence. The native structure ensures interaction with endogenous RNA processing machinery and regulatory partners, leading to properly cleaved miRNA.

The organization of the HIV-based expression vector contains the following features **(Fig.17):**

- **WPRE element—**enhances stability and translation of the cytomegalovirus (CMV)-driven transcripts. Primary miRNA are expressed using conventional pol-II promoter, the CMV promoter ensures a high level of expression from a single copy of integrated miRNA construct
- **SV40 polyadenylation signal—**enables efficient termination of transcription and processing of recombinant transcripts
- **Hybrid RSV-5'LTR promoter—**provides a high level of expression of the full-length viral transcript in producer 293 cells
- **Genetic elements (cPPT, GAG, LTRs)**—necessary for packaging, transducing, and stably integrating the viral expression construct into genomic DNA
- **SV40 origin—**for stable propagation of the pMIRNA1 plasmid in mammalian cells
- **pUC origin—**for high copy replication and maintenance of the plasmid in *E.coli* cells

- **Ampicillin resistance gene—**for selection in *E.coli* cells
- **copGFP-**fluorescent marker to monitor cells positive for transfection and transduction. The human EF1α promoter drives this protein marker

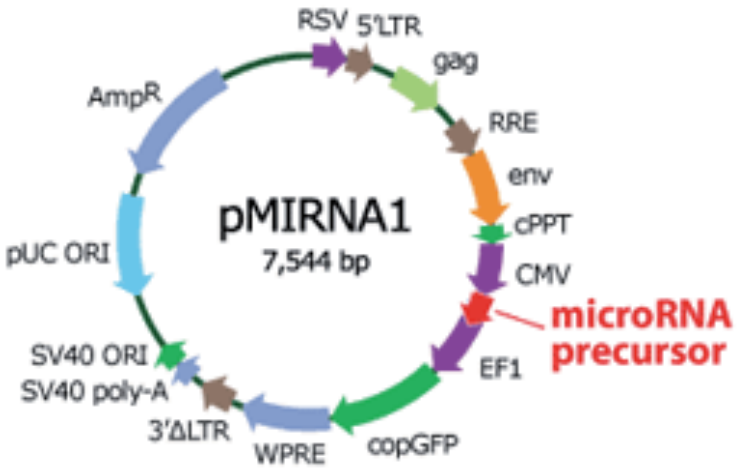

Figure 17. The organization of the HIV-based expression vector. (Image obtained from https://www.systembio.com/downloads/Manual_MicroRNA_Constructs_web.ver2.pdf)

For packaging of constructs in pseudoviral particles, pSPMD2G (packaging plasmid) and pSPAX2 (envelope plasmid) vectors (Abgene, Life Technologies/Thermo Fisher Scientific, Waltham, MA, USA) were used. Three 10cm culture plates (p100) treated with 5ml gelatine were used to seed 4.10^6 Hek 293T cells 24h before the transfection with Lipofectamine 2000 following manufacturer's instructions. Cells were incubated with the transfection complex for 6h. Then, 6ml of fresh RPMI medium 10% FBS were added. Thirty six hours later, culture supernatant was collected and centrifuged at 2500rpm for 5min at RT to remove cell debris, filtered with sterile syringe filter 0,45µm PES (VWR International, Wayne, PA, USA) and stored in 15ml tubes at -80°C until the target cells infection (2,5ml/p60 for 24h).

72h after infection, we prepared a suspension of $1,5.10^6$cells/500µl RPMI medium 10% FBS filtered with 30µm filter (Partec, Göttingen, Germany) to isolate infected cells, which expressed high levels of copGFP, by FacsAria sorting (BD Bioscience, San Jose, CA, USA). The miRNA expression levels of these cells were assessed by RT-qPCR.

3.4. Proliferation Assay

3.4.1. For Transfected Cells

A suspension of 5.10^3cells/100µl free-antibiotics RPMI medium 5% FBS were seeded into 96-well tissue culture plates treated with L-Polylysine diluted with PBS (5:100; Sigma-Aldrich, St Louis, MO, USA) the day before transfection. Cell number was determined at 96h after transfection.

PC-3 and PC-3M cells were fixed for 30min at RT in 4% formaldehyde, washed in cold PBS and stained with 50µl crystal violet solution 0,01%. After 30min, wells were washed twice with PBS, and 10% acid acetic was added. After 15min, the absorbance was measured using a BioTek ELx800 plate reader to directly test wavelengths of 590nm.

Since LNCaP cell line has low anchoring potential and does not produce a uniform monolayer in culture, we assess its proliferation using CellTiter 96 Assay (Promega Biotech Iberica, Madrid, Spain) following manufacturer's instructions, based on metabolic conversion of 3-[4,5-dimethylthiazol-2-yl]-2,5-diphenyl tetrazolium bromide (MTT). 20µl of the kit reagent were added to each well, mixed by swirling the plates and returned to the incubator. After 2-3 hours, the absorbance was measured by dye solution using a BioTek ELx800 plate reader to directly test wavelengths of 490nm.

All data are presented as the mean value for sextuplicate wells, and referenced to the negative control.

3.4.2. For Stable Cells

A suspension of 5.10^3cells/2ml RPMI medium 10% FBS were seeded into 6-well tissue culture plate. PC cell number was determined at 6-12 days counting cells by using Neubauer chamber or 500µl crystal violet staining 0,01% following the protocol described above. Data are presented as the mean value for triplicate wells, and referenced to the negative control.

3.5. Viability Assay

A suspension of 5.10^3cells/100µl free-antibiotics RPMI medium 5% FBS were seeded into 96-well tissue culture plates treated with L-Polylysine (5:100; Sigma-Aldrich, St Louis, MO, USA) the day before transfection. The percentage of dead cells was determined at 96h after transfection.

PC cells were treated directly into their culture supernatant with 2µl Hoechst dye (1mg/ml) and 2µl propidium iodide (PI, 0,05mg/ml) for 10min at RT. Then, images of the cells were taken with the 20x objective of a Nikon Eclipse TE2000-S inverted microscope. Data was presented as the mean value of three photos for each well for triplicate, and referenced to the negative control.

3.6. Detection of Cell Cycle Progression by Flow Cytometry

The fraction of stable cells in each cell cycle stage was analysed by flow cytometry, staining DNA content with PI. Cells were seeded into two 10cm plates (p100) at 60% of confluence ($7,5.10^5$). After 24h, cells ($1,5.10^6$cells/ml) were fixed in 70% ice-cold ethanol and stored for at least 15min in a 1,5ml tube at -20°C to fix.

For the PI staining, cells were centrifuged at 5000rpm for 10min at 4°C and washed twice with cold PBS. The pellet was re-suspended in 500µl of a solution that contains: IP (20µl/ml; 1mg/ml) and RNase A (20µl/ml; 10mg/ml), both purchased from Sigma-Aldrich, St Louis, MO, USA), and incubated for 1h at RT. The number of cells in each peak, corresponding to cells in G1, S and G2/M, was represented as the percentage of total cell number by using FCS Express software. The results are shown as the average of 2 independent assays.

3.7. Clonogenic Assay

A suspension of 500 PC-3M stable cells in 1ml RPMI medium 10% FBS were seeded into 12-well tissue culture plate. After a week, cell colonies were rinsed with PBS and stained with 1ml crystal violet solution 0,01%, following the protocol described above. After swirling and pipetting up and down, 0,5ml of stain was placed in a 24-well plate and the absorbance was

measured at 590nm using the BioTek ELx800 plate reader.

A suspension of 1000 PC-3 stable cells in 1ml RPMI medium 10% FBS with metilcelulose 1% (Sigma-Aldrich, St Louis, MO, USA) were seeded into low-adherent 24-wel special tissue culture plate to measure spheroid formation. The cell medium was renewed every 3 days. After 15 days, spheroids were photographed.

Data are presented as the mean value for triplicate wells, and referenced to the negative control. Furthermore, the colonies were photographed with a Nikon Eclipse TE2000-S inverted microscope.

3.8. Wound Healing Assay

To determine the rate of cell motility in PC-3 and PC-3M cells (4.10^4), they were seeded into 24-well plates and transfected as described above. Cells were grown to confluence for 24h (4.10^4cells/well) or 48h ($1,5.10^4$cells/well), and a straight line (wound) was then gently performed at the bottom of the dish with a 10µl pipette tip. Afterwards, cells were washed, incubated in medium with 2% FBS, and kept in a computer controlled mini-incubator, which provided a stabilized temperature of 37 C with 95% humidity, 5% CO, and optical transparency for microscopic observations. The incubator was fastened to an inverted microscope (Live Cell Imaging CellR, Olympus, Japan) to monitor cell migration. Images were taken with the 4x objective every 30 minutes at predetermined wound sites (3 sites per condition, performed in triplicate) and were analysed using the Image J software (Wright Cell Imaging Facility, USA). Initial wound area (μm^2) and time needed to close the wound (hr) were the variables used to calculate the migration speed of the cells. Data are presented as the mean value for triplicate wells, and referenced to the negative control.

3.9. Transwell Migration and Invasion Assays

PC cells were seeded (6.10^4cells/well) into 24-well tissue culture plate and transfected as described above. Cells were harvested by trypsinization and seeded (5.10^4cells/insert) onto Transwell migration inserts **(Fig.18)** or Matrigel Invasion Chamber inserts (BD Bioscience, San Jose, CA, USA) with 8µm diameter pore membranes in 500µl RPMI medium 2% FBS (cell

suspension contains trypsin) at 48h after transfection, with the lower chamber containing 700µl RPMI medium 20% FBS and incubated for 24 hours at 37°C.

To quantify migrating cells, cells remaining on the topside of the membrane were removed using a cotton-tipped swab, and the nucleus of cells that had migrated to the underside were stained with Hoechst (1:200; 1mg/ml) and photographed with the 20X objective of a Nikon Eclipse TE2000-S inverted microscope (4 pictures/well). Data was presented as the mean value of 4 photos for each well for triplicate, and referenced to the negative control. The migration experiments were performed at least two times.

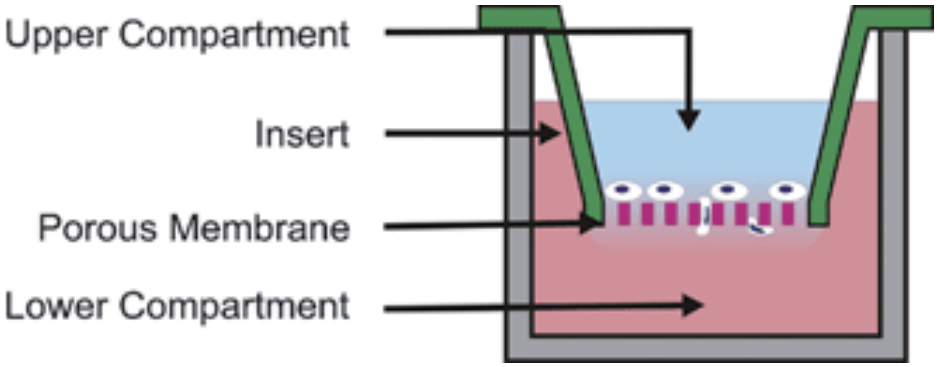

Figure 18. Transwell migration Insert (image obtained from http://pubs.rsc.org/services/images/RSCpubs.ePlatform.Service.FreeContent.ImageService.svc/ImageService/Articleimage/2008/LC/b711887b/b711887b-f3.gif)

4. EXOSOMES FROM URINE AND CELL MEDIA

4.1. Exosomes Purification

All exosomes were purified following a differential ultracentrifugation method.

Urine supernatants stored at -80ºC were thawed and first centrifuged at 16,000xg for 30min at 4ºC, to pellet the fraction of larger MVs and any possible remaining cell debris. The supernatant was ultracentrifuged at 100,000xg for 120min (Sorvall ultracentrifuge, with AH-629 rotor). The resulting pellet was washed with cold PBS and centrifuged again at 100,000xg, 60min. For protein studies, the final pellet was resuspended in 50µL PBS, of which 5µl were stored for the

nanoparticle tracking analysis (NTA), and the rest was mixed with 50µl RIPA 2X buffer.

In order to isolate exosomes from culture supernatant, cells were grown to 90% confluence in 5 15cm (p150) culture plates, and incubate with 15ml of exosomes-free complete RPMI medium for 48h before collecting culture supernatant. The supernatant was centrifuged at 10,000xg for 30min at 4ºC to remove dead cells and stored at 4ºC until exosome purification by ultracentrifugation. The resulting pellet was resuspended in 200µl PBS, of which 50µl are used to RNA extraction and 10µl diluted in 490µl PBS (1:50) for the NTA.

In an effort to improve this basic method, we assayed several modifications, as described below.

4.1.1. DTT Treatment

For urine supernatant, in order to break the THP fibers and release the exosomes that could remain trapped in their net, the first pellet obtained was treated with DTT (200mg/ml) at 37ºC for 10min, and centrifuged again at 16,000xg, 30min. The supernatant was mixed with the initial one before proceeding with the ultracentrifugation steps.

4.1.2. RNAse A Treatment

If the samples are used for analysis of RNA or miRNA content, the pellet resulting from the first ultracentrifugation was treated with 500µl RNAse A (0,4mg/ml) (Sigma-Aldrich, St Louis, MO, USA) to degrade any RNA that may have co-precipitated with the exosome fraction. The RNase A was removed during the second ultracentrifugation step.

4.2. Sizing and Quantification

The NTA was conducted in collaboration with the Grup d'Enginyeria de Materials (GEMAT) in Institut Químic de Sarrià, Ramon Llull University. Vesicles present in purified samples were analysed by NTA using the NanoSight LM14 system (NanoSight Ltd., Amesbury, UK), configured with a high sensitivity digital camera system (Hamamatsu C11440 ORCA-Flash2.8, Hamamatsu City, Japan). Videos were analysed using the NTA-software (version 2.3), with the minimal

expected particle size, minimum track length, and blur set to automatic. Camera shutter speed and camera gain were set to maximum. Camera sensitivity and detection threshold were set close to maximum (15 or 16) and minimum (2 to 5), respectively, to reveal small particles. Ambient temperature was ranging from 23 to 25ºC. Samples were diluted in miliQ particles-free water. One video of 60s duration was recorded for each sample. We considered the particle concentration reliable when it was equal or more than 10^8particle/ml.

5. MOLECULAR BIOLOGY

5.1. Protein Extraction

5.1.1.For Cell Lines

Cells were scrapped from the culture plates and centrifuged at 500xg for 5min at RT, washed with PBS and centrifuged again at 500xg 5min. RIPA 1X lysis buffer was then added to the cell pellet and it was kept in a shaker at 4ºC for at least 30min to facilitate the rupture of the cells. After this incubation, cells were disrupted by sonication (LABSONIC M, Sartorius Stedim Biotech, Göttingen, Germany) at 100% amplitude for 4 pulses of 5 seconds each separated by 5 seconds pauses on ice. Finally, cell lysis product was centrifuged at max speed for 15min and the supernatant was stored at -20ºC.

5.1.2. For Purified Exosomes

Pellets recovered from the ultracentrifugation and resuspended in RIPA 1X lysis buffer were frozen at -80ºC. After thawing, samples were disrupted by sonication (LABSONIC M, Sartorius Stedim Biotech, Göttingen, Germany) at 100% amplitude for 4 pulses of 5 seconds each separated by 5 seconds pauses on ice. Finally, cell lysis product was centrifuged at max speed for 15min and the supernatant was stored at -20ºC.

5.2. Protein Quantification

For urinary exosomes and cell lines, protein was quantified using the DC Protein Assay (Bio-Rad, Bio-Rad Laboratories, Hercules, CA, USA), following the manufacturers instructions. Samples, usually diluted 1 in 20 (exosomes) and 1 in 10 (cell lines), were compared in triplicates against serially diluted BSA as standard.

On the other hand, exosomes from culture supernatant in PBS were directly quantified using the MicroBCATM Protein Assay kit (Thermo Scientific, Waltham, MA, USA).

5.3. Western Blotting

Proteins were separated by 10-12% SDS-PAGE under reducing or non-reducing conditions and transferred to PVDF membranes. For blocking, membranes were soaked in 5% non-fat dried milk in TBS-Tween20 (0.01%). Proteins were immunodetected using antibodies against the protein of interest, always overnight at 4°C. Then the membranes were washed and incubated with a secondary HRP-coupled antibody 1h at room temperature. Finally, HRP signal was revealed using the Immobilon Western HRP Substrate (Merck Millipore, Darmstadt, Germany). The intensity of the bands was densitometrically quantified using the Image J software v1.45s.

5.3.1. Antibodies

Exosome markers: anti-TSG101 (dilution 1:500; Abcam, Cambridge, MA, USA), anti-CD81 (dilution 1:1000; Santa Cruz Biotechnology, Santa Cruz, CA, USA), anti-CD63 (dilution 1:1000; Santa Cruz Biotechnology, Santa Cruz, CA, USA).

MiRNAs related pathways: E-cadherin (dilution 1:2500; BD Bioscience, San Jose, CA, USA), N-cadherin (dilution 1:2000; BD Bioscience, San Jose, CA, USA), cyclin A (dilution 1:200; Santa Cruz Biotechnology, Santa Cruz, CA, USA), cyclin B1 (dilution 1:1000; Merck Millipore, Darmstadt, Germany), cyclin D1 (dilution 1:1000; Santa Cruz Biotechnology, Santa Cruz, CA, USA), cyclin E (dilution 1:1000; Abcam Cambridge, MA, USA), p21 (dilution 1:1000; Santa Cruz Biotechnology , Santa Cruz, CA, USA), ERK (dilution 1:1000; Merck Millipore, Darmstadt,

Germany), pERK (dilution 1:1000; CS), Tubulin (dilution 1:1000; CS).

Secondary antibodies: Rabbit anti-Mouse Immunoglobulins/HRP (dilution 1:2000; Dako Cytomation), Goat anti-Rabbit Immunoglobulins/HRP (dilution 1:2000; Dako Cytomation) and Rabbit anti-Goat Immunoglobulins/HRP (dilution 1:2000; Dako Cytomation).

5.4. Plasmid Isolation

We picked a single and isolated colony from the bacterial plate and grew in a 3ml liquid culture LB-ampicillin (1:1000, 100μg/ml) shaking at 30ºC. After 6-10h, all culture volume was added into an Erlenmeyer with LB-ampicillin shaking at 30ºC ON. Before plasmid isolation, we created a bacterial stock from the culture adding glycerol (1:1) and stored at -80ºC. Plasmids were isolated using the Plasmid midi kit (Qiagen, Hilden, Germany), following the manufacturer's instructions.

5.5. RNA Extraction

Total RNA was extracted from exosomes and cell lines using the miRNeasy mini kit (Qiagen, Hilden, Germany) following manufacturer's instructions. The synthetic sequence of mature miRNA cel-miR-39 (5μl; 1nM) (Applied Biosystems, Foster City, CA, USA) was added for exosomes purified from culture supernatant. RNA was extracted by homogenization in 700μl Qiazol lysis buffer. Finally, RNA was dissolved in 30-50μl RNase-free H_2O.

From FFPE tissue samples, total RNA was extracted using FFPE miRNeasy mini kit (Qiagen, Hilden, Germany) following manufacturer's instructions. RNA was dissolved in 20μl RNase-free H_2O.

Urine pellets were centrifuged at 5000xg for 30min at 4ºC to remove the RNALater, and homogenised in 700μl Trizol (Life Technologies/Thermo Fisher Scientific, Waltham, MA, USA). Total RNA was extracted using the QIAamp viral RNA mini kit (Qiagen, Hilden, Germany) following manufacturer's instructions. RNA was dissolved in 60μl RNase-free H_2O.

RNA from cell lines and tissue samples was quantified using the NanoDrop 1000 (Thermo Scientific, Waltham, MA, USA).

5.6. Retrotranscription (RT) and real-time Quantitative Polymerase Chain Reaction (qPCR)

MiRNA was reverse-transcribed using the TaqMan microRNA reverse transcription kit and miRNA-specific stem-looped primers (Applied Biosystems, Foster City, CA, USA). Furthermore, cDNA product from urinary exosomes and sediment was preamplified using the TaqMan preamp master mix 2X and TaqMan qPCR probes (Applied Biosystems) following manufacturer's instructions.

Amplification reactions were performed as specified by the manufacturer using TaqMan miRNA-specific primer-probe and TaqMan universal master mix II, with UNG and a 7900 real time PCR system (Applied Biosystems, Foster City, CA, USA). MiRNAs Ct values were obtained from SDS software v2.2.4 and expression suite software v1.0.1 from Applied Biosystems. Expression data were normalized to endogenous genes or geometric mean (geomean). Each reaction was performed in triplicates.

5.7. Low Density TaqMan miRNA Array

Multiplex RT-qPCR was performed using the TaqMan Array Human MicroRNA A+B Cards v3.0 and TaqMan Custom Array according the manufacturer's instructions. RNA was RT using the Megaplex RT Primers and the TaqMan microRNA reverse transcription kit, and cDNA pre-amplified with the Megaplex preamp primers according to the manufacturer's recommendations. qPCR was performed on the ABI 7900 machine. Expression was normalized to RNU6B-2 (U6), RNU44 (U44) and RNU48 (U48) provide as an endogenous control on the arrays, in addition to PSA mRNA and geomean. Cq values above 32 were indicative of no expression according to the manufacturer's recommendations.

6. TARGET PREDICTION AND PATHWAY ANALYSIS

Before starting functional assays, we conducted bioinformatics study to predict the target genes regulated by miRNAs, using different algorithms, including TargetScan, PicTar and followed by additional experimentally verified targets from miRTarbase. Functional pathway and network analyses were performed through the Ingenuity Pathway Analysis (v9.0, Ingenuity(R) Systems, USA).

7. STATISTICAL ANALYSIS

All qPCR experiments were conducted according to the MIQE guidelines. Each amplification reaction was performed in triplicate. For each gene has been adjusted its threshold. Data was presented as means ±SE and p-value ≤ 0,05 was considered statistically significant. The parametric Student's t-test and nonparametric Man-Whitney were used for comparing two groups (cancer vs. non-cancer). All the figures represent miRNA levels relative to an endogenous control, transformed into quantities using the formula $2^{-\Delta\Delta Ct}$.

The raw human MicroRNA Card array data was statistically analysed in the same way, although each sample was analysed only once. The same analysis has been performed with each of the endogenous genes included in the plate (U6, U44 and U48), and PSA. For discovery, the two plates (A and B) were analysed in the same study, for which the threshold of endogenous genes coincided.

Receiver operating characteristic (ROC) analysis by logistic regression was used to study the feasibility of using the particular miRNA profile to discriminate PC patients from healthy controls. The results were represented as the AUC with 95% of confidential interval.

Correlations analysis was conducted using Spearman's test for continuous variables, Wilcoxon, Kruskal–Wallis or Mann–Whitney's U-test for categorical variables.

All analyses were calculated using SPSS v20 (IBM, Inc.) statistical software. Statistical analysis of the cell culture data was performed by means of Student's t-test and nonparametric Man-Whitney test.

The construction of a diagnostic miRNA signature was statistically analysed by using R (The Core Team, v.3.1.2, Vienna, Austria) and Bioconductor packages. PSA expression levels were used to normalize the raw C_t measurements. Missing values were imputed by nearest neighbor averaging (k=10) using the impute package, while variables with more than 80% of missing values were removed.

A total of 80 models were compared; five different feature selection methods (t-test, Limma, Wilcoxon, Lasso and Random forest) combined with 4 classifiers (LDA, Random Forest (RF), Support Vector Machine (SVM) and Penalized logistic regression (PLR)) were built, by using 3, 5, 10 and 25 variables. The area under the curve (AUC) was the metric used to select the best model, although the accuracy, sensitivity, specificity were also monitored.

Nested cross-validation (1,000 iterations) was used to build and compare the models; an external 5-fold stratified cross-validation to estimate the parameters and an inner 4-fold stratified cross-validation to optimize each model, using the CMA package.

RESULTS

1. STANDARIZATION OF METHODS FOR ISOLATION AND QUANTIFICATION OF URINARY MIRNA

Since miRNA identification is a multi-step process that includes: sample collection, RNA purification, RNA quantification, quality control and RNA profiling, the first purpose was to describe some of the technical parameters that could be relevant to miRNA expression profiling in urine samples. Because the best technical approaches to isolate miRNAs were still unknown for urine samples, we compared different techniques to optimise the best conditions for the miRNAs detection by RT-qPCR in order to improve the validity and reliability of our results.

1.1. MiRNA from Prostate Cells

We extracted the total RNA (including miRNAs) from exfoliated cells in urine by several methods and the expression of one miRNA (hsa-miR-130b), described as suitable reference gene (RG) for miRNA expression analysis in PC (124), was analysed in a pool of samples. Furthermore, a synthetic RNA (spike-in) was used as positive control for Exiqon RT-qPCR. Two pellets were analysed for each extraction protocol to evaluate the method variability **(Table 10)**.

As results, we obtained that the best miRNA extraction method was the QIAamp Viral RNA kit, followed by the MiRNeasy Mini kit from Qiagen, both based on a silica-based column system. The spike-in control, added at the moment of the retrotranscription, was similar for each sample, thus cDNA synthesis and qPCR have been equally efficient for all samples.

Due to the small amount of starting material and that some methods that we used required a RNA-carrier addition, we assessed the quality of samples through the analysis of PSA expression from non-dilute cDNA by TaqMan RT-qPCR. Additionally, we compared the 3 RT-qPCR platforms available, based on Sybr Green or TaqMan technology, which differ in the RT and PCR reagents **(Table 11)** (125). RT and qPCR conditions were modified for urine sample.

Table 10. Comparison between different miRNA extraction methods.

Sybr Green	RNA extraction method	Pellet (Pool A and B)	Cp Mean ± SD	
			hsa-miR-130b	Spike-in
Exiqon	QIAamp Viral RNA kit (Qiagen)	1 (A)	38,4 ± 0,3	19,3 ± 0,03
		2 (A)	37,3 ± 0,2	19,3 ± 0,03
	Urine Total RNA Purification kit (Norgen)	3 (A)	Undet.	19,7 ± 0,04
		4 (A)	Undet.	19,5 ± 0,03
	ZR Urine RNA Isolation kit (Zymo)	5 (A)	Undet.	20,8 ± 0,10
		6 (A)	Undet.	19,6 ± 0,02
	Phenol: Clorophorm (Lab)	7 (A)	Undet.	22,8 ± 0,10
		8 (A)	Undet.	20,3 ± 0,01
Qiagen	QIAamp Viral RNA kit (Qiagen)	1 (B)	33,9 ± 1,0	
	MiRNeasy Mini kit (Qiagen)	2 (B)	35,3 ± 2,3	

RNA extraction methods were evaluated by RT-qPCR. MiRNA expression (Cp) is represented as mean ± SD. Grey cells indicate no values. The black line separates two independent tests. After the first test, MiRNeasy Mini kit was added to compare it with the best method above. Undet: undetermined.

Table 11. Comparison of the 3 RT-qPCR platforms.

Sample	Target	Cp//Ct Mean ± SD		
		Exiqon	Qiagen	TaqMan
1 (A)-QIAamp Viral RNA kit (Qiagen)	hsa-miR-130b	38,4 ± 0,30	34,8 ± 0,70	30,2 ± 0,50
	U6		30,5 ± 0,02	24,4 ± 0,20
	PSA			24,9 ± 0,30

The comparison of the 3 platforms is represented as expression levels Cp (Sybr Green) or Ct (TaqMan). Results are mean ± SD. Grey cells indicate no values.

As shown in **table 11**, TaqMan RT-qPCR was the most sensitive method for the detection of small RNA.

For the Sybr Green method, melting curve analysis indicated that there were at least no primer-dimers and non-specific products in this assay (data not shown).

PSA expression levels demonstrated the presence of exfoliated prostate cells in urine.

Finally, we analysed the need to add a pre-amplification step for miRNAs detection **(Fig.19)**. According to the TaqMan protocol, a RNA concentration <350ng requires an additional step of cDNA amplification before performing the qPCR.

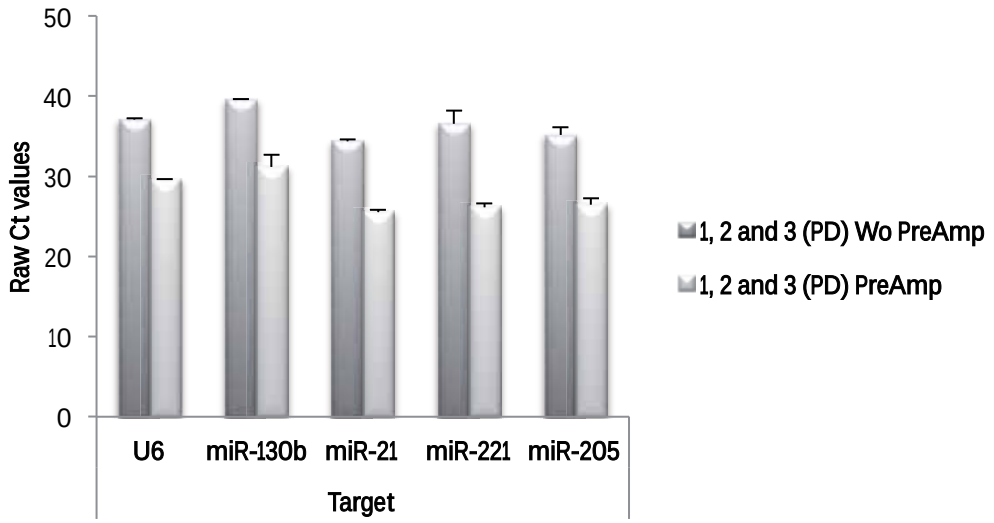

Figure 19. Plot of miRNA expression in pooled samples (PD) with and without (wo) pre-amplification. Results are mean ± SD. Gene expression is expressed as Ct values.

After carrying out an RT-qPCR for a set of miRNA and two described reference genes U6 and hsa-miR-130b, the results showed that the pre-amplification step was necessary for a more efficient qPCR, because it improved the detection of low-expressed miRNAs without, apparently, introducing a bias in their detection.

1.2. Cell-free MiRNA

Because it had not been described any protocol for the isolation of cell-free miRNAs from a urine samples, we decided to use the QIAamp Circulating Nucleic Acid kit from Qiagen following a protocol indicated for blood samples. This fraction also includes miRNAs of vesicles like exosomes. In this case, the concentration of RNA could not be measured because of the presence of the RNA carrier.

On the other hand, the exosomal fraction from urine samples was isolated by ultracentrifugation and total RNA was extracted using the best miRNA extraction methods for the pellet, QIAamp Viral RNA Mini kit and MiRNeasy Mini kit. With the last one, total RNA was quantified using 2 different methods, Nanodrop and Ribogreen, and its quality was assessed using Picochip **(Fig.20)**.

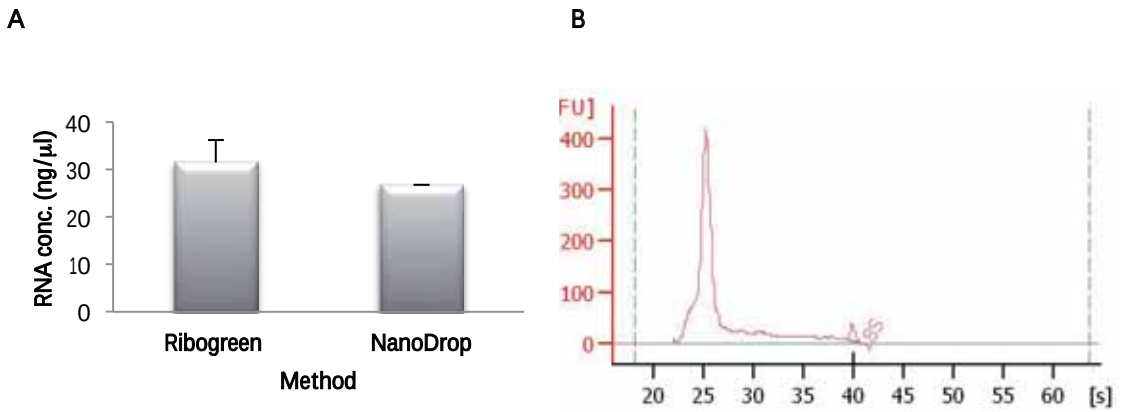

Figure 20. (A) RNA concentration measured by Ribogreen and Nanodrop methods. The quantification of RNA by Nanodrop gives us information about RNA purity (OD 260/280: 1,83, protein contamination; OD 260/230: 1,16, guanidine salts). **(B)** RNA quality was measured by Picochip. 18S and 28S ribosomal RNA were used as indicators of RNA integrity.

The results showed a low concentration of RNA. The values obtained with the Nanodrop were below 20ng/µl. However, Ribogreen dye, which measures RNA with greater sensitivity at low concentrations, was more reliable, but did not give us any information about RNA integrity or purity.

Because exosomes contain less ribosomal RNA than cells (61), and we did not get ribosomal RNA (28S and 18S) in the Picochip analysis, we could confirm that our samples were not contaminated with cellular content.

Furthermore, in order to assess the effectiveness of exosomal isolation by ultracentrifugation, we analysed the quality of samples from 2 pools, one including control patients and the other with PC patients, because it has been observed that MVs population could be affected by alterations in the prostate. NTA was performed to characterise the heterogeneity of vesicles population and exosomes purity was confirmed through the detection of several exosomal specific markers by WB **(Fig.21)**.

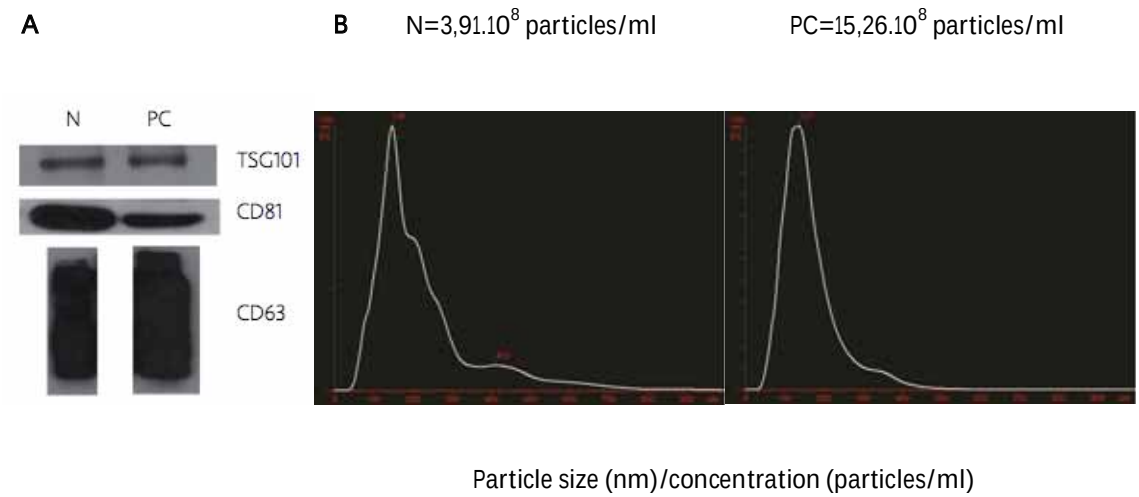

Figure 21. (A) Western blot of 3 exosomal markers. Membrane proteins: TSG101, CD81 and CD63. **(B)** Measurement by NTA. The histogram shows the overall size distribution and particle counts of the normal (left graph) and PC pool (right graph).

The general particle size correlated with the expected size for exosomes (≤150nm), and was similar between the two types of samples (normal pool 137nm and PC pool 148nm). We found that the number of particle/ml was larger in the case of the PC samples (15,26.10^8 particles/ml). Furthermore, for all exosomal protein markers we got a positive result, thus indicating that exosomes are a representative part of the total protein in the sample.

For the exosomes and extracellular fractions, the expression levels of hsa-miR-191-5p, described before in prostate tissue (101,126), and U6, U44 and U48, all of them usually used as housekeeping genes for prostate tissue and circulating miRNAs (127) were measured by TaqMan RT-qPCR. In addition, to demonstrate that these ncRNAs came from the prostate, we also analysed the expression of some prostate specific mRNAs **(Fig.22)**.

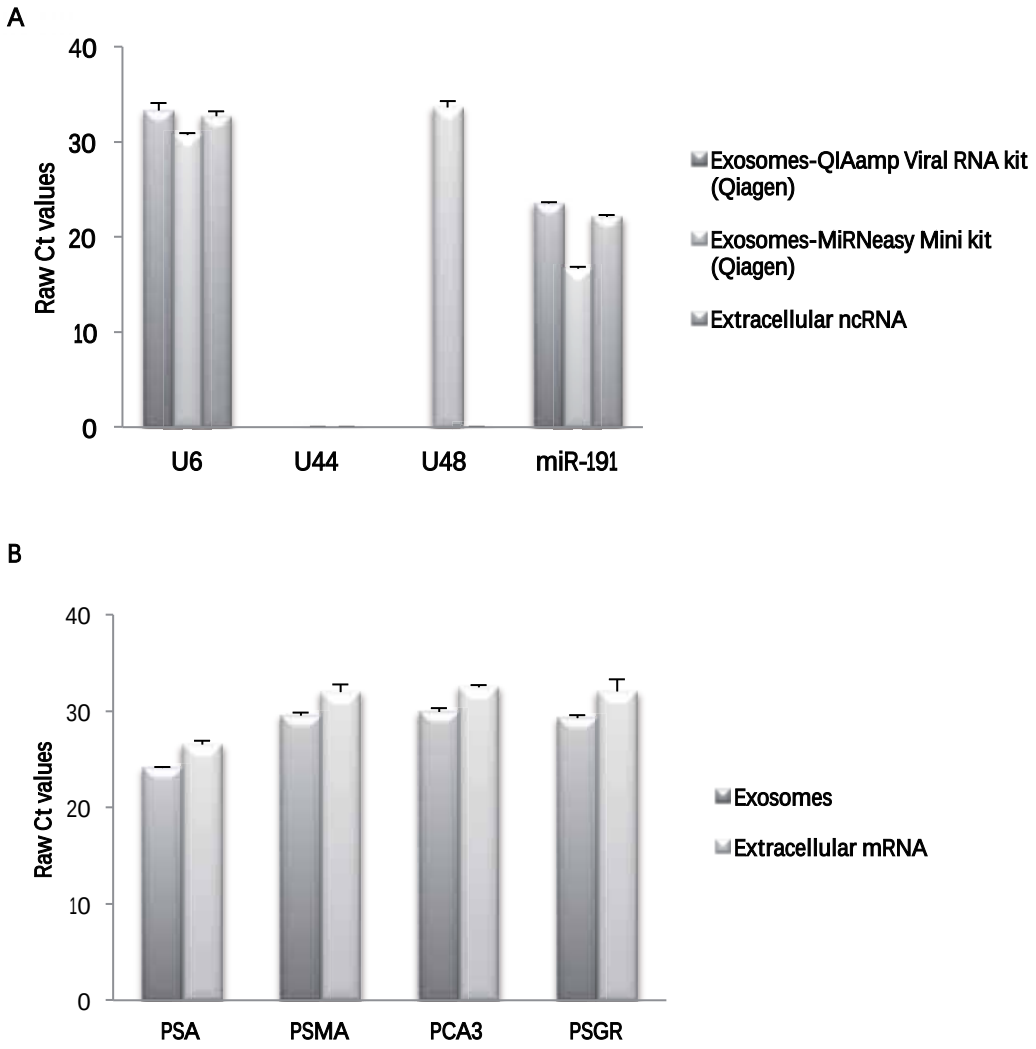

Figure 22. Cell-free RNA expression levels (A) Plot of ncRNAs expression for both fractions, comparison of 2 RNA extraction methods for exosomes (B) Plot of prostate specific mRNA expression. Exosomal RNA was extracted with the MiRNeasy Mini kit (Qiagen).

The results showed that the best miRNA extraction method for exosomes was the MiRNeasy Mini kit, by which we detected the U6, U48 and hsa-miR-191-5p. However, we only detected U6 and hsa-miR-191-5p with higher Ct values for the extracellular fraction, suggesting the necessity

to improve the extraction or detection method or indicating that these endogenous genes are not the most suitable genes to study circulating miRNAs.

All prostate specific mRNA were detectable in our MV-derived RNA material, thus indicating that exosomes derived from the prostate are a representative part of the total exosomes in the sample.

2. MIRNA AS URINARY DIAGNOSTIC BIOMARKERS FOR PROSTATE CANCER

2.1. Pilot Study

MiRNA has been emerged as crucial regulator of gene expression (128). In order to demonstrate that we were able to detect miRNAs deregulated in the urine sediment of PC patients compared to the controls (n=40), we analysed the expression of 20 miRNAs by RT-qPCR described as deregulated in PC in studies previously published until 2011 **(Table 12).**

2.1.1. Qualitative Data Analysis

First of all, a quality study of data was performed by using a software package named **Array Quality Metrics**. It generates an automatic quality report for the sample data and has different methods for the detection of outliers. Data were analysed from different points of view:

a) **Between sample comparisons.** Spatial arrangement of points and the colour pattern of the plots A and B respectively indicated any clustering of the samples either because of biological or unintended experimental factors (batch effects) **(Fig.23A).** Plot of distance between samples showed patients 6, 8, 15 and 33 as outliers **(Fig.23B).**

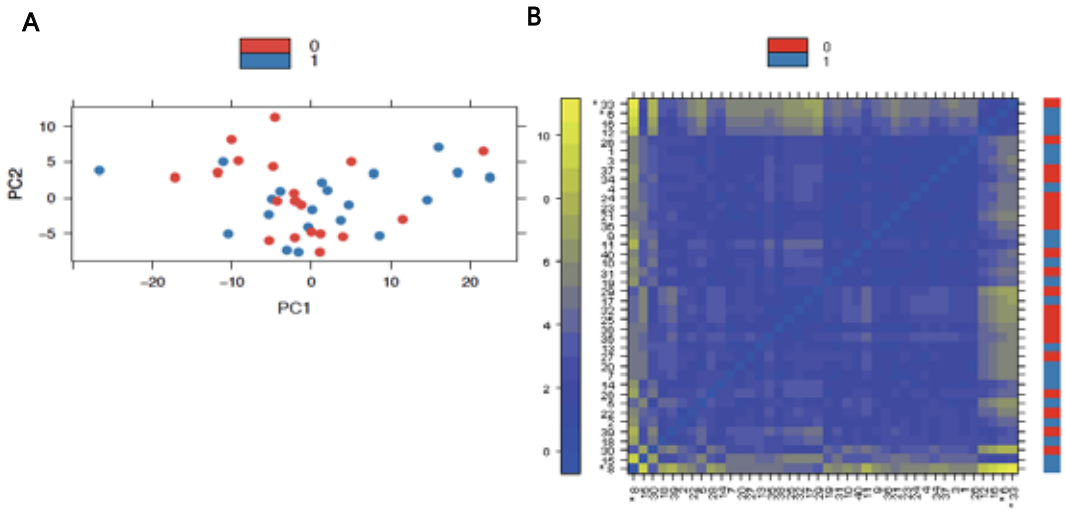

Figure 23. (A) Principal component analysis (PCA). **(B)** Distance between samples.

b) Sample intensity distributions. Plots indicated samples distribution; differences between them may indicate an experimental problem **(Fig.24)**. Because the boxplot of patient 8 was significantly different from the others, it was consider an outlier **(Fig.24A)**.

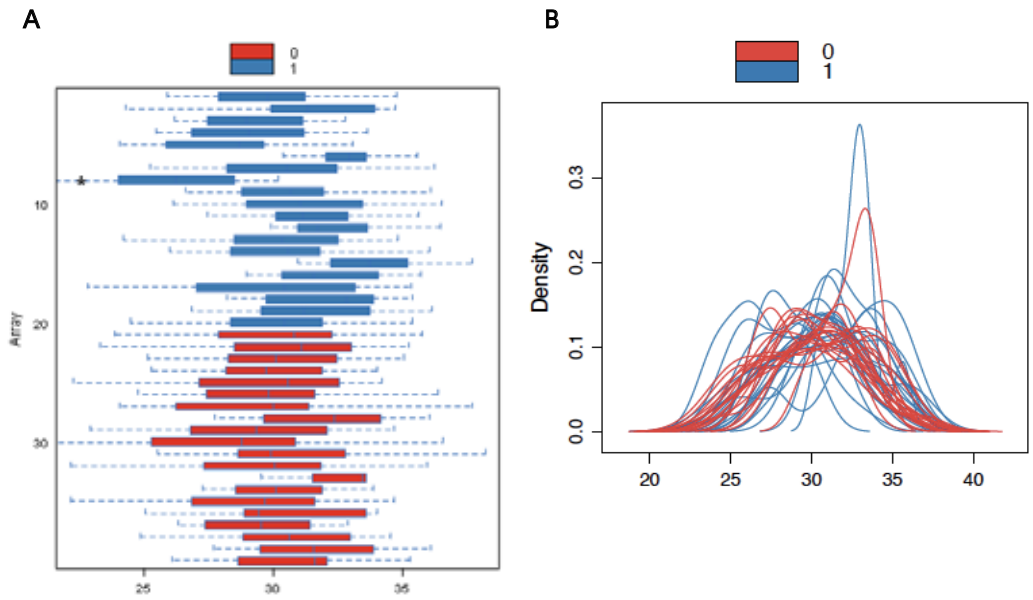

Figure 24. (A) Boxplot. Each box corresponds to one patient. **(B)** Density plots.

c) **Individual array quality**. The outlier detection criterion based on Hoeffding's statistic D_a also indicated that the patient 8 must be classified as an outlier, because it exceeded the threshold of 0,5, which is indicated by the vertical line **(Fig.25)**.

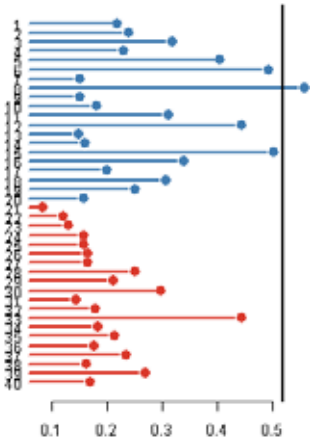

Figure 25. Outlier detection for MA plots.

Taking into account the results shown above, patient 8 was the most significantly outlier, therefore we excluded him from the further analysis.

Table 12: Related PC miRNAs selected from literature for the pilot study.

miRNA name	Chr	Str	Cluster	Family	Mature sequence	Samples	Expression (C vs. PC)	Related functions	References
hsa-let-7c	21	+	hsa-miR-99a	let-7c	UGAGGUAGUAGGUUGUAUGGUU	Tissue	Up/Down	Unknown	(129–131)
hsa-miR-100	11	-	hsa-let-7a-2	miR-10	AACCCGUAGAUCCGAACUUGUG	Tissue	Down	Unknown	(100,129)
hsa-miR-101	1	-	hsa-miR-3671	miR-101	UACAGUACUGUGAUAACUGAA	Cells and tissue	Up/Down	Proliferation, invasion and growth	(131–134)
hsa-miR-135b	1	-	None	miR-135	UAUGGCUUUUCAUUCCUAUGU	Tissue	Up	Unknown	(100)
hsa-miR-141	12	+	hsa-miR-200c	miR-8	UAACACUGUCUGGUAAAGAUGG	Cells, tissue and serum	Up/Down	Proliferation	(100,133,135–139)
hsa-miR-143	5	+	hsa-miR-145	miR-143	UGAGAUGAAGCACUGUAGCUC	Cells and tissue	Down	Proliferation, apoptosis, migration and invasion	(100,129,131,140–143)
hsa-miR-145	5	+	hsa-miR-143	miR-145	GUCCAGUUUUCCCAGGAAUCCCU	Cells and tissue	Down	Proliferation, apoptosis, cell cycle, migration and invasion	(98,100,129–131,141,142,144–148)
hsa-miR-146a	5	+	None	miR-146	UGAGAACUGAAUUCCAUGGGUU	Cells and tissue	Down	Proliferation, migration and invasion	(149)

hsa-miR-191	3	-	hsa-miR-425	miR-191	CAACGGAAUCCCAAAAGCAGCUG	Tissue	Up	Unknown	(101)
hsa-miR-194	1	-	hsa-miR-215	miR-194	UGUAACAGCAACUCCAUGUGGA	Tissue	Up/Down	Unknown	(98)
hsa-miR-200b	1	+	hsa-miR-200a and -429	miR-8	UAAUACUGCCUGGUAAUGAUGA	Cells	Down	Migration, invasion and adhesion	(150)
hsa-miR-205	1	+	None	miR-205	UCCUUCAUUCCACCGGAGUCUG	Cells and tissue	Down	Apoptosis, migration, invasion, growth, clonability and viability	(98,100,145,151,152)
hsa-miR-21	17	+	None	miR-21	UAGCUUAUCAGACUGAUGUUGA	Cells, tissue (human/xeno-graft) and serum	Up	Proliferation, apoptosis, migration, invasion and angiogenesis	(101,129,131,133,135,153–158)
hsa-miR-210	11	-	None	miR-210	CUGUGCGUGUGACAGCGGCUGA	Tissue	Up	Unknown	(129)
hsa-miR-218	4	+	None	miR-218	UUGUGCUUGAUCUAACCAUGU	Tissue	Up/Down	Unknown	(98,101,131)
hsa-miR-221	X	-	hsa-miR-222	miR-221	AGCUACAUUGUCUGCUGGGUUUC	Cells, tissue (human/xeno-graft) and serum	Up/Down	Proliferation, growth and clonability	(98,100,101,131,135,145,157,159–163)
hsa-miR-26a	3	+	None	miR-26	UUCAAGUAAUCCAGGAUAGGCU	Cells, tissue and serum	Up/Down	Unknown	(98,129,132,164,165)
hsa-miR-32	9	-	None	miR-32	UAUUGCACAUUACUAAGUUGCA	Tissue	Up	Unknown	(98,101)

hsa-miR-34c	11	+	hsa-miR-34b	miR-34	AGGCAGUGUAGUUAGCUGAUUGC	Cells and tissue	Down	Proliferation, apoptosis, migration, invasion and growth	(133,166–168)
hsa-miR-96	7	-	hsa-miR-183 and -182	miR-96	UUUGGCACUAGCACAUUUUUGCU	Tissue	Up	Unknown	(145)

Selected miRNA name, chr, str, cluster, family and mature sequence were adapted from miRbase database, while miRNA related references from PubMed (until 2011). References described miRNAs deregulated in PC compared to the control from different human or xenograft samples, and/or determined their related functions. Chr: chromosome; str: strand.

2.1.2. Candidate Reference Genes

Based on the literature, we chose 3 RGs to normalise the 20 miRNAs: hsa-miR-130b, U6 and PSA (124,169).

Because a suitable RG should be well detected and especially, remain stable among all samples, we measured their expression levels in 40 patients by RT-qPCR and analyse their stability using the coefficient of variation (CV).

Table 13. Details of candidates RGs.

Gene name	Average Ct	SD	CV (%)	P-value (Benign vs. PC)	PC Gleason score	
					r_s	P-value
hsa-miR-130b	32,97	2,70	8	0,85	0,11	0,64
U6	29,99	1,99	7	0,52	0,40	0,08
PSA	29,58	2,51	8	0,98	-0,01	0,95

The expression of candidate RGs is represented as the average of expression levels (Ct). CV (%) was calculated from the average Ct and SD. P-value obtained by t-test compared both groups, benign and PC. Spearman's correlation was used to correlate gene expression with PC Gleason score, divided in 3 groups (<7, =7 and >7). CV: coefficient of variation; SD: standard deviation; r_s: Spearman rank-order coefficient.

As shown in **table 13**, U6 was the most stable gene, and together with PSA were more highly expressed than hsa-miR-130b. Furthermore, 7 of 40 patients did not express hsa-miR-130b; therefore we excluded it as candidate RG.

In any case there were significant differences between groups or correlation with Gleason score, indicating a stable expression in PC samples.

On the other hand, PSA and U6 expression pattern did not correlate (Pearson's correlation; p-value: 0,99; r: -0,002) **(Fig.26)**. For this reason, we did not expect to find similar results after normalising with both genes. However, because we still did not know what was the best way to analyse miRNA data, we considered equally interesting miRNAs obtained significantly deregulated from both normalizations.

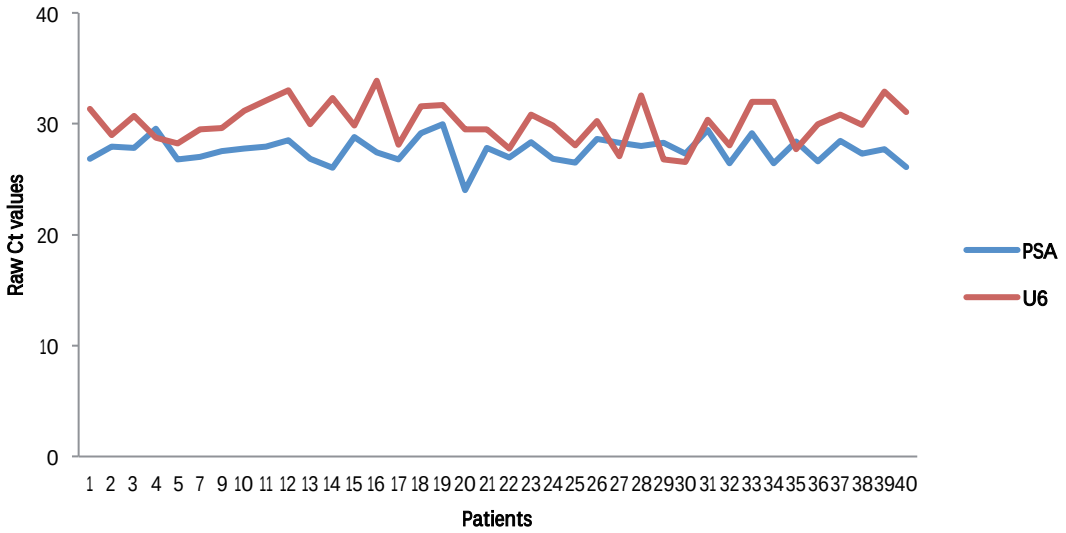

Figure 26. The variation of the RG expression is represented as Ct values obtained of each urine sample included in the study.

2.1.3. Deregulated MiRNAs Detection in Prostate Cancer

The expression levels of 20 previously described miRNAs were analysed by RT-qPCR in urine samples from 20 PC patients and 20 benign controls. The results obtained showed 6 miRNAs significantly deregulated in PC patients compared to controls (p-value<0,05). MiR-26a, miR-145, miR-191 and miR-210 were found under-expressed while miR-100 and -194 were over-expressed in PC samples **(Table 14)**.

Furthermore, in order to elucidate the putative diagnostic properties of the most promising miRNAs (p-value<0,05 and detected in at least 50% of samples for both groups), receiver-operating characteristic (ROC) curves (plot of sensitivity vs. 1-specificity) were calculated.

As it can be observed in **table 15**, although selected miRNAs showed acceptable AUC values of 0,6-0,7, only in the case of under-expressed miRNAs normalised by PSA presented interesting specificity and sensitivity values.

Table 14. MiRNAs differentially expressed in PC compared to benign control urine samples.

miRNA	PC (n)	Benign (n)	P-value (RG=PSA)	Fold change	P-value (RG=U6)	Fold change
hsa-miR-100	**20**	**19**	**0,630**	**1,0**	**0,057***	**1,0**
hsa-miR-101	6	11	0,692	1,4	0,922	1,3
hsa-miR-130b	16	17	0,865	2,0	0,540	1,3
hsa-miR-135b	16	18	0,772	1,0	0,361	1,1
hsa-miR-141	20	19	0,457	1,4	0,254	1,2
hsa-miR-143	8	13	0,285	1,1	0,434	1,1
hsa-miR-145	**17**	**19**	**0,04***	**3,0**	**0,184**	**1,2**
hsa-miR-146a	19	20	0,306	1,0	0,736	1,2
hsa-miR-191	**20**	**19**	**0,025***	**2,1**	**0,339**	**1,2**
hsa-miR-194	**18**	**18**	**0,843**	**1,6**	**0,044***	**1,1**
hsa-miR-200b	20	20	0,339	1,4	0,574	1,3
hsa-miR-205	15	18	0,425	1,4	1,000	1,3
hsa-miR-21	20	20	0,273	1,2	0,286	1,2
hsa-miR-210	**20**	**19**	**0,034***	**2,7**	**0,350**	**1,0**
hsa-miR-218	20	20	0,299	1,6	0,866	1,1
hsa-miR-221	19	19	0,378	1,4	0,564	1,0
hsa-miR-26a	**20**	**20**	**0,038***	**2,1**	**0,866**	**1,2**
hsa-miR-32	2	6	0,134	-	0,505	-
hsa-miR-34c	3	2	0,248	1,7	0,564	1,0
hsa-miR-96	7	3	0,606	1,3	0,909	2,2
hsa- let-7c	20	20	0,415	1,3	0,448	1,1
U6	19	20	0,24	1,2	-	-

Expression levels of miRNAs are represented as fold change of PC patients vs. benign controls. Values that are significantly different by Mann-Whitney are indicated by *p-value< 0,05. Fold changes were corrected by 3SD as measure of variability.

Table 15. Performance of urinary miRNAs to discriminate PC from benign patients.

	MiRNA	AUC	95% CI of AUC	Sensitivity (%)	Specificity (%)
Over-expressed (U6)					
1	**hsa-miR-100**	0,67	0,50-0,84	94	5
2	**hsa-miR-194**	0,67	0,49-0,84	94	0
Under-expressed (PSA)					
1	**hsa-miR-145**	0,67	0,50-0,85	94	30
2	**hsa-miR-26a**	0,68	0,50-0,85	94	40
3	**hsa-miR-191**	0,69	0,53-0,86	94	35
4	**hsa-miR-210**	0,69	0,52-0,86	94	30

AUC: Area under curve; CI: coefficient interval.

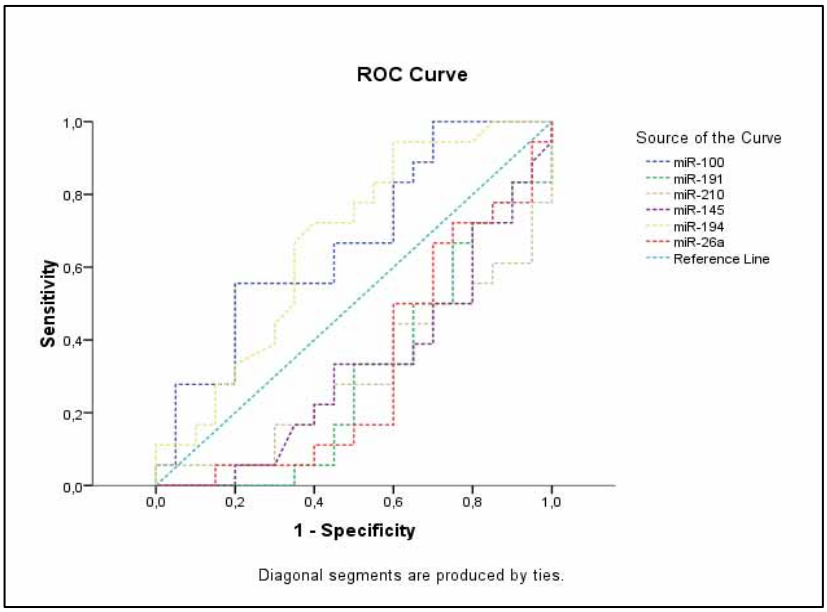

Figure 27. ROC curve to discriminate PC patients from those with non-malignant prostate alterations. ROC analysis was performed from the expression of all selected miRNAs.

2.2. MiRNA High Throughput Profiling in Prostate Cancer

Once confirmed that we were able to detect changes in miRNA levels between PC and benign patients, we decided to perform a further study in which more than 700 miRNAs were analysed using the TaqMan microfluidic Cards in the same cohort of patients as the pilot study (discovery phase). Subsequently, we selected the most significant miRNAs to validate them in a new larger cohort of patients (validation phase) to explore their potential use as diagnostic biomarkers for PC detection.

2.2.1. Discovery Phase

2.2.1.1. Candidate Reference Genes

Based on the miRNA array profiling data and our previous results (pilot study), we chose to analyse the stability of 3 small RNAs (U6, U44, U48), PSA and the geometric mean (geomean) in order to select the best option to be used as RG.

Since U6, U44 and U48 have been the most used RGs to analyse miRNA data, they are included in microfluidic cards (A and B) by the company, however, we used the same data obtained from the pilot study for PSA.

As shown in **table 16**, both geomean and U44 presented significantly different expression between groups (card A); therefore we excluded them for further analysis. However, PSA was more stable than snoRNAs, whose expression showed a large intragroup variability. In any case there were significant differences between groups or correlation with Gleason score, indicating a stable expression in PC samples.

On the other hand, U6 and U48 pattern expression had a good correlation between cards (Pearson's correlation; U6 p-value: <0,01, r: 0,84; U48 p-value: <0,01, r: 0,97) **(Fig.28)**.

PSA only correlated with U6 (card B) (Pearson's correlation; p-value: 0,032, r: 0,34), but the correlation coefficient was very low.

Table 16. Characteristics of candidate reference genes.

Candidates RGs CARD A	Average Ct value	SD	CV (%)	P-value (Benign vs. PC)	Gleason score r_s	 P-value
U6	14,8	2,9	19,3	0,30	-0,03	0,91
U44	**18,3**	**3,1**	**17,0**	**0,02***	**-0,29**	**0,21**
U48	18,9	2,5	13,4	0,08	-0,01	0,95
Geomean	**28,8**	**0,1**	**3,5**	**0,05***	-0,02	**0,95**
CARD B						
U6	16,3	2,8	17,2	0,10	0,06	0,81
U44	20,2	2,6	12,8	0,20	0,23	0,33
U48	19,6	2,5	12,5	0,07	0,12	0,63
Geomean	30,4	0,6	1,9	0,80	0,03	0,91
PSA	29,6	2,5	8,0	0,98	-0,01	0,95

The expression of candidate RGs is represented as the average of expression levels (Ct). CV (%) was calculated from the average Ct and SD. Values that are significantly different between benign and PC by t-test are indicated by *p-value< 0,05. Spearman's correlation was used to correlate gene expression with PC Gleason score, divided in 3 groups (<7, =7 and >7). CV: coefficient of variation; SD: standard deviation; r_s: Spearman rank-order coefficient.

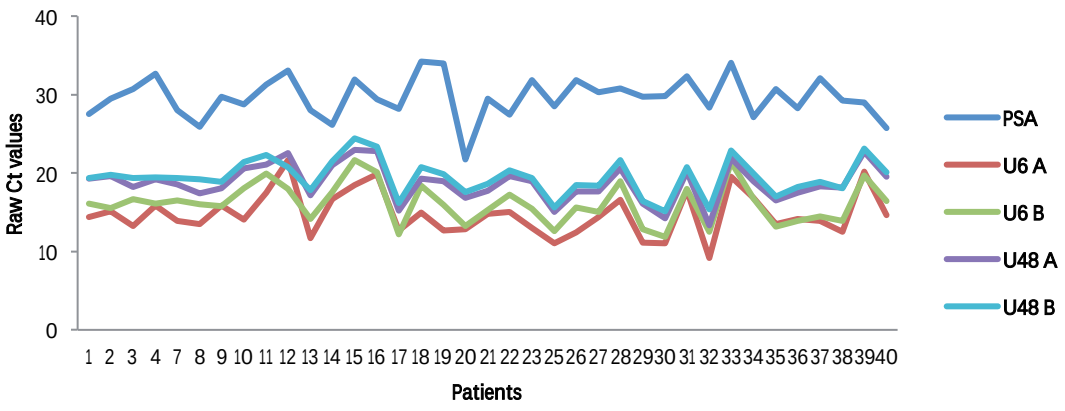

Figure 28. Analysis of RG expression levels variability in urine samples of PC and control patients.

2.2.1.2. Deregulated MiRNAs in Prostate Cancer

Taking together PSA, U6 and U48 normalization results, we obtained 113 significantly deregulated miRNAs **(Table 17, 18 and 19)**. Most of them came from PSA normalization method (80%), and approximately 7% of them were common for other two normalisations genes. Since U6 and U48 presented a high correlation, as we seen above, most of their significant miRNAs were the same, 58% and 48%, respectively. Only miR-223 and miR-520a were significantly deregulated by 3 RGs **(Fig.29)**.

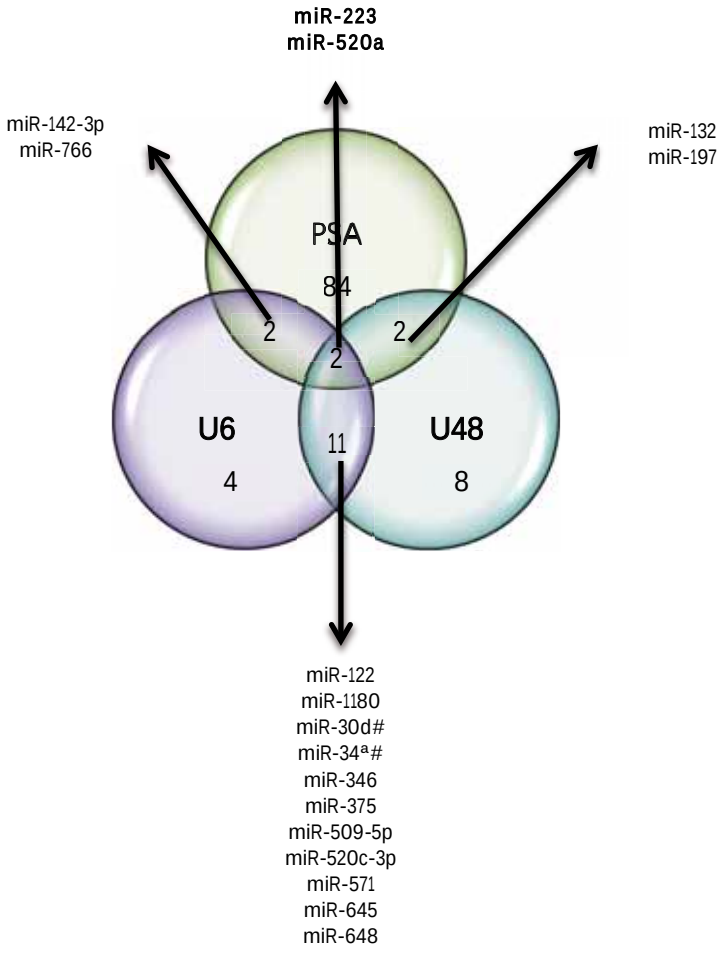

Figure 29. Venn diagram illustrating the overlapping significant miRNAs (indicated with arrows) from the 3 RGs normalization: PSA (green), U6 (purple) and U48 (blue).

Table 17. Significantly deregulated miRNAs after PSA normalization.

miRNA	PC (n)	Benign (n)	P-value (PSA)	AUC	Expression
hsa-let-7d	20	20	0,014	0,728	Down
hsa-let-7e	20	20	0,045	0,685	Down
hsa-let-7f	18	19	0,033	0,705	Down
hsa-let-7g	20	20	0,002	0,780	Down
hsa-miR-103	17	19	0,014	0,740	Down
hsa-miR-106a	20	20	0,006	0,753	Down
hsa-miR-106b	18	20	0,019	0,722	Down
hsa-miR-1201	18	19	0,029	0,711	Down
hsa-miR-1233	20	20	0,03	0,700	Up
hsa-miR-1248	15	13	0,032	0,739	Up
hsa-miR-125a-3p	15	16	0,033	0,725	Down
hsa-miR-1260	20	20	0,025	0,708	Down
hsa-miR-1267	15	17	0,043	0,710	Down
hsa-miR-1290	20	20	0,028	0,703	Down
hsa-miR-1291	18	20	0,035	0,700	Down
hsa-miR-130b	9	16	0,008	0,826	Down
hsa-miR-132	16	19	0,022	0,727	Down
hsa-miR-133a	19	17	0,001	0,811	Down
hsa-miR-140-3p	15	17	0,047	0,706	Down
hsa-miR-142-3p	20	20	0,005	0,758	Down
hsa-miR-145	19	20	0,008	0,750	Down
hsa-miR-146b	20	20	0,023	0,710	Down
hsa-miR-147b	17	20	0,01	0,750	Down
hsa-miR-148a	19	18	0,013	0,740	Down
hsa-miR-149#	19	20	0,018	0,721	Up

hsa-miR-15b	17	20	0,016	0,732	Down
hsa-miR-16	20	20	0,006	0,755	Down
hsa-miR-17	20	20	0,015	0,725	Down
hsa-miR-181a	19	20	0,01	0,742	Down
hsa-miR-186	18	19	0,031	0,708	Down
hsa-miR-191	20	20	0,002	0,785	Down
hsa-miR-193a-5p	19	20	0,015	0,729	Down
hsa-miR-195	19	20	0,015	0,729	Down
hsa-miR-197	20	20	0,002	0,780	Down
hsa-miR-19b	20	20	0,017	0,720	Down
hsa-miR-20a	20	19	0,015	0,729	Down
hsa-miR-21	20	20	0,03	0,700	Down
hsa-miR-210	19	20	0,012	0,734	Down
hsa-miR-212	18	20	0,028	0,708	Down
hsa-miR-214	19	18	0,009	0,752	Down
hsa-miR-222	20	20	0,009	0,743	Down
hsa-miR-223	20	20	0,002	0,783	Down
hsa-miR-223#	15	18	0,007	0,774	Down
hsa-miR-24	20	20	0,008	0,745	Down
hsa-miR-25	17	19	0,015	0,737	Down
hsa-miR-26a	20	20	0,003	0,770	Down
hsa-miR-26b	20	20	0,003	0,778	Down
hsa-miR-27a	16	20	0,026	0,719	Down
hsa-miR-28	17	20	0,019	0,727	Down
hsa-miR-28-3p	20	20	0,014	0,728	Down
hsa-miR-30b	20	20	0,012	0,733	Down
hsa-miR-30c	20	20	0,025	0,708	Down

hsa-miR-320	20	20	0,017	0,720	Down
hsa-miR-324-3p	17	19	0,041	0,700	Down
hsa-miR-324-5p	18	19	0,013	0,740	Down
hsa-miR-328	19	20	0,013	0,732	Down
hsa-miR-342-3p	20	20	0,007	0,750	Down
hsa-miR-345	19	20	0,012	0,734	Down
hsa-miR-34a	19	19	0,032	0,704	Down
hsa-miR-370	13	19	0,048	0,709	Down
hsa-miR-374	19	20	0,009	0,745	Down
hsa-miR-422a	17	20	0,038	0,700	Down
hsa-miR-425-5p	20	20	0,02	0,715	Down
hsa-miR-454	20	20	0,007	0,748	Down
hsa-miR-484	20	20	0,007	0,750	Down
hsa-miR-490	20	20	0,004	0,768	Down
hsa-miR-505#	15	17	0,015	0,753	Down
hsa-miR-516-3p	18	20	0,031	0,706	Down
hsa-miR-520a	19	20	0,003	0,776	Down
hsa-miR-520a#	18	19	0,021	0,722	Down
hsa-miR-526b	20	20	0,011	0,735	Down
hsa-miR-548b-5p	13	18	0,031	0,731	Down
hsa-miR-551b#	15	18	0,021	0,737	Down
hsa-miR-574-3p	20	20	0,023	0,710	Down
hsa-miR-590-5p	10	19	0,017	0,774	Down
hsa-miR-601	16	16	0,009	0,770	Down
hsa-miR-628-3p	16	16	0,029	0,727	Down
hsa-miR-652	16	20	0,03	0,713	Down
hsa-miR-659	20	20	0,021	0,713	Up

hsa-miR-720	20	20	0,02	0,715	Down
hsa-miR-744#	16	15	0,013	0,763	Down
hsa-miR-766	19	20	0,001	0,800	Down
hsa-miR-92a	20	20	0,007	0,750	Down
hsa-miR-939	19	20	0,033	0,700	Down
hsa-miR-99a	19	20	0,012	0,734	Down
mmu-miR-140	19	20	0,003	0,774	Down
mmu-miR-374-5p	20	20	0,007	0,750	Down
mmu-miR-491	16	20	0,001	0,822	Down
mmu-miR-93	19	20	0,018	0,721	Down
rno-miR-7#	18	19	0,009	0,752	Down

Table 18. Significantly deregulated miRNAs after U6 normalization.

miRNA	PC (n)	Benign (n)	P-value (U6)	AUC	Expression
hsa-miR-1180	16	19	0,028	0,719	Up
hsa-miR-122	18	20	0,008	0,751	Up
hsa-miR-142-3p	20	20	0,023	0,710	Up
hsa-miR-183	14	14	0,024	0,250	Up
hsa-miR-198	16	19	0,037	0,293	Up
hsa-miR-216b	16	17	0,034	0,717	Down
hsa-miR-223	20	20	0,009	0,740	Up
hsa-miR-30d#	20	19	0,02	0,717	Up
hsa-miR-346	19	18	0,039	0,301	Up
hsa-miR-34a#	15	17	0,01	0,767	Up
hsa-miR-375	20	20	0,035	0,305	Down
hsa-miR-509-5p	16	15	0,009	0,225	Up

hsa-miR-520a	19	20	0,015	0,729	Down
hsa-miR-520c-3p	20	20	0,006	0,756	Up
hsa-miR-571	20	19	0,022	0,715	Up
hsa-miR-645	18	20	0,027	0,710	Down
hsa-miR-648	15	18	0,034	0,717	Up
hsa-miR-766	19	20	0,032	0,299	Up
mmu-miR-615	16	10	0,051	0,269	Up

Table 19. Significantly deregulated miRNAs after U48 normalization.

miRNA	PC (n)	Benign (n)	P-value (U48)	AUC	Expression
hsa-miR-1180	16	19	0,021	0,729	Up
hsa-miR-1208	20	20	0,024	0,709	Up
hsa-miR-122	18	20	0,006	0,763	Up
hsa-miR-1247	20	19	0,029	0,704	Up
hsa-miR-1275	20	20	0,014	0,726	Up
hsa-miR-1300	18	17	0,041	0,703	Up
hsa-miR-132	16	19	0,037	0,293	Up
hsa-miR-197	20	20	0,021	0,288	Up
hsa-miR-223	20	20	0,007	0,250	Up
hsa-miR-30d#	20	19	0,029	0,704	Up
hsa-miR-346	19	18	0,016	0,731	Up
hsa-miR-34a#	15	17	0,008	0,775	Up
hsa-miR-362	9	17	0,033	0,758	Up
hsa-miR-375	20	20	0,019	0,718	Up
hsa-miR-494	20	18	0,016	0,729	Up
hsa-miR-509-5p	16	15	0,011	0,767	Up

hsa-miR-520a	19	20	0,026	0,292	Down
hsa-miR-520c-3p	20	20	0,002	0,791	Up
hsa-miR-571	20	19	0,018	0,722	Up
hsa-miR-645	18	20	0,016	0,729	Up
hsa-miR-648	15	18	0,02	0,739	Up
hsa-miR-660	18	20	0,035	0,700	Up
hsa-miR-886-3p	20	20	0,023	0,710	Up

Discrimination between groups is represented as AUC of PC patients vs. benign controls. The expression of miRNAs, up or down, is relative to control. Values that are significantly different by Mann-Whitney are indicated by p-value.

2.2.2. Validation Phase

Due to the promising results obtained in the discovery phase, 48 miRNAs were selected to be validated in a new cohort of patients (n=154) by the same methodology used in the discovery. Because PSA was the most stable candidate, it correlated with snoRNAs, and furthermore, it came from exclusively prostate cells, we selected those miRNAs differentially expressed in PC patients after normalising data with PSA as RG.

2.2.2.1. Candidate Reference Genes

Before normalizing data, we analysed candidate RGs to confirm that they kept stable. As shown on **table 20**, PSA remained the most stable gene. In any case there were significant differences between groups or correlation with Gleason score, indicating a stable expression in PC samples.

On the other hand, PSA continued correlating with U6 (Pearson's correlation; p-value: 0,005, r: 0,23), and also with U48 (Pearson's correlation; p-value: 0,019, r: 0,19). However, U6 and U48 correlated each other with a higher correlation coefficient than other genes (Pearson's correlation; p-value <0,001, r: 0,72).

Table 20. Details of candidate RGs.

Candidates RGs	Average Ct values	SD	CV (%)	P-value (Benign vs. PC)	Gleason score	
					r_s	P-value
U6	18,3	2,5	13,8	0,06	-0,16	0,22
U48	20,8	2,5	12	0,34	-0,14	0,28
PSA	25,8	2,4	9,5	0,18	-0,24	0,06

The expression of candidate RGs is represented as the average of expression levels (Ct). CV (%) was calculated from the average Ct and SD. Values that are significantly different between benign and PC by t-test (U6 and U48) or by Mann-Whitney (PSA) are indicated by *p-value< 0,05. Spearman's correlation was used to correlate gene expression with PC Gleason score, divided in 3 groups (<7, =7 and >7). CV: coefficient of variation; SD: standard deviation; r_s: Spearman rank-order coefficient.

2.2.2.2. MiRNAs as Diagnostic Markers for Prostate Cancer Detection

The expression levels of 48 miRNAs candidates were analysed by RT-qPCR using Custom microfluidic Cards (Life Technologies) in benign controls and PC patients. A total of 33 significantly deregulated miRNAs were obtained, most of them under-expressed in PC (73%) **(Table 21)**.

Although all p-values are interesting, to search a new biomarker it is important take into account its specificity and sensibility (AUC value) and, furthermore, it should be detected in all the patients. Therefore, as shown in **table 21**, hsa-miR-147b, hsa-miR-28, hsa-miR-548-5p and hsa-miR-648 were the most promising candidates as biomarkers because they could be found in most of the patients (≥80%) and their AUC value was about ≥ 0,65.

Table 21. Significantly deregulated miRNAs by PSA normalization.

miRNA	PC (n=62)	Benign (n=92)	P-value	AUC	Expression
hsa-let-7g	62	92	**0,039***	0,59	Down
hsa-miR-1291	57	86	**0,021***	0,61	Down
hsa-miR-130b	51	82	**0,038***	0,59	Down
hsa-miR-132	56	84	**0,029***	0,6	Down
hsa-miR-142-3p	61	91	**0,008****	0,61	Down
hsa-miR-145	62	91	**0,050***	0,58	Up
hsa-miR-147b	60	89	**0,013***	0,65	Down
hsa-miR-193a-5p	62	92	**0,002****	0,64	Down
hsa-miR-197	60	90	**0,018***	0,61	Down
hsa-miR-222	62	92	**0,024***	0,6	Up
hsa-miR-223	50	77	**0,048***	0,59	Down
hsa-miR-223#	62	92	**0,017***	0,6	Down
hsa-miR-24	62	91	**0,037***	0,59	Up
hsa-miR-26a	50	70	**0,026***	0,6	Down
hsa-miR-26b	62	92	**0,041***	0,59	Down
hsa-miR-27a	62	92	**0,023***	0,61	Down
hsa-miR-28	60	92	**0,003****	0,65	Down
hsa-miR-28-3p	59	92	**0,010****	0,61	Down
hsa-miR-324-5p	22	33	**0,013***	0,61	Down
hsa-miR-328	47	78	**0,002****	0,63	Down
hsa-miR-342-3p	62	91	**0,028***	0,6	Down
hsa-miR-345	62	92	**0,001*****	0,62	Down
hsa-miR-362	61	84	**0,030***	0,57	Down
hsa-miR-375	47	84	**0,010****	0,62	Down

hsa-miR-454	60	91	**0,018***	0,6	Up
hsa-miR-484	61	91	**0,009****	0,62	Up
hsa-miR-520a	62	92	**0,029***	0,59	Up
hsa-miR-548b-5p	43	62	**0,008****	0,66	Up
hsa-miR-648	57	88	**0,000*****	0,77	Up
hsa-miR-766	56	85	**0,028***	0,6	Down
mmu-miR-140	53	83	**0,013***	0,61	Down
mmu-miR-491	62	92	**0,003****	0,62	Up
mmu-miR-93	60	86	**0,039***	0,59	Down

Expression levels of miRNAs. Discrimination between groups is represented as AUC of PC patients vs. benign controls. The expression of miRNAs, up or down, is relative to control. Values that are significantly different by Mann-Whitney are indicated by *p-value< 0,05, **p-value< 0,01 and ***p-value< 0,001. AUC: area under the curve.

2.2.2.3. Validation of MiRNAs Candidates in FFPE Tissue Samples

After obtaining a list of differentially expressed miRNAs in urine, we wanted to verify whether these changes actually came from prostate tissue alterations. To carry out this analysis the four most promising miRNAs of the validation phase, based on their p-value and AUC value, were selected (hsa-miR-147b, hsa-miR-28, hsa-miR-548-5p and hsa-miR-648).

Firstly, we optimized the miRNA detection method in FFPE comparing 2 RNA extraction kits. In order to analyse the results, we performed an RT-qPCR of hsa-miR-130b in 2 PC patients (A and B). In addition, spike-in control was used for Exiqon RT-qPCR **(Table 22)**.

Table 22. Comparison of different miRNA extraction methods.

RNA extraction method	Patient	RNA amount (ng/µl)	OD 260/280	Cp Mean ± SD (Exiqon)	
				hsa-miR-130b	Spike-in
MiRNeasy FFPE kit (Qiagen)	**A**	**298,5 ± 0,10**	**1,9 ± 0**	**34,9 ± 0,01**	**19,4 ± 0,05**
	B	**303,5 ± 4,50**	**1,9 ± 0,01**	**34,3 ± 0,10**	**19,2 ± 0,08**
High Pure FFPE RNA Isolation kit (Roche)	A	35,5 ± 0,80	1,8 ± 0,01	38,2 ± 0,70	19,3 ± 0,18
	B	33,9 ± 0,30	1,8 ± 0,03	37,5 ± 1,50	19,4 ± 0,03

RNA extraction methods were evaluated by RT-qPCR. MiRNA expression (Cp) is represented as mean ± SD.

As results, we obtained that the best miRNA extraction method was the MiRNeasy FFPE kit. The spike-in control was similar for each sample, thus cDNA synthesis and qPCR have been equally efficient for all samples.

To analyse miRNAs expression, we used U44 and U48 as RGs, both are typically used to normalise miRNA data derived from RT-qPCR in tissue (170,171). Although U6 is also usually used, we excluded it from the further analysis because its expression levels in tissue samples were higher than U44 and U48 (Ct>32) (data not shown).

U44 and U48 expression pattern was highly correlated (Pearson's correlation, p-value: <0,001, r: 0,9); however, we selected U44 as endogenous gene because it was more stable than the other (CV: 4%). There were no significant differences between groups or correlation with Gleason score, indicating a stable expression in PC samples **(Table 23)**.

Table 23. Details of candidate RGs.

Candidates RGs	Average Ct value	SD	CV (%)	P-value (Benign vs. PC)	Gleason score	
					r_2	P-value
U44	30,8	1,2	4	0,93	-0,38	0,29
U48	29,5	1,9	6	0,86	-0,44	0,21

The expression of candidate RGs is represented as the average of expression levels (Ct). CV (%) measured using average Ct and SD. Spearman's correlation was used for correlation between gene expression and Gleason score divided in 3 groups (<7, =7 and >7). CV: coefficient of variation; SD: standard deviation; r_s: Spearman rank-order coefficient.

Once analysed the expression levels of 4 more interesting miRNAs in FFPE samples from PC patients, only miR-28 showed a significantly deregulated levels. We found it under-expressed in human prostate tumours (p-value<0,05) with a fold change of 2 and AUC value of 0,8 (100% sensitivity, 40% specificity) **(Fig. 30).**

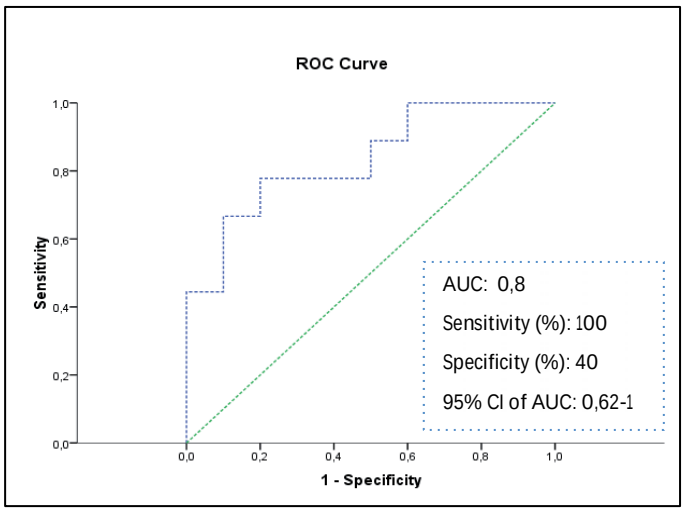

Figure 30. ROC curve to discriminate PC patients from those with non-malignant prostate alterations. AUC: area under the curve; CI: coefficient interval.

2.2.2.4.Construction of a Diagnostic MiRNA Signature

In order to enhance the predictive value of individual miRNAs expression, we determined a miRNA-based diagnostic classifier based on the combination of miRNAs expression taking into account the 48 miRNAs of the validation phase (n=154)

We build 80 models based on 5 variable selectors (t-test, Limma, Wilcoxon, Lasso and Random Forest (RF)), 4 classifiers (linear discriminant analysis (LDA), RF, support vector machine (SVM) and penalized logistic regression (PLR)) and 4 variables (3, 5, 10 and 25) to find the best miRNA profile. Those algorithms were validated by cross-validation. We selected the best model from the AUC values and then by the misclassification, sensitivity and specificity. Furthermore, in order to improve the robustness of the statistical analysis, ROC analysis of the 3 miRNAs was combined with bootstrapping as an internal validation.

In the **figure 31**, we can observe the comparison of the best models for each classifier.

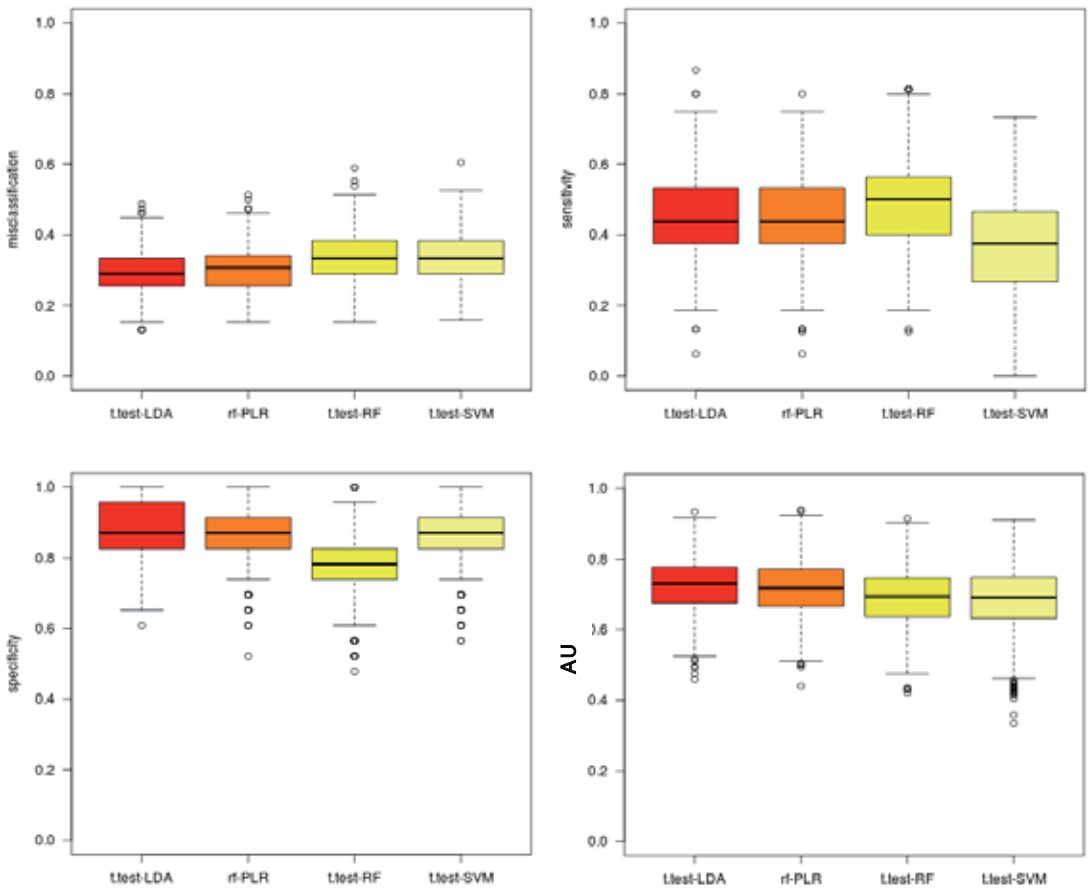

Model	Misclassification	Sensitivity	Specificity	AUC
T-test + LDA	**0,297**	**0,441**	**0,880**	**0,738**
RF + PLR	0,302	0,437	0,786	0,690
T-test + RF	0,333	0,490	0,786	0,690
T-test+ SVM	0,335	0,368	0,865	0,687

Figure 31. Comparison of the best models for each classifier.

As result, the best model was obtained by t-test and LDA classifier with 3 miRNAs (variables): hsa-miR-648, hsa-miR-147b and hsa-miR-193a-5p. Their combination into a single predictor enhanced the AUC up to 0,738. However, although the specificity was high (88%), the sensitivity was quite low (44%).

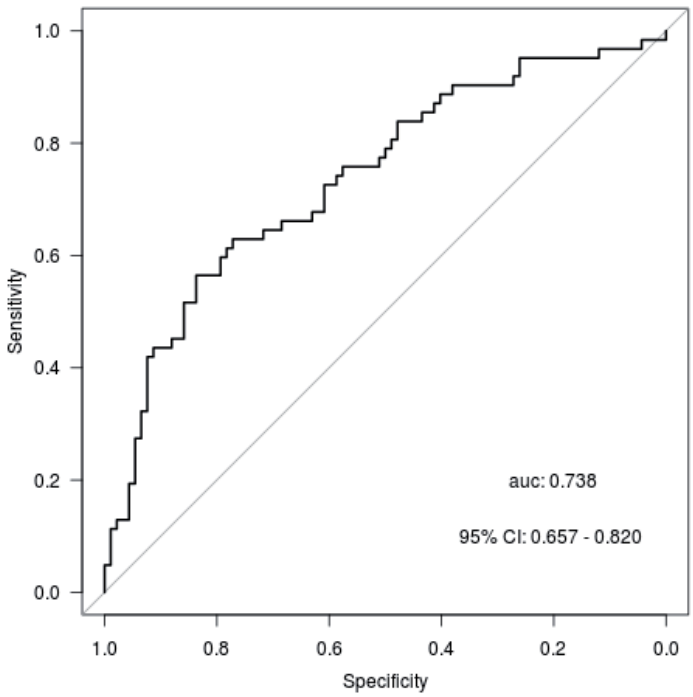

Figure 32. ROC curve from combined hsa-miR-648 + hsa-miR-147b + hsa-miR-193a-5p to discriminate PC patients from those with non-malignant prostate alterations.

3. FUNCTIONAL CHARACTERIZATION OF MIRNAS IN PROSTATE CANCER

In addition to identify deregulated miRNAs as potential PC diagnostic biomarkers from urine samples, we characterized some of them *in vitro* to contribute to the elucidation of the PC pathogenesis. We selected 3 miRNAs from the pilot study (hsa-miR-100-5p "miR-100", hsa-miR-191-5p "miR-191" and hsa-miR-210-3p "miR-210") and the most promising from the validation phase (hsa-miR-28-5p "miR-28"), the role of which had not been described so far in PC.

On the other hand, in collaboration with the group of Dr. Ochiya in the National Cancer Center (NCC), Tokyo, we assessed exosomes as therapeutic delivery system for one tumour suppressor miRNA (miR-210).

First of all, in order to select which was our most appropriate *in vitro* model, we determined selected miRNA expression levels in 3 PC cell lines (PC-3, LNCaP and PC-3M) in conjunction with U6, U44 and U48 as endogenous genes **(Fig.33)**. After analysing their expression levels, it could be observed that the 3 miRNAs presented detectable levels in all cell lines.

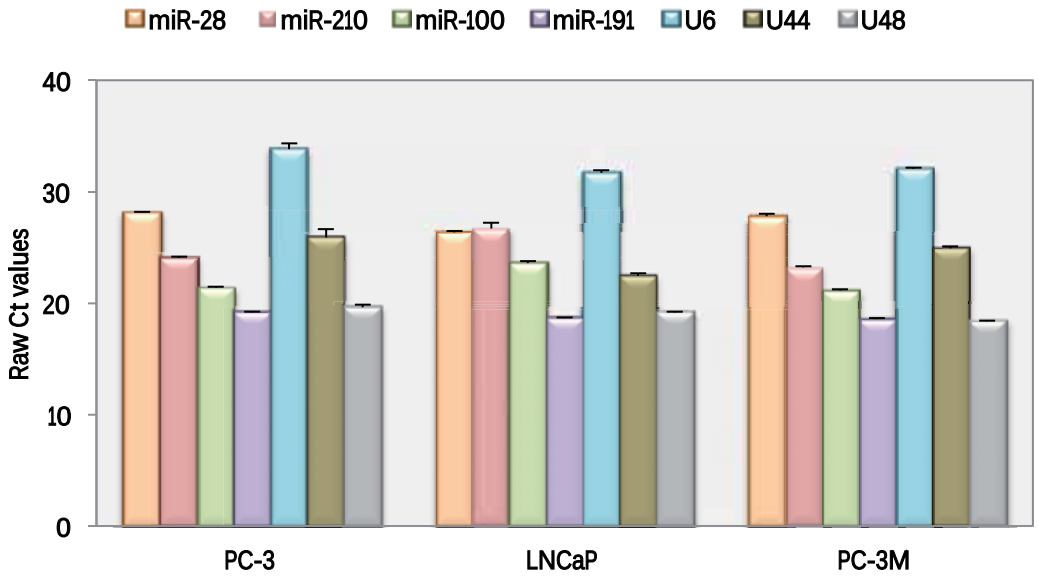

Figure 33. Expression levels in 3 human PC cell lines analysed by TaqMan RT-qPCR.

3.1. MiR-28 and miR-210 Decreased Cancer Cell Proliferation

Since the most fundamental trait of cancer cells involves their ability to sustain chronic proliferation (103), we studied the influence of miRNAs on PC cells proliferation by transfecting PC-3 and LNCaP cells with a mimic or antisense inhibitor synthetic oligonucleotide to transiently amplify or inhibit miRNAs expression.

We evaluated the efficiency of transfection by analysing mature miRNA relative expression at RNA level 24h after transfection at the same concentration of 50nM **(Fig.34A)**. However, this was only possible for the mimics. Therefore, we added a positive control based on fluorescent oligonucleotide (Block-iT) as independent condition in each experiment **(Fig.34B)**.

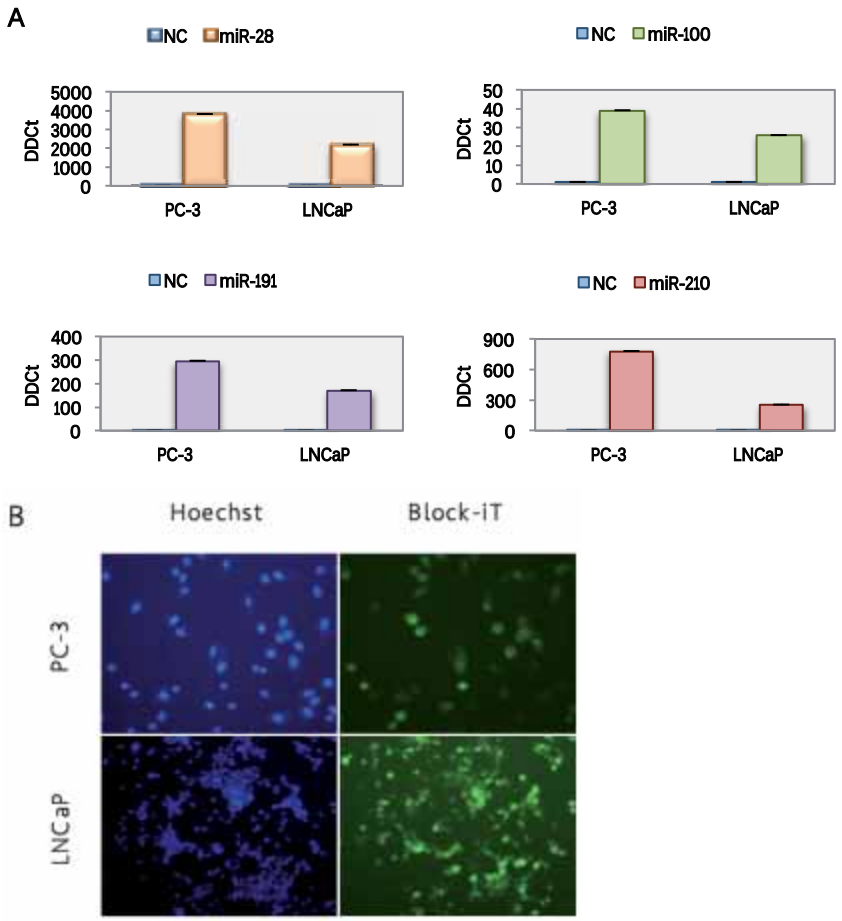

Figure 34. (A) Relative expression of miRNA in transfected PC cell lines. The levels of mature miRNAs were detected using TaqMan RT-qPCR and normalized to the U44. **(B)** Transfection efficiency of miRNA inhibitors measured by Block-iT fluorescence (transfected cells) compared with Hoechst staining (nucleus).

Effectiveness of transfection of PC cell lines assessed by Block-iT indicated that approximately 84% of PC-3 and 73% of LNCaP were transfected using our transfection conditions.

Once optimized transfection protocol, we performed a proliferation assay. The results showed that the over-expression of miR-28 in LNCaP cell line and miR-210 in PC3, significantly decreased proliferation activity compared to NC (38% and 21%, respectively) 96h after transfection. However, the inhibition of miRNAs expression levels did not show any effect. **(Fig.35)**.

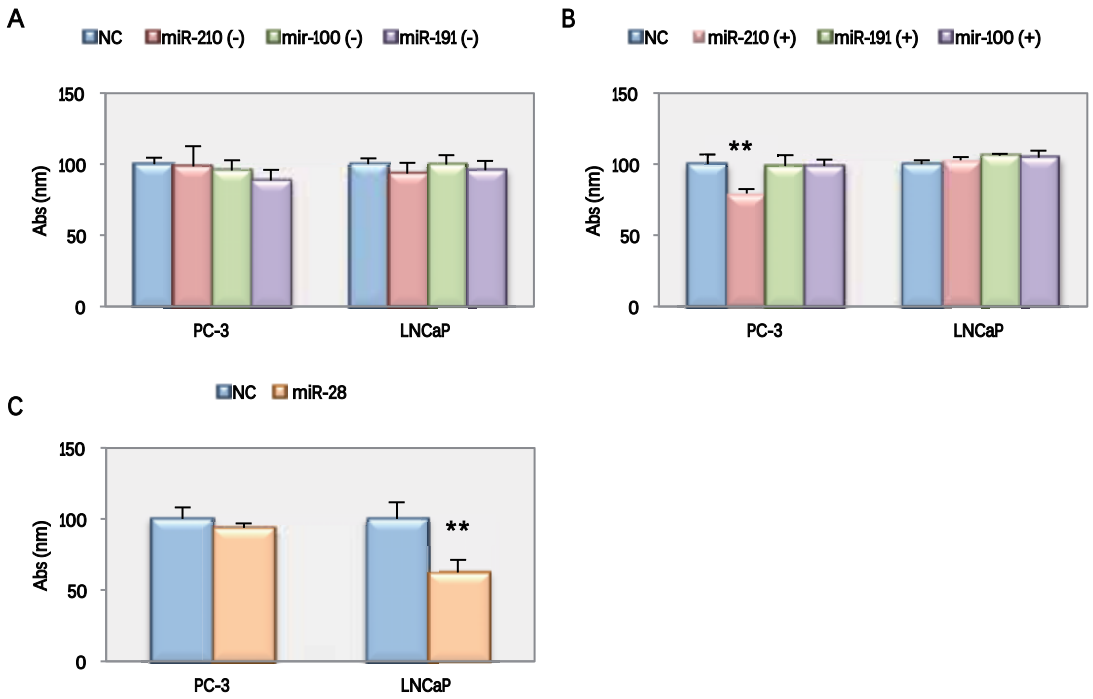

Figure 35. **(A)** Effects of miR-210, miR-191 and miR-100 under-expression on PC cell lines proliferation. **(B)** Effects of miR-210, miR-191 and miR-100 over-expression on PC cell lines proliferation. **(C)** Effects of miR-28 over-expression on PC cell lines proliferation. Results are represented as absorbance 96h after transfection using Cell Titer reagent in LNCaP (490nm) and crystal violet (590nm) in PC-3. The bars represent the mean ± SD. Values that are significantly different by t-test from the NC are indicated by **p-value<0,01. NC: negative control, (-): presence of miRNA inhibitor and (+): presence of mimic.

Taking into account these results, we selected miR-28 and mir-210 for further analysis.

3.1.1. Lentiviral MiR-210 Overexpression Enhanced the Effect on Cell Proliferation

To study the long-term effect of miR-210 over-expression, we analysed miRNA expression level in PC-3 cells at 24h, 48h, 72h and 96h after transfection.

As shown in **figure 36** and as it expected after transient transfection, the relative expression of miR-210 decreases around 50% 72-96h after transfection.

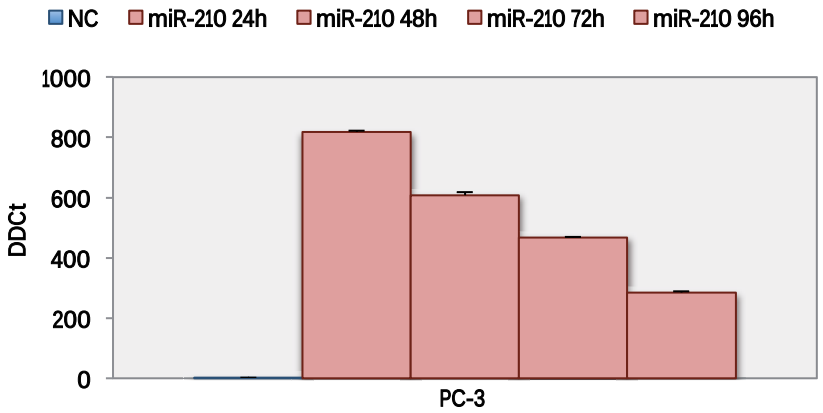

Figure 36. Relative expression levels of mature miR-210 24h, 48h, 72h and 96h after mimic transfection in PC-3 cells. The bars represent the mean ± SD of expression levels normalized to U44 as endogenous control gene.

In order to enhance the effects on proliferation of our candidate and be able to perform longer *in vitro* assays, a lentiviral-based pre-miR-210 infection was standardized in PC-3 cell line **(Fig.37)**. Simultaneously, we infected pre-miR-210 PC-3M and LNCaP cell lines, and evaluated the efficiency of infection by analysing mature miR-210 relative expression at mRNA level 24h after transfection **(Fig.38)**.

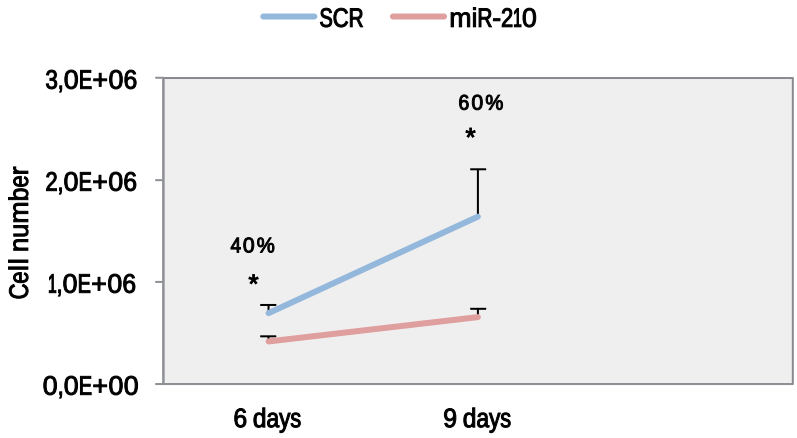

Figure 37. Effects of miR-210 over-expression on infected PC3 cell line proliferation. Results are represented as number of cells 6 and 9 days after infection (mean± SD). Cell proliferation assay was performed in triplicate. Values that are significantly different by t-test from the SCR (negative control) are indicated by *p-value<0,05.

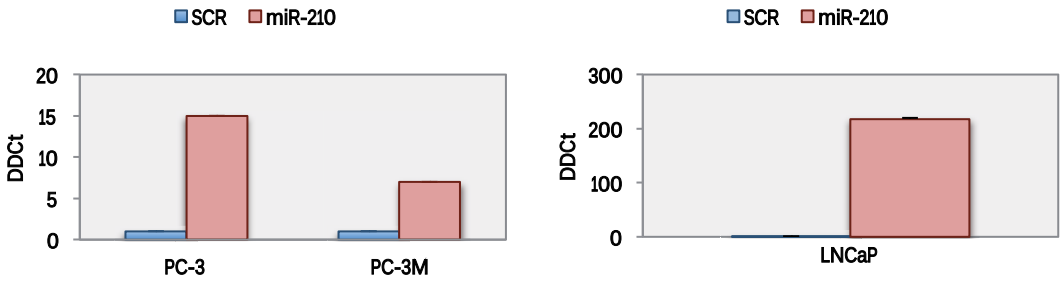

Figure 38. Relative expression of miR-210 in infected PC cells with pre-miR-210. The level of mature miR-210 was detected using TaqMan RT-qPCR, and normalized to the U44 control.

As shown on **figure 37**, after lentiviral infection the proliferation inhibition was enhanced, especially after 9 days (60%) compare with the transient cells. However the proliferation did not stop completely, therefore, in order to work with a more homogeneous population of cells we sorted by FACS only those cells that overexpressed the miR-210. Then, we repeated the proliferation assay observing again that miR-210 was able to significantly decrease more than 50% the proliferation activity of PC-3 cells. In LNCaP cells with miR-210 did not presented any effect, but in PC-3M the proliferation decreased significantly (39%) **(Fig.39)**.

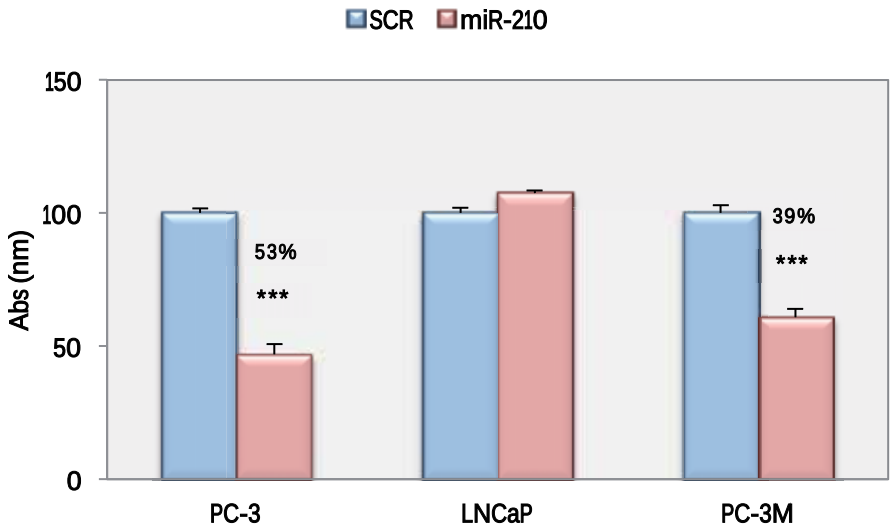

Figure 39. Effect of miR-210 over-expression on PC cell lines proliferation. Results are represented as absorbance at 590nm (crystal violet). The bars represent the mean ± SD. Values that are significantly different by t-test from the NC are indicated by ***p-value<0,001. SCR (negative control).

3.2. Effect of Stable MiR-210 Overexpression on the Cell Cycle

To analyse whether the observed decrease on PC-3 and PC-3M cells proliferation was due an arrest at any stage of the cell cycle, or a transition delay upon infection with pre-miR-210, we analysed their DNA content by flow cytometry.

Cell cycle analysis showed that the majority of PC-3 and PC-3M cells were accumulated in G1 and only a small fraction of cells were synthesizing DNA (S phase) or in G2/M **(Fig.40A)**. However, we did not observed significant differences in the proportion of cells in G1, S or G2/M phases between SCR and pre-miR-210-infected cells **(Fig.40B)**. Nevertheless, we analysed the expression at protein level of cyclin B1, D1 and E, and WAF1 (p21) (all implicated in cell cycle progression) to explore if their expression was affected by miR-210 over-expression.

Due to lack of cells lines that stably expressed miR-28, we added protein samples from miR-28 LNCaP transfected cells to this analysis in order to unveil the mechanism by which the transient over-expression of miR-28 also decreased the proliferation rate **(Fig.41).**

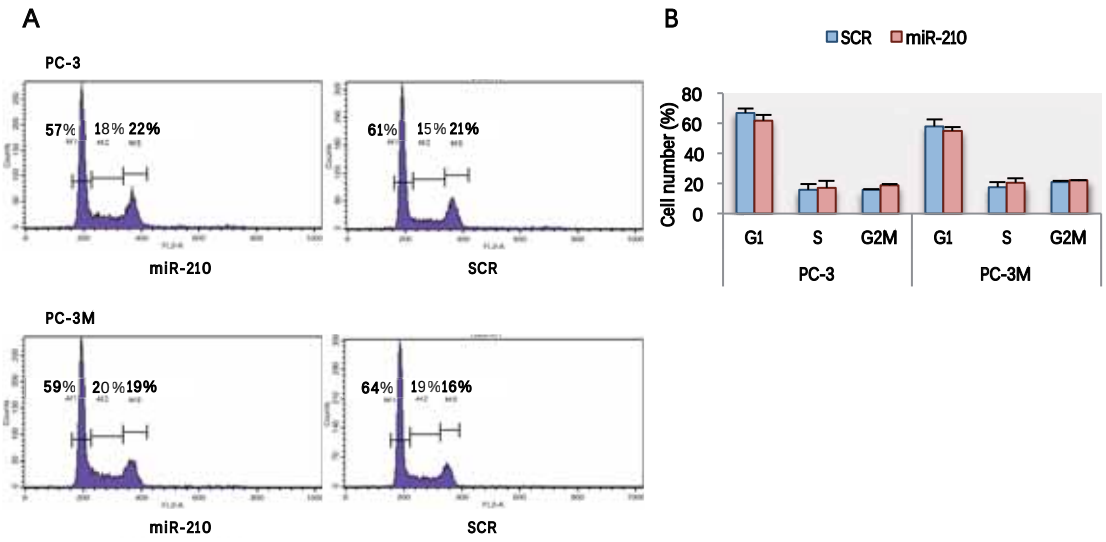

Figure 40. (A) SCR and pre-miR-210 infected PC-3 and PC-3M cells were subjected to FACS analysis. Representative images are shown. **(B)** Proportions of cells in the G1, S and G2M phases. The bars represent the mean ± SD (n=2).

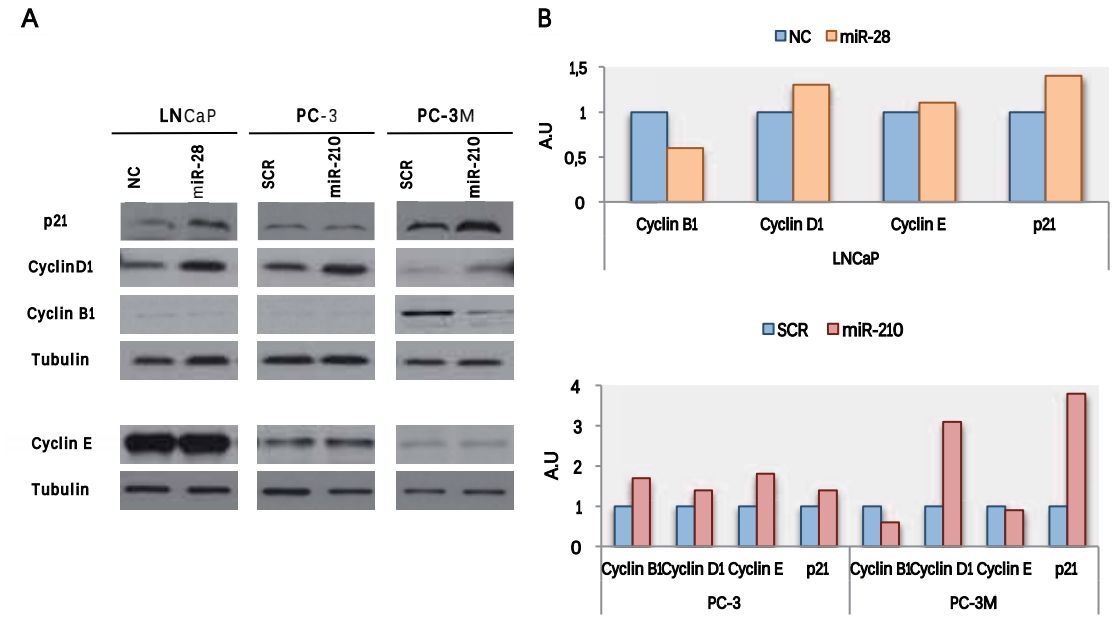

Figure 41. (A) A representative western blot analysis of p21 and cyclins D1, B1 and E protein levels is shown. **(B)** Results were assessed by densitometry and normalized to those of tubulin protein (n=1).

As shown in **figure 41,** the overexpression of miR-210 in PC-3M cells caused a marked decrease in cyclin B1 levels that was accompanied by higher p21 expression, as expected. Concomitantly, cyclin D1 levels were increased upon miR-28 (in LNCaP) or miR-210 (in PC-3 and PC-3M) overexpression, whereas cyclin E levels were not significantly changed. All together, these results are in agreement with lower proliferation rates upon miR-210 overexpression in PC-3M and suggest a delay on the G1-S transition of the cell cycle when this miRNA is overexpressed.

3.3. Stable MiR-210 Overexpression Decreased Clonogenic Capacity

It is known that within neoplastic prostatic cells, there are some with self-renewal potential (CSCs) that contribute to the tumour growth, evolution and heterogeneity (172).

In order to determine the ability of cell lines such as PC3 or PC3M that stably over-expressed miR-210 to form clones (clonogenicity), we performed a colony formation assay as one of the clonogenic cell survival assays.

Briefly, a clonogenic cell survival assay measures the velocity with which cell colonies or aggregates (called spheroids) are formed under culture conditions and the size of such colonies or aggregates. The test may reveal a reduction in their number or sizes in response to a treatment.

As results, miR-210 stably expressed reduced the self-renewal capacity of PC-3M cells **(fig. 42A)**, but not of PC-3 cells. Because we did not obtain expected results for PC-3 cell line by the colony formation assay, we decided to perform a sphere formation assay. As shown in **figure 42B**, there were more PC-3 cells over-expressing miR-210 (miR-210-PC-3) that remain single, died or formed small spheroids or tumourspheres. On the other hand, control cells formed large cell spheroids, indicating that they survived and maintained the ability to proliferate indefinitely.

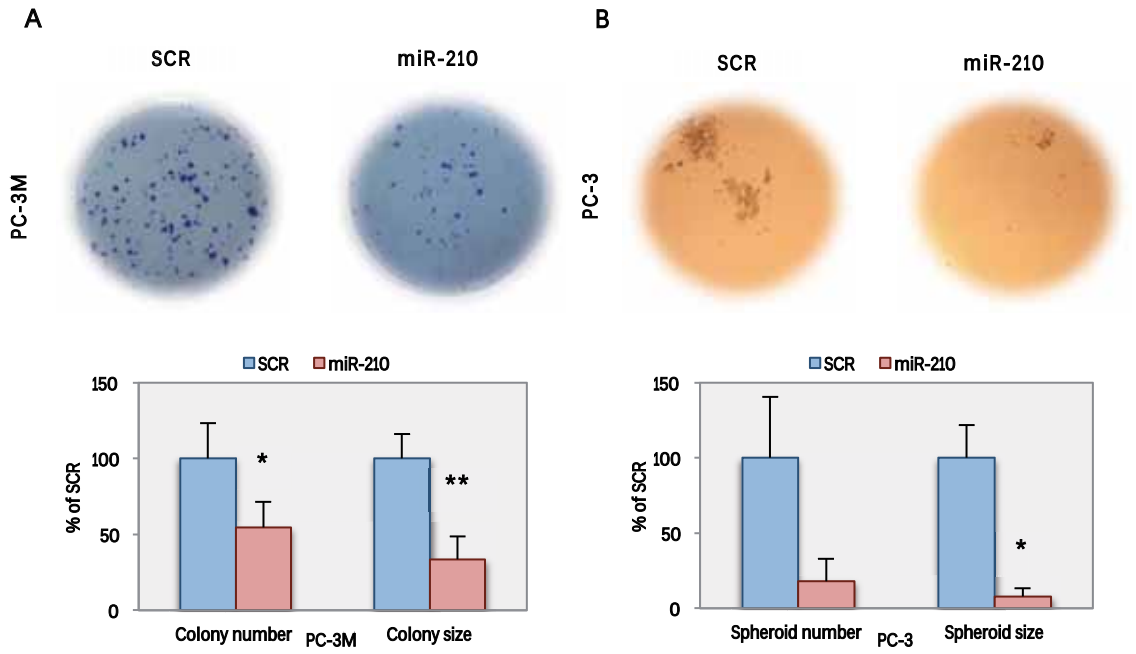

Figure 42. (A) Effect of miR-210 overexpression in PC-3M clonogenic capacity. Images of colonies stained with crystal violet were taken after 10 days of growth. **(B)** Effect of miR-210 overexpression in PC-3 spheroid formation capacity. Images of spheroids were taken after 10 days of growth. The bars represent the number of colonies/spheroids and their size as mean ± SD (% of SCR). Values that are significantly different by t-test from the SCR are indicated by *p-value<0,05, **p-value<0,01. SCR: scramble.

3.4. MiR-28 and MiR-210 Induced Cell Death

The next step was to investigate whether miR-28 and miR-210 overexpression decreased proliferation activity through an increased apoptosis or cellular death. Hoechst-PI staining was conducted on our modified cell lines. Hoechst was used to stain cellular nucleus, whereas PI (propidium iodide) is a marker of membrane integrity.

As results, miR-28 and miR-210 transfected PC cells showed an increased number of PI positive cells (dead cells) compared to NC 96h after transfection, many of which contained highly compacted DNA and fragmented chromatin stained by Hoechst (apoptotic cells). Specifically, miR-210 expression increased significantly the cell death in PC-3 and PC-3M (6,8 and 3,6 times, respectively) compared with NC. The same effect was observed in LNCaP that over-expressed miR-28 (1,2 times) **(Fig. 43)**.

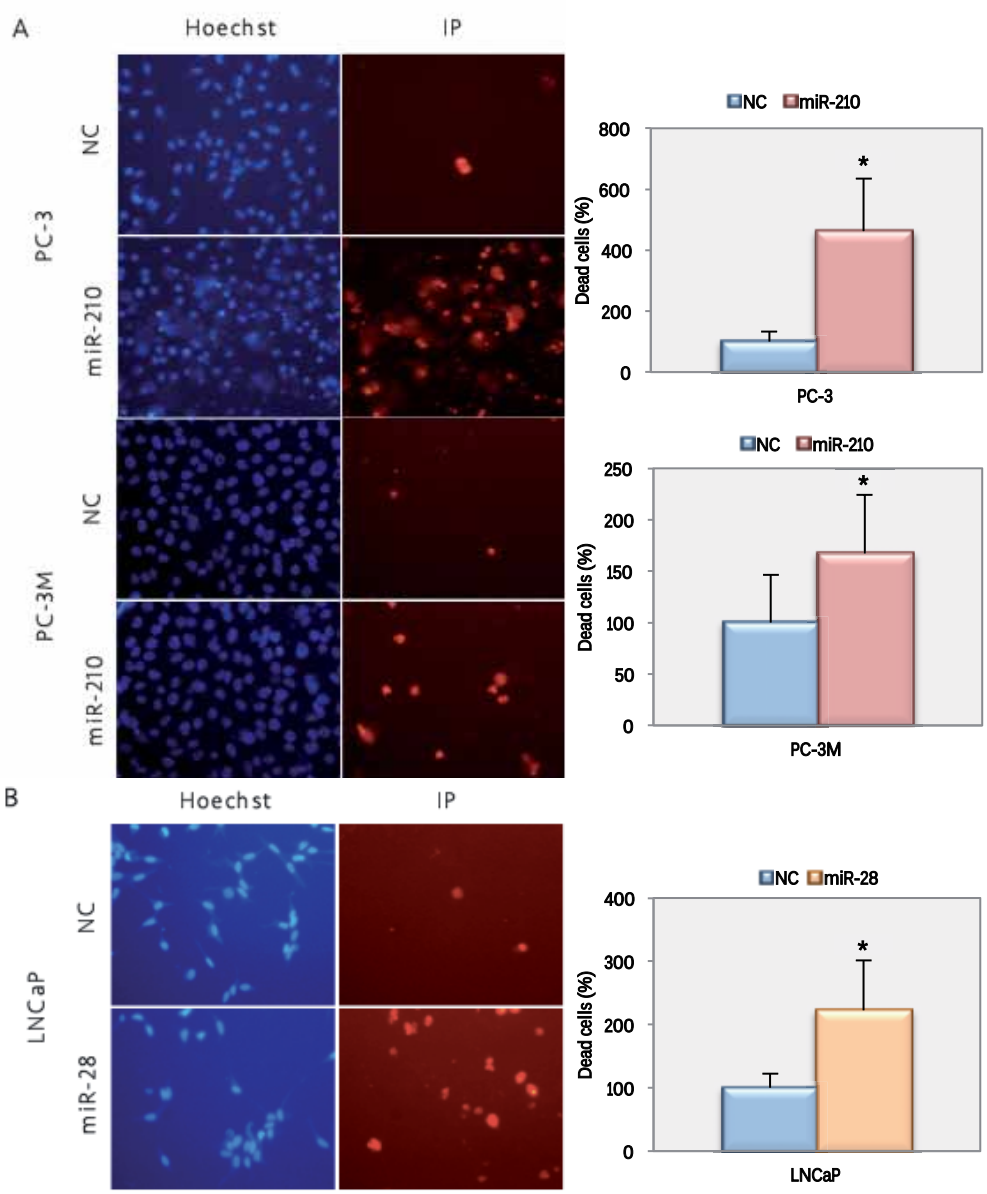

Figure 43. (A) Effect of miR-210 over-expression in PC-3 and PC-3M on cell viability. **(B)** Effect of miR-28 over-expression in LNCaP on cell viability. Images were taken 96h after transfection. The bars represent the number of death cells as mean ± SD (% of NC). Values that are significantly different by t-test from the NC are indicated by *p-value<0,05. NC: negative control.

3.5. MiR-28 and MiR-210 Overexpression Effect in Metastatic Potential

Two of the most important properties of a metastatic cell are its migration and invasion capacity. Thus, these characteristics of aggressiveness were studied in our modified cell lines.

The migration ability of miR-28-LNCaP, miR-210-PC-3 and miR-210-PC-3M was evaluated by transwell migration assay. Moreover, due to their capacity to from a monolayer, the migration capacity of PC3 and PC3M was also evaluated performing a wound healing assay.

Concerning to LNCaP cells, miR-28 over-expression changed significantly their capacity of migration after 24h of seeding cells in transwells **(fig.44)**. Since LNCaP cell line grows without forming monolayers, it was not possible to corroborate results with the wound healing technique.

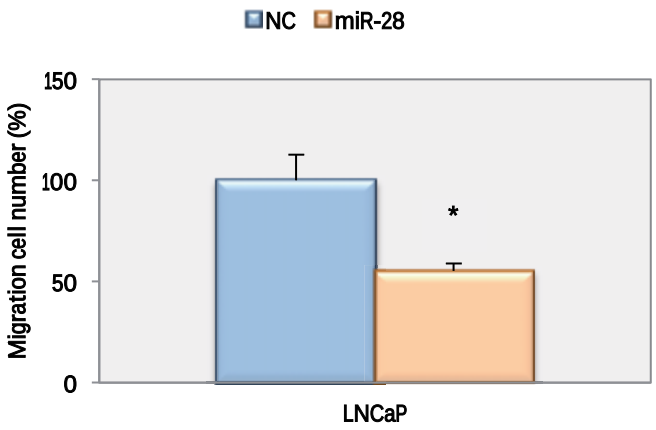

Figure 44. Effect of miR-28 over-expression in LNCaP cell line migration capacity. Results of transwell migration assay are expressed as number of migrating cell (% of control). The bars represent mean ± SD (n=3). Values that are significantly different by t-test from the NC are indicated by *p-value<0,05. NC: negative control.

On the other hand, miR-210-PC-3 cells increased significantly their migration capacity in both wound healing and transwell assays after 24h. However, we did not obtain any effect for PC-3M cells **(Fig.45)**.

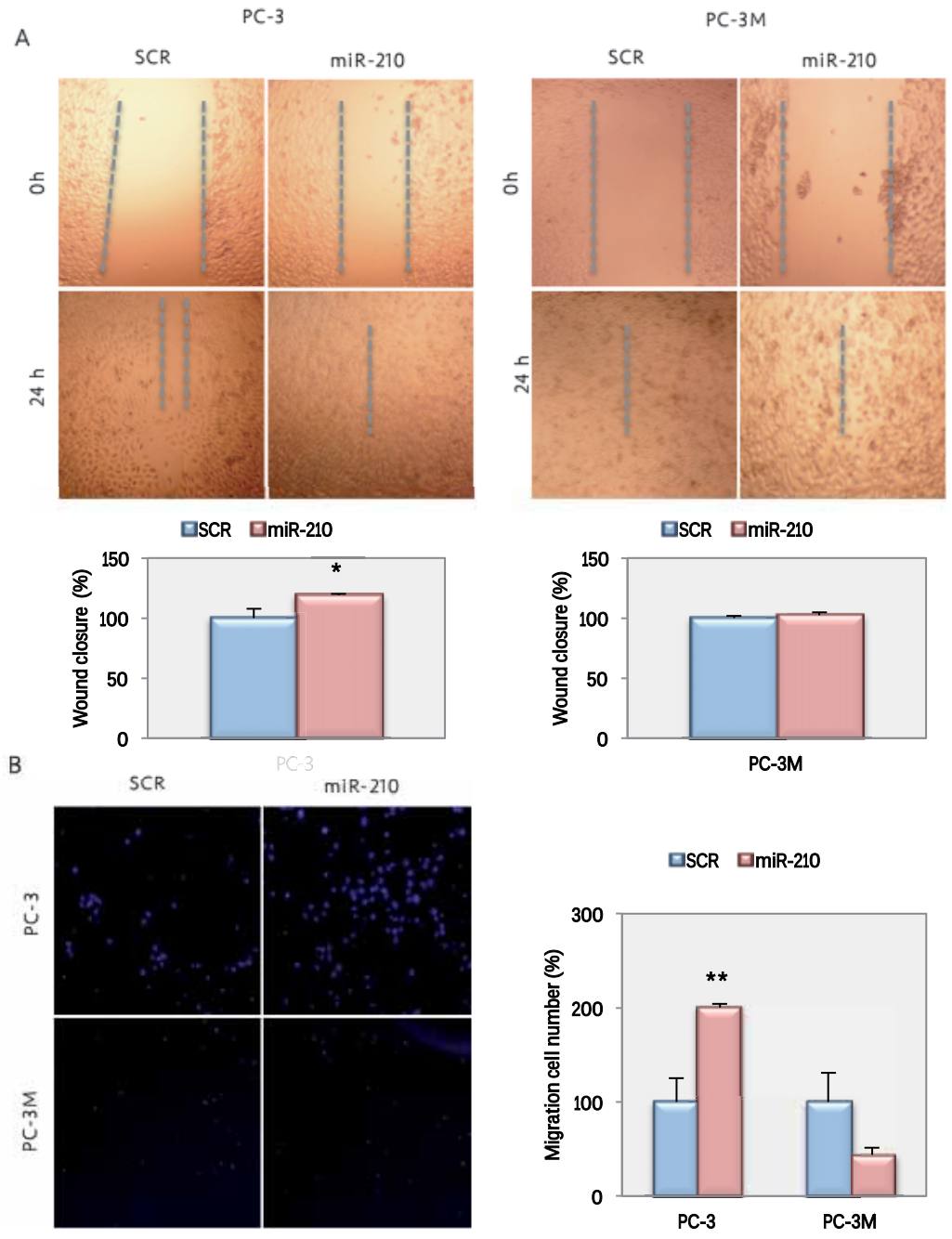

Figure 45. Effect of miR-210 over-expression on PC-3 and PC-3M cells migration capacity. **(A)** The results of wound healing assay are presented as the difference between the wound-healing speed (μm2/h) before and after 24h of transfection calculated using Image J software. **(B)** Migration transwells values are presented as number of migrating cells stained with Hoechst after 24h of transfección. The bars represent the mean ± SD (n=3). Values that are significantly different by t-test from the SCR are indicated by *p-value<0,05 and **p-value<0,01. SCR: scramble.

Subsequently, the invasion ability of miR-28-LNCaP, miR-210-PC-3 and miR-210-PC-3M was evaluated by transwell invasion assay. However, results did not indicate significant effect for any cell line **(Fig.46)**.

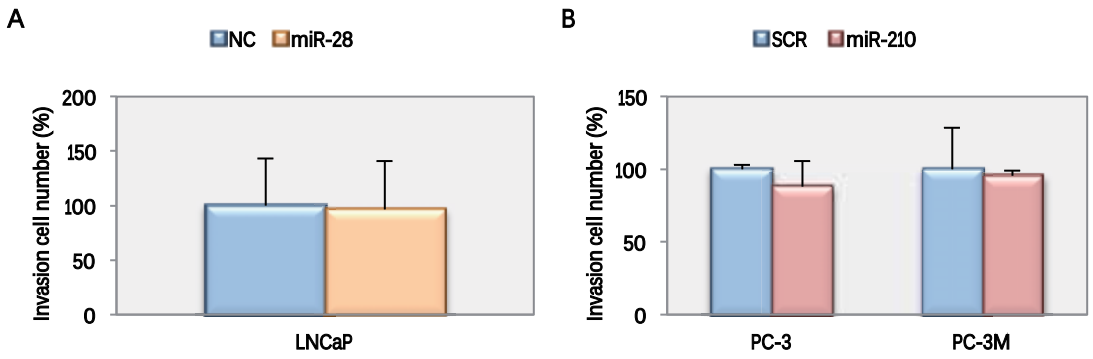

Figure 46. (A) Effect of miR-28 over-expression in LNCaP cells invasion capacity. **(B)** Effect of miR-210 over-expression in PC-3 and PC-3M cells invasion capacity. Results of transwell invasion assay are expressed as number of invasion cell (% of control). The bars represent mean ± SD (n=3). NC: negative control; SCR: scramble.

Furthermore, to examine whether EMT may be associated with the changes observed in the migration capacity, the protein levels of E-cadherin, N-cadherin, Erk and phospho-Erk were evaluated in the protein extracts of the same PC cell lines.

As shown in **figure 47**, there were not differences in E-cadherin and N-cadherin levels between miR-210-cells and control cells. Therefore, EMT seems not to be the mechanism responsible of the effects observed on miR-28-LNCaP and miR-210-PC-3 cells migration. However, p-Erk, that has been implicated in the migration of numerous cell types (173), showed an important decreased in LNCaP that over-expressed miR-28.

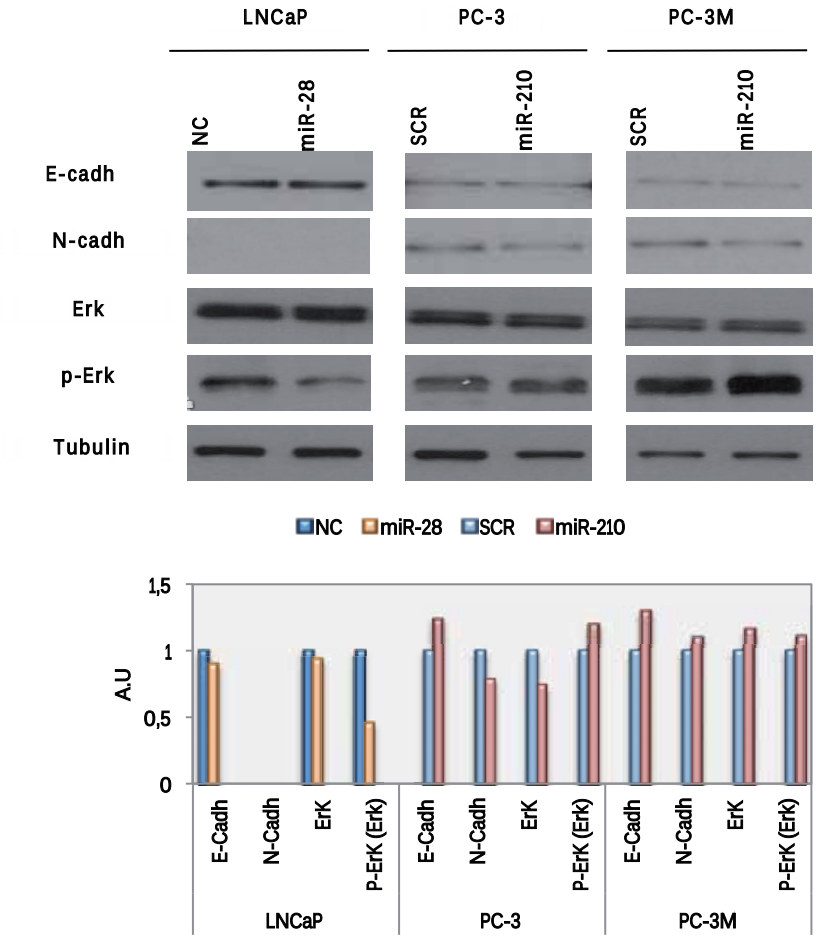

Figure 47. EMT proteins expression levels in stably miR-210-PC3 and miR-210-PC-3M and in transient miR-28-LNCaP. Western blot of E-cadherin (120KDa), N-cadherin (130KDa), Erk1/2 (44/42KDa) and phospho-Erk 1/2 (44/42KDa), and the control tubulin (52KDa) was performed on total cell extracts. The bars represent densitometry analysis of the bands using Image J software (% of Control). E-cadh: E-cadherin; N-cadh: N-cadherin and p-Erk: phospho-Erk; NC: negative control; SCR: scramble.

3.6. MiR-28 and MiR-210 Targets: Bioinformatics Analysis

To complete the miR-28 and miR-210 characterization, we performed an *in silico* functional analysis to find out which pathways could be involved in the effects on proliferation, viability and migration that had been observed in our previous experiments.

We further studied miRNAs targets through different specialized software for the identification of experimentally validated or predicted mRNA targets.

Some of the most commonly used databases are: TargetScan (predicted targets), PicTar (predicted targets) and miRTarbase (experimentally validated targets).

In order to create a common miRNA target list, we matched all targets previously unified with the same identifier (ID) by the gene ID converter called BioMart Central Portal (http://central.biomart.org/converter/#!/ ID_converter/gene_ensembl_config_2).

As results, a total of 122 and 291 genes were identified as targets of miR-210 and miR-28, respectively. Regarding to miR-210, ephrin A3 (EFNA3), glycerol-3-phosphate dehydrogenase 1-like (GPD1L) and DENN/MADD domain containing 6A (DENND6A) genes were present in all 3 analysis. On the other hand, miR-28 showed only OUT deubiquitinase, ubiquitin aldehyde binding 1 (OTUB1) gene as a common target, which has been recently validated as deregulated gene in PC (174) **(Fig.48)**.

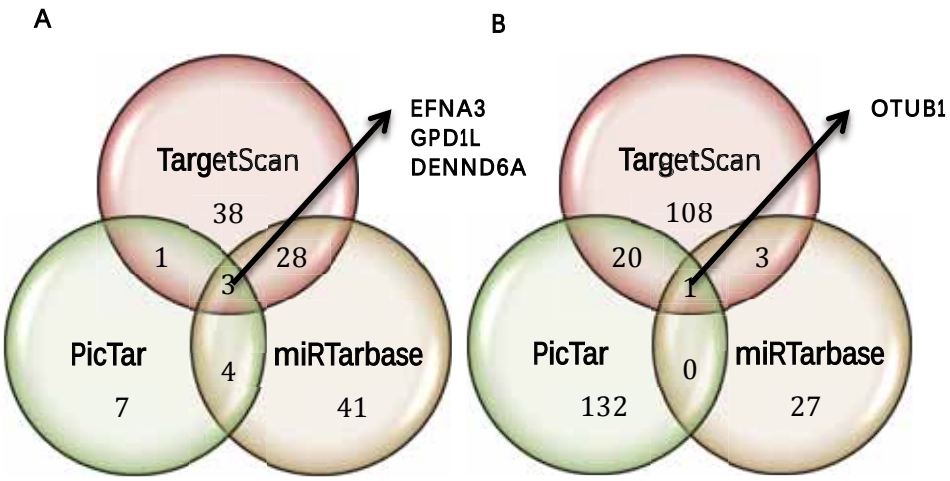

Figure 48. Venn diagram of miR-210 **(A)** and miR-28 **(B)** illustrating the overlapping targets from the 3 databases: TargetScan (red), PicTar (yellow) and miRTarbase (orange). Black arrows indicate common genes in TargetScan, PicTar and miRTarbase databases.

Then, we analysed the known role of miRNA targets using the software Ingenuity Pathways Analysis (IPA) that allow us to identify miR-28 and miR-210 biological functions and related pathways.

According with our previous results, IPA data analysis confirmed that miR-210 and miR-28 were both involved in cancer as one of their top diseases **(Fig.49A and 50A)**. Targets of both miRNAs seemed to be implicated in cell cycle and cell viability regulation as one of the main biological functions. MiR-210 targeted mRNA of genes implicated in DNA double-strand break repair and cell cycle (Fig. 29B), whereas some of the most important canonical pathways of miR-28 were ERK5, PI3K/AKT, ERK/MAPK and insulin receptor signalling. Interestingly, the *in*

silico results showed a direct effect of mir-28 on PC related signalling pathways. **(Fig.50B)**. Targets of miR-28 in PC signalling reflected its function as tumour suppressor gene, since the inhibition of them (RAS, ERK1/2, GSK3β3 and CREB) resulted in growth arrest and cellular apoptosis **(Fig.51)**.

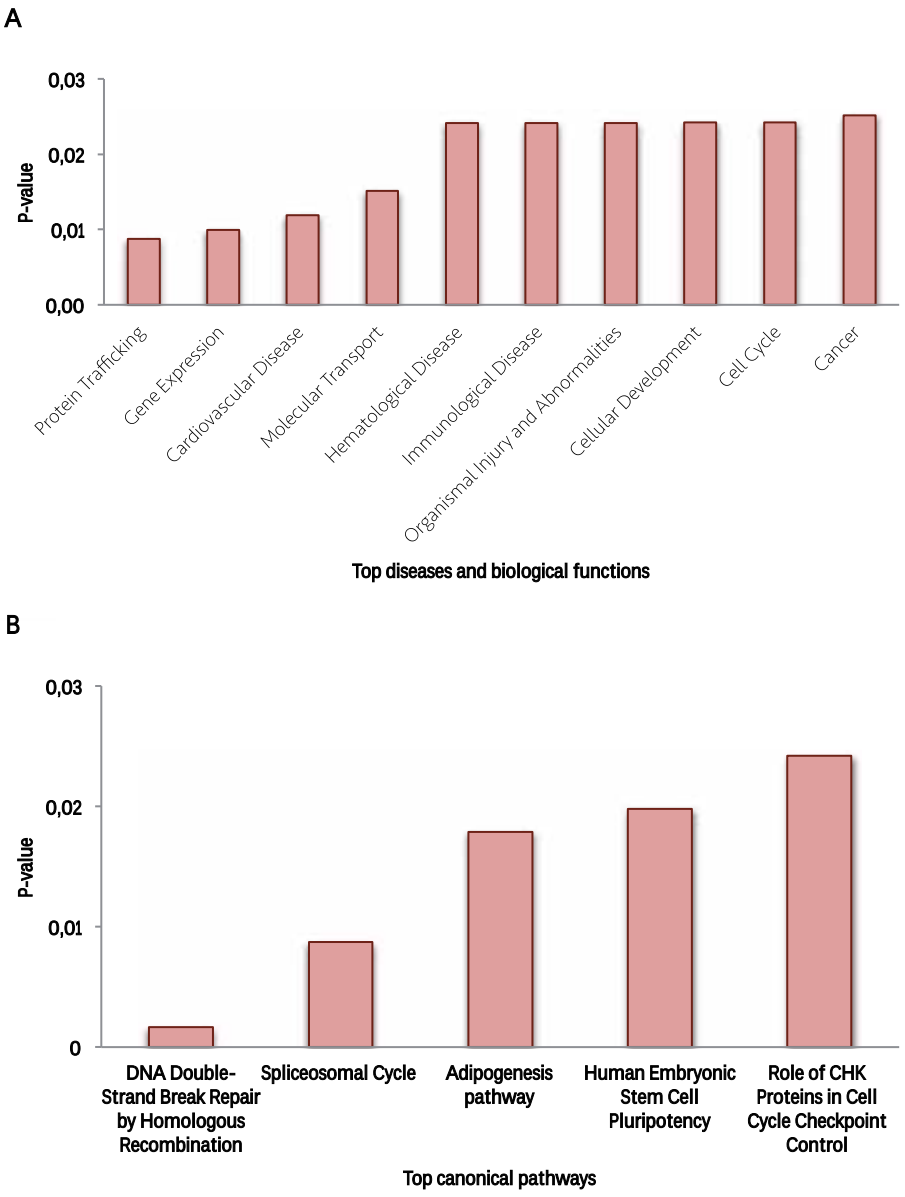

Figure 49. (A) Top diseases and biological functions of miR-210. **(B)** Top canonical pathways of miR-210. Results are represented by p-value.

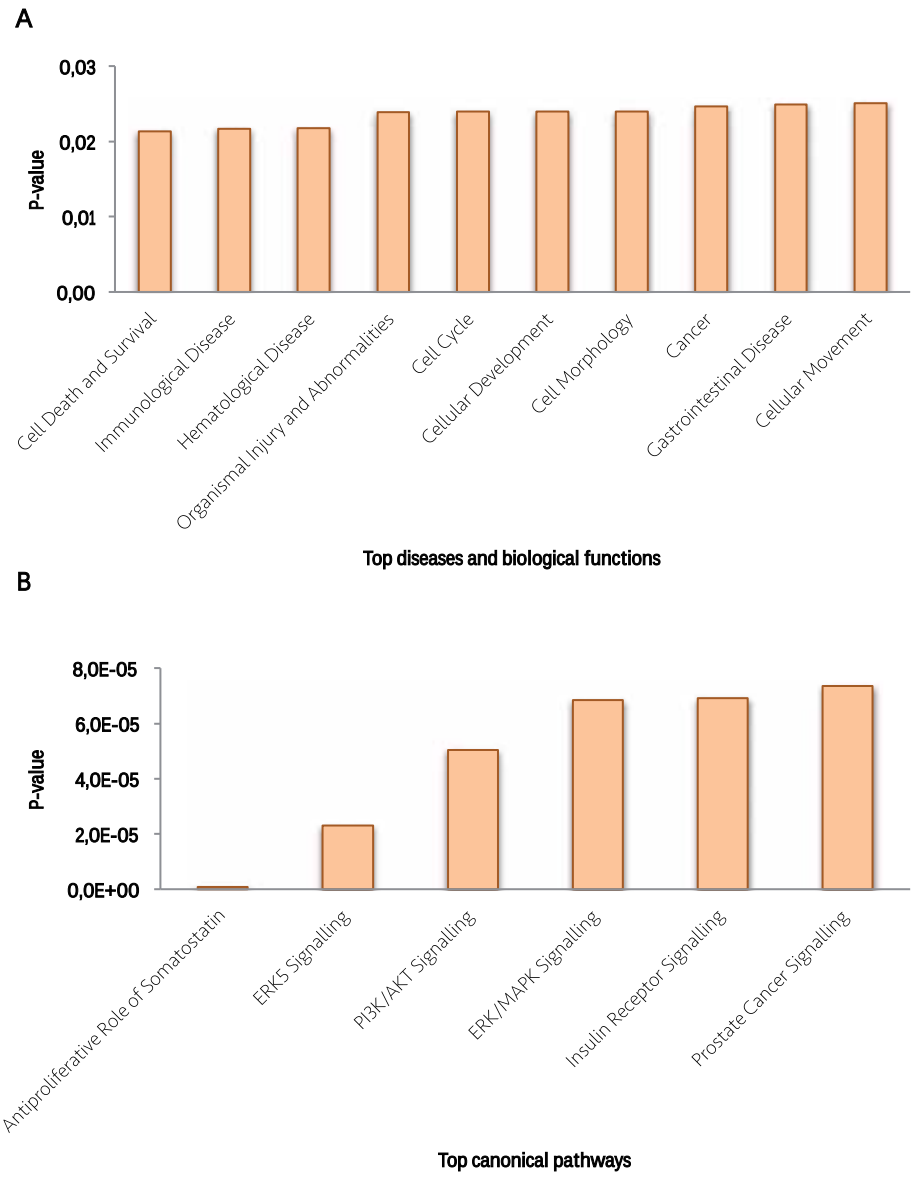

Figure 50. (A) Top diseases and biological functions of miR-210. **(B)** Top canonical pathways of miR-28. Results are represented by p-value.

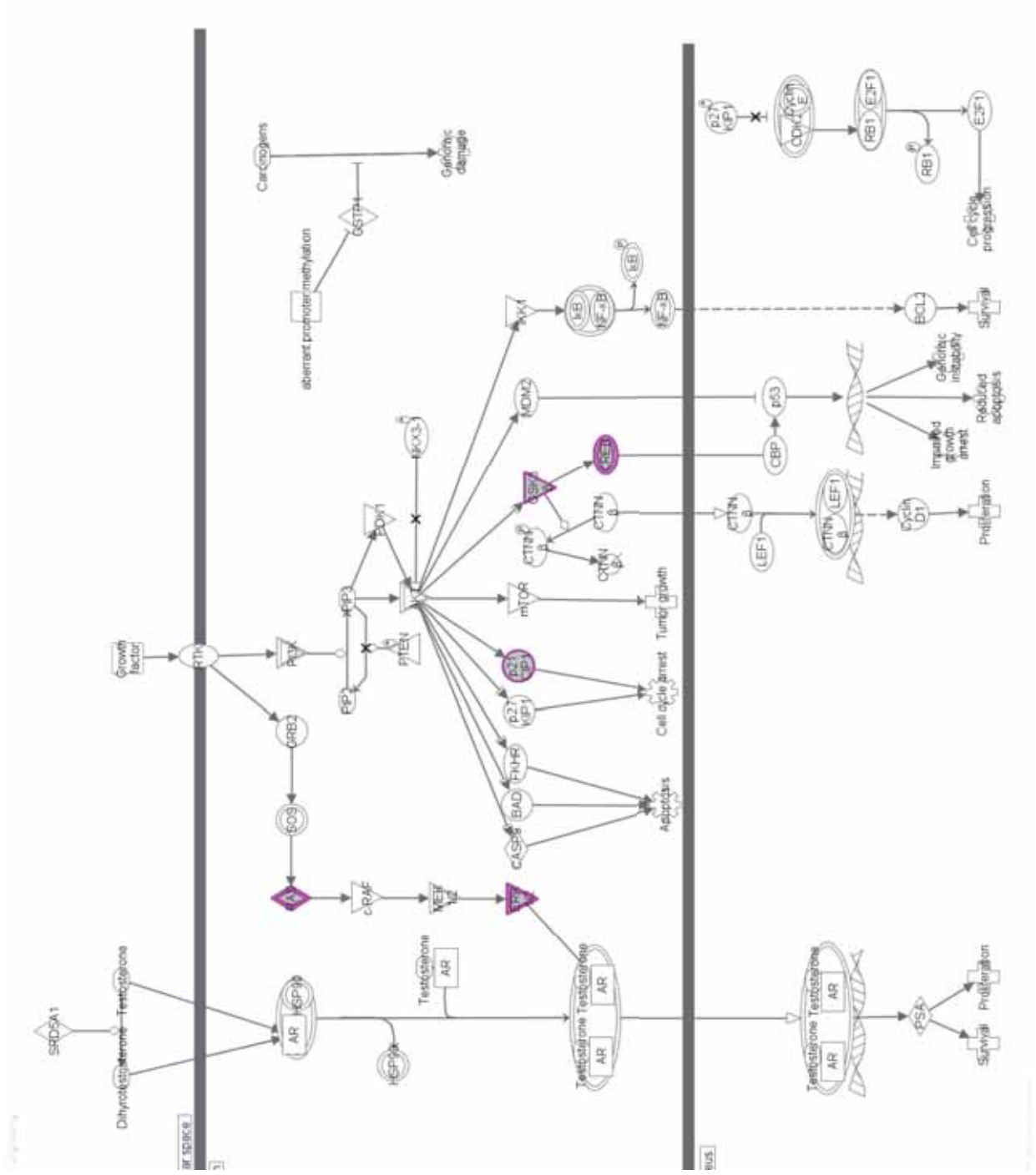

Figure 51. PC signalling pathway. MiR-28 predicted targets marked in purple and yellow respectively.

3.7. Detection of MiR-210 in the Exosomes of Prostate Cells

Since the exosome has been recently described as potential therapeutic delivery system because of its characteristics such as containing functional tumour suppressive miRNAs, we decided to evaluate whether miR-210 that we identified in our previous *in vitro* experiments as a tumour suppressor gene in PC cells, could be used as a therapeutic tool through transfecting it by exosomes derived donor cell-enriched media.

In collaboration with Dr.Ochiya's group from the National Cancer Center (NCC, Tokyo, Japan), PNT-2 cell line was selected as exosomes donor cell, since it has been described that they secrete exosomal miRNAs downregulated in PC cells and capable of inhibiting prostate tumour growth (121). On the other hand, as we found previously that miR-210 inhibited PC-3 and PC-3M cells proliferation, we selected them as recipient cells to incorporate PNT-2 exosomes. Therefore, we hypothesized that PNT-2 cells had more miR-210 than the recipient cells PC-3 and PC-3M.

Firstly, we checked the miR-210 expression level in PNT-2, PC-3 and PC-3M cells by TaqMan RT-qPCR. As shown in **figure 52**, PC-3 presented higher levels of miR-210, whereas PC-3M and PNT-2 showed similar levels.

Then, exosomes of PNT-2, PC-3 and PC-3M cells were isolated from culture media and assessed the quality of samples by using the NTA. Furthermore, in order to corroborate the exosomes isolation method reliability, protein levels of CD81 and CD63 in PC-3 were analysed since both have been described as specific exosome markers. As results, the general particle size correlated with the expected size for exosomes (≤150nm), and was similar between the three types of prostate cells (PC-3 cells 127nm, PC-3M cells 122nm and PNT-2 cells 137nm). The number of particle/ml was higher in PC-3M cells ($18,5.10^8$ particles/ml) **(Fig.53A)**. Moreover, we only got a positive result in PC-3 for exosomal protein markers, thus indicating that exosomes are a representative part of the total protein in the sample and that the ultracentrifugated culture media was not contaminated with FBS exosomes **(Fig.53B)**.

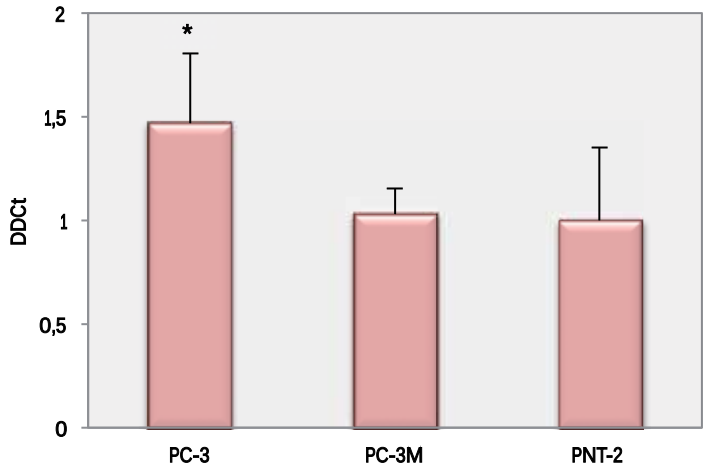

Figure 52. Relative expression of miR-210 in parental PC cells. The level of mature miR-210 was detected using TaqMan-qPCR and normalized to the U6 control. PC-3 cells significantly express more miR-210 than PC-3M and PNT-2 cell lines. The levels of mature miR-210 were detected using TaqMan RT-qPCR and normalized to the U6. The bars represent the mean ± SD (n=3). Values that are significantly different by t-test are indicated by *p-value<0,05.

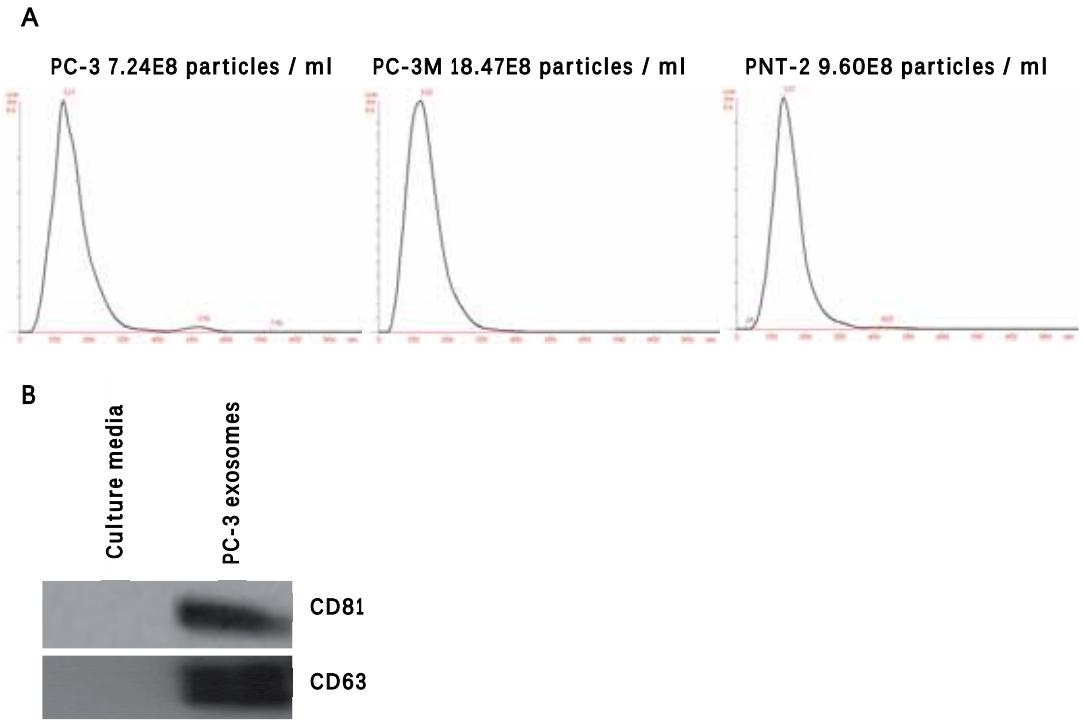

Figure 53. (A) Measurement by NTA. The histogram shows the overall size distribution and particle counts of the prostate cells. **(B)** Western blot of 2 exosomal markers in ultracentrifugated culture media and PC-3 cells exosomes. Membrane proteins: CD81 (26KDa) and CD63 (30-65KDa).

Finally, the amount of exosomes miR-210-contained was analyses by TaqMan RT-qPCR. The results showed that PC-3M cells presented a significant higher level than PC-3 and PNT-2 cells, which contained similar levels of miRNA. Because there was not any described reference gene to normalize data from the exosomes, we decided to use the total protein quantification **(fig.54)**.

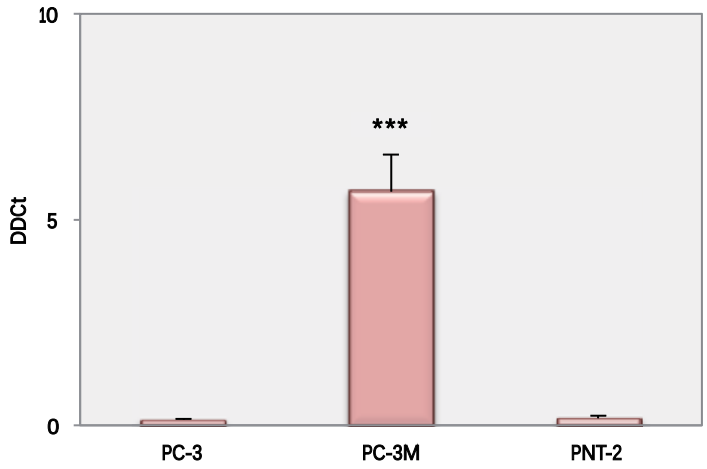

Figure 54. Relative expression of miR-210 in the exosomes of PC cells. The levels of mature miR-210 were detected using TaqMan RT-qPCR and normalized to the total protein amount. The bars represent the mean ± SD (n=3). Values that are significantly different by t-test are indicated by ***p-value<0,001.

DISCUSSION

PC is one of the most common cancers and one of the leading causes of cancer-related death in the industrialized countries. The introduction of PSA markedly altered and benefited the initial diagnosis of men with PC. As a result of PSA screening, the lifetime risk of PC diagnosis increased to 16% whereas the lifetime risk of dying from the disease was 3.4%, suggesting that nonlethal PC is mostly detected by PSA screening. It is now obvious that over-detection of potentially indolent disease by the widespread use of PSA testing has resulted in patients over-treatment. Thus, nowadays a clinical dilemma in the management of PC is to distinguish men with aggressive disease who need definitive treatment from men whose disease does not require such intervention (175). In order to improve the utility and benefit of PSA screening, it has been suggested that the practice should be decreased for low-risk individuals or those unlikely to benefit from screening, halting further screening when appropriate, and utilizing observational strategies in patients unlikely to suffer clinically significant effects of PC over their anticipated life expectancy (176).

In summary, a great number of the PBs practiced are unnecessary, causing pointless discomfort to the patient and extra expenses to the health care system. In the last years, a lot of effort has been put into the identification of new biomarkers for PC that would improve the current situation. However, so far only PCA3, a non-coding RNA found in the urine sediments obtained after DRE, has been translated into the clinics. This RNA is currently utilized in a commercially available test under the name PROGENSA® PCA3, approved by the US FDA in 2012 (177,178). In this assay, PCA3 and KLK3 mRNAs are quantified, and the PCA3 Score is calculated as the ratio of PCA3 and KLK3 (PCA3 mRNA/KLK3 mRNA x 1000). PROGENSA® PCA3 assay has been demonstrated to be useful when combined with other patient information to aid in the decision of whether to recommend a repeat PB in men 50 years or older who have had at least one previous negative PB (179), but its utility for PC early diagnosis is still under investigation.

Because of the location of the prostate in the body, in direct contact with the urethra, desquamated cells and secreted products can be detected in urine, reflecting the physiological state of tissue. Deregulation of miRNAs in serum/plasma or tissue has been associated with many diseases including PC, suggesting the possible use of miRNAs as diagnostic biomarkers also in other body fluids, such as urine. The main aim of this thesis was to develop a minimally invasive method, using a miRNAs signature as a biomarker, for the early diagnosis of PC in urine obtained after DRE.

1. OPTIMIZATION OF MIRNAS ISOLATION AND QUANTIFICATION FROM URINE SAMPLES

When the present project was initiated, no studies about the identification of urinary miRNAs deregulation in PC had been performed. As the first purpose, because urine is a complex mixture that can be subfractionated, we standardized miRNA isolation and quantification from the two urinary fractions that contained nucleic acids (cell pellet and supernatant). Clinical samples used were pools of urine collected after prostatic massage by DRE, in order to be representative of the study population.

Because there was no comparison between the miRNA isolation and quantification strategies from body fluids, we decided to extract total RNA containing miRNAs comparing different RNA extraction methods that are valid to purify small RNAs from cells or body fluids. On the other hand, we chose RT-qPCR as quantification method, since it is considered to be the gold standard to quantify miRNA expression due to its sensitivity and specificity.

Firstly, the expression of miRNA-miR-130b from urine sediment was analysed, since it has been described as stably expressed in prostate tissue (124). We determined that prostate cells were present in our samples through the analysis of PSA transcript by TaqMan RT-qPCR.

In our hands, the best results from the miRNA extraction were from the QIAamp Viral RNA mini kit (Qiagen). Subsequently, we compared three of the most known commercially available miRNA RT-PCR assays (Exiqon's miRCURY LNA Universal RT microRNA PCR assay, Qiagen SYBR green–based miScript PCR System and Life Technologies' TaqMan miRNA Assay). Expression levels were more accurate by using TaqMan system compared with those obtained with Exiqon and Qiagen. Furthermore, miRNA raw Ct values improved after the preamplification step of RT product due to miRNAs are a small fraction of total RNA, forcing us to work with preamplificated cDNA.

The TaqMan assay has been described as one of the most specific and sensitive method for miRNA profiling, and is also one of the most widely used (125). It consists of a unique stem-loop RT primer designed to quantify only mature miRNAs and is miRNA specific. This primer produces a primer/mature miRNA chimera that extends the 3' end of the miRNA, generating a longer RT product for the specific primers and probe to anneal during the PCR step. On the other hand, Exiqon and Qiagen assays employ a universal tailing RT primer platform that make them more sensitive but less specific (180).

On the other hand, because in the last years exosomes are being studied intensively in body fluids as a source of new diagnostic biomarkers, but there was still no studies for urinary miRNAs in PC, we decided to optimized also the procedure for isolation of exosomes from urine, extract their RNA cargo, and analysed gene expression by TaqMan RT-qPCR. In addition, we compared obtained results with the entire fraction of circulating RNAs.

One of the most significant challenges involving the use of exosomes for the discovery of new biomarkers is the lack of standard and reliable isolation methods. The isolation of exosomes from biological fluids is rather complex, since these contain protein complexes and, certainly, other kinds of vesicles, which are frequently co-isolated with the population of interest. Here, we isolated exosomes by the most frequently used method based on differential ultracentrifugation. In addition, our protocol contains an additional step of RNAase A to remove cellular nucleic acids, and a DTT treatment to break the THP fibbers that trap the vesicles during the initial centrifugation cycles. Finally, the presence of exosomes as significant part of the obtained material has been verified by WB and NTA.

Despite the quality of samples, in this case we also had to work with preamplified cDNA because the low quantity of eluted RNA. The expression of 3 snoRNAs (U6, U44 and U48), frequently used as miRNA RGs (127), and miRNA-miR-191 that has been described in prostate tissue (101,126) were analysed. Although almost all these targeted genes were identify from the entire fraction of circulating RNAs and exosomes, the best expression was obtained in the case of total RNA extracted from exosomes by using the miRNeasy Mini kit (Qiagen).

In order to use exosomal miRNAs as biomarkers, a more efficient and simple isolation method for exosomes and their RNA content is a challenge for the future because ultracentrifugation is a quite tedious and time consuming protocol. Moreover, it would be very convenient that this method allow us purify exclusively prostatic exosomes, thus facilitating data analysis. Here we demonstrated that part of purified RNA of both fractions comes from prostate secretions from the analysis of specific prostate mRNAs: PSA, PCA3, prostate-specific G-coupled receptor (PSGR), and prostate specific membrane antigen (PSMA), indicating that what we found in the urinary exosomes reflects what is happening in the prostate gland.

2. MiRNA PROFILING

2.1. Importance of Choosing the Correct Normalization Method

The core of the project presented in this second objective of the thesis was to analyse the differences in the miRNA expression levels between urinary cells derived from PC versus benign samples. The results obtained would show us whether urinary miRNAs could be used as diagnosis biomarkers to distinguish patients with PC from those with benign diseases. This comparison was achieved by miRNA expression measurement applying an RT-qPCR approach for relative quantification, since RT-qPCR is the most commonly used method for the identification of specific miRNAs deregulation. However, there are several technical and biological variables in a qPCR experiment to require normalization.

The main objective of the normalization step is to remove as much variation as possible between groups except for that difference that is a consequence of the disease state itself. The method of choice to normalise miRNA measurements can significantly impact on the discovery of "differentially expressed" miRNAs and should be carefully considered.

Firstly, we sought to find suitable RGs to normalize the expression levels of miRNA. It was a very challenging task since it has not been described a standard RG for this purpose so far. At the beginning of this work, there were only two articles published about miRNA normalization in PC (124,169), and they showed conflicting results. Urine contains a highly variable mixture of cells of different origins and, to date, there is no consensus about the best way to normalize miRNA expression data retrieved from this source. Moreover, miRNA normalisation has an additional difficulty concerning other molecules. Since miRNAs regulate multiple genes within the same pathway, relatively small changes in their expression may be biologically significant. Furthermore, miRNAs represent a small fraction of total RNA (0,01%) in a sample, and it can vary significantly across different samples. Therefore, the normaliser of choice should mirror any change in the miRNA expression (181).

In our work, in order to avoid erroneous expression results due to an incorrect normalisation approach, we decided to apply different normalisation strategies in parallel and finally compare the obtained results.

The criteria that define a valid miRNA standard must be the same biotypes as the targets, highly conserved across species, highly abundant, perfectly compatible to different techniques, and

more importantly, stably and universally expressed irrespective of biological variance, medical conditions and treatment. Further, a normalizer should have similar storage stability, extraction, and quantification efficiency as miRNA, and then be in the miRNA assay design (170).

Currently, normalise miRNAs after RT-qPCR to one RG U6, U44 or U48 is generally accepted. The Applied Biosystems Megaplex miRNA assay pool (Applied Biosystems, Warrington, UK) and associated RT–PCR arrays, such as Applied Biosystems TaqMan Low-Density Arrays (Applied Biosystems), recommend using the average of these three snoRNAs.

U6, U44 and U48 are located in the nucleolus and constitute a group of single stranded ncRNAs of variable length (60-300nt in length) mostly required for ribosomal RNA (rRNA) maturation (182,183). Those snoRNAs have high abundance, are stably expressed and are similar in size compared with miRNAs. Furthermore, it is unlikely that these ncRNAs are involved in pathways that regulate miRNAs; therefore they fulfil the prerequisites for endogenous controls in miRNA studies (184). However, a number of tissue-specific snoRNAs have recently been identified that apparently do not target conventional substrates and are presumed to guide processing of primary transcripts of protein-coding genes, and some of them are located at an intronic region within genes that are associated with cancer (170). Recent evidence suggests they are deregulated in cancer and demonstrate capability to affect cell transformation, tumorigenesis and metastasis (185).

We found that snoRNAs have a highly variable expression across urine samples. Furthermore, we observed U6 and U44 significantly deregulated in PC compared to benign controls. Therefore, we discarded them as a suitable urinary miRNA RGs and only used U48. Although U48 was more stable than U6 and U44, its CV remained high, suggesting that it could introduce noise when is used as reference control.

SnoRNAs instability may be because of biological differences and/or methodology. It has been seen that U44 and U48 are located in intronic regions, harboured by the same host gene that often exhibit distinct temporal profiles. For example, RNU44 is located at an intronic region of human growth arrest specific 5 non-protein coding RNA (GAS5), and its relative expression was correlated with GAS5 gene. On the other hand, RNU48 is also an intronic snoRNA, within chromosome 6 open reading frame 48 (c6orf48 or G8). C6orf48 is part of the major histocompatibility complex III tissue-protective factor produced in response to chronic inflammation, and polymorphisms in the c6orf48 gene are associated with susceptibility to

infection (170). U6, highly conserved across evolution, has multiple copies in the genome, and appears to be up regulated in cervical cancer and correlate with progression (186).

The normalization of miRNA RT-qPCR assays using reference miRNA can be robust as well (181). In our study, the suitability of miR-130b has been also applied because it was found to be a stable endogenous reference miRNA to characterize the differential miRNA expression in PC from tissue samples (124). However, as results we obtained that miR-130b was difficult to detect in urine; therefore, we also excluded it as candidate RG. Moreover, in a current study by Chen and collaborators they demonstrated that the expression of miR-130b was significantly down-regulated in PC cell lines and clinical PC tissues, and that it also had a role in cancer progression (187).

PSA mRNA has been proposed to RNA normalisation such as in the first publication of the urinary PCA3 test (188). Moreover, in a study of several mRNAs expression in urine as PC biomarkers of our lab, it was also been described (189). Taking into account these studies, PSA mRNA as RG for the presence of prostate cells, which are released from the prostate by the DRE in urine, was included in our analysis. As results, we obtained that PSA was the most stable gene to be used as reference control.

However, the use of RNAs as RGs for miRNA profiling studies is an issue full of controversies. MRNAs have different extraction efficiencies, are degraded more easily and have to be reverse transcribed by other techniques, thereby increasing technical errors (181). Furthermore, several studies suggested that PSA mRNA levels might indeed be an independent marker for PC, since those patients who present with negative biopsy usually tend to have fewer cells of prostatic origin in their post-DRE urine than their malignant counterparts. One possible explanation could be the loss of cell-to-cell and cell-to-extracellular contacts in cancer (190). Larne and collaborators (2014) showed that the synthesis and serum levels of PSA are directly affected by miR-183. However, the effect on PSA mRNA level was less pronounced than the effect on the protein level, and the correlation between miR-183 and PSA encoding transcript is also weaker than to the protein (191). On the other hand, it has been seen that PSA could be involve in PC physiopathology, since its increased expression was demonstrated in cancer samples compared to benign hyperplasia or that discriminate metastatic samples from benign tissue in conjunction with TMPRSS2-ERG fusion genes and androgen receptor, with good specificity and sensitivity (192,193).

2.2. Identification of Deregulated MiRNAs in Prostate Cancer

MiRNAs are highly preserved in almost all types of analysed biological material providing greater sensitivity than other species of RNAs or proteins mainly because its natural structure and biogenesis. However, the measurement of miRNAs in tissue for diagnostic purposes is limited and non-invasive measurement of molecular markers has become a priority.

Since the beginning of the miRNAs project so far, many articles have been published for tissue and serum/plasma samples, while very few for urine. Therefore, we performed a pilot study using TaqMan RT-qPCR technology in order to unveil if we were able to detect deregulated miRNAs in PC urine samples.

We analysed the expression of 20 miRNAs the expression of which had been seen to be deregulated in PC tissues in 40 urine samples (PC: 20 and benign control: 20). Using a univariate analysis approach and PSA mRNA as control, we have demonstrated the differential expression of 6 miRNAs, 4 under-expressed (hsa-miR-145, -26a, -191 and -210) and 2 over-expressed (hsa-miR-100 and -194). Moreover, our results for miR-145 and miR-194 overlapped with other studies, where miR-145 is under-expressed, and miR-194 is over-expressed in PC compared to non-malignant tissue samples (98,100,130,131,145). However, for the other miRNAs we obtained contradictory results, e.g. miR-191, -26a are over-expressed (98,101), and miR-100 under-expressed (100). The AUC for these markers ranged from 0.67 to 0.69. Fixing the sensitivity at 94%, the obtained specificities for the individual markers were from 0% to 40%.

Although several diagnostic miRNA profiling studies have been performed on PC, their results are inconclusive and no single miRNA expression signature has been found yet. Different methods of sample collection, varied study designs, and diverse specificity of the platforms used, could explain some of these inconsistencies. However, even without an agreement in which would be miRNA-profiling signature for PC diagnosis, it is patent the relevance of some miRNAs that appear strongly up- or down-regulated in prostate tumours and could even classify PC regarding tumour stage, castration resistance or invasion capacity (55). For this reason, we performed a discovery in order to identify a specific miRNA expression profile for the diagnosis of PC.

TaqMan array microfluidic cards have emerged as additional alternative of RT-qPCR that represents the traditional way to analyse miRNA expression when a large number of genes have to be quantified. Thus, TaqMan miRNA array profiling of >700 human miRNAs from the pilot study patients was performed, and the best 48 candidates significantly deregulated were validated in a larger and independent cohort of 154 patients by TaqMan custom miRNA array profiling.

We obtained a list of 113 miRNAs from the discovery phase that showed a differential expression between PC and benign urine samples. Among the 48 validated miRNAs, we found 4 (hsa-miR-147b, hsa-miR-28, hsa-miR-548-5p and hsa-miR-648) still unknown for PC that could present a special interest for PC diagnosis because of their significance and predictive value. Consequently, we validated them in 10 matched FFPE tissue samples (PC: 10 and benign control: 10) from RP by TaqMan RT-qPCR in order to determine whether the observed changes in urine come from the prostate. Interestingly, miR-28 was found significantly deregulated in PC tissue compared to benign control normalising by U44. However, perhaps the data set was too small to draw any conclusions respect to the other candidates, thus, a larger cohort would be need to test them.

Although validated urinary miRNAs are interesting as potential PC diagnostic biomarkers, they not exceeded PSA predictive value. Since a single marker may not necessarily reflect the nature of tumour, we constructed a multi-gene panel or "fingerprints" through multivariate analysis in order to improve the diagnostic predictive value of single miRNA. We established a multiplex model by the combination of three miRNAs, hsa-miR-648, hsa-miR-147b and hsa-miR-193a-5p. As result, we obtained that this model slightly improves serum PSA AUC value (multiplex model AUC=0.74 *vs.* PSA AUC=0.61). The most exciting aspect is that the specificity of the panel was of 88%, compared to the 33% of PSA. However, one major panel limitation is the poor sensitivity (44%). In any case, the field of biomarkers from urine is still in its infancy, and important challenges need to be addressed before it can be translated into a clinical routine. These challenges include the development and standardization of isolation methods and criteria for normalisation between samples.

First of all, it would be necessary reduce sample variability, by improving normalisation methods, and try to enrich the sample with prostate epithelial cells. In the study by Anderson and collaborators (2014), they enriched exfoliated tumour cells fraction in urine for bladder cancer using a membrane filter with a defined pore-sized (microfiltration), increasing the sensitivity for DNA-based detection (194). Another option would be to establish a rate between our control gene and an epithelial cell specific gene, such as GAPDH. However, it has been seen

that GAPDH is not the best option because it was observed to be deregulated in advanced PC (195).

AIthough recently Hanke and collaborators (2010) reported the use of individual miR-152 as RG in urine (196) so far there is no conclusive findings about the best method of standardization and further studies need to be done in this field.

Taking into account the use of miRNAs as biomarkers for the early detection of PC, our results can provide a strong basis for future PC biomarker research in urine sediment. This new approach may help identifying more specific biomarkers through non-invasive method, which will allow us to distinguishing more specifically PC from other benign conditions and, therefore, reducing PC related over-diagnosis and the economic costs at the same time.

3. FUNCTIONAL RELEVANCE OF MIRNAS IN PROSTATE CANCER

3.1. Characterization of MiR-28 and MiR-210 in Prostate Cancer

This part of our project had as a main objective analyse the functional role and therapeutic potential of the most promising urinary miRNAs that we had found deregulated in the urinary sediments of PC patients. Firstly, we selected miRNAs from the pilot study (miR-100-5p, miR-191-5p and miR-210-3p) whose function was still unknown for PC to be characterized *in vitro,* while we performed the discovery and validation phases. Subsequently, we added miR-28-5p, since it was verified in both urine and tissue samples. All these genes were found significantly under-expressed in PC urine samples.

Functional assays were carried out by generating miRNA loss-of-function and/or overexpression in different PC cell lines. Transfection of the PC-3 and LNCaP PC cell lines with a synthetic miR-210-3p and miR-28-5p mimic respectively, resulted in a decrease of their proliferative capacity and viability, suggesting a potential relevance of these miRNAs in tumorigenic properties of these cells.

Thus far, miR-210 has been investigated extensively in cancer, since it is the most consistently and predominantly up-regulated miRNA in response to hypoxia (197). However, this miRNA cannot simply be described as oncogene or tumour-suppressor gene, because of the wide array of targets involved in regulating different cellular functions (198). In order to study its role in PC, we further performed cell cycle, clonogenicity, migration and invasion assays.

Results indicated that the stably over-expression of miR-210 reduced significantly PC-3 and PC-3M proliferation as well as their clonogenic capacity. Although flow cytometric data for miRNA-treated cells did not reveal any arrest in the cell cycle, we observed differences in the expression of regulatory proteins. The restoration of miR-210 expression in PC-3M led to substantial increased in the expression of cyclin-dependent kinase inhibitor p21, followed by a decreased in cyclin B1 that pays an essential role as a positive regulator of cyclin-dependent kinase 1 (Cdk1) activity in cell cycle progression at the G2/M transition stage (199). Moreover, miR-210 over-expression increased PC-3 motility, suggesting that not only acts as tumour suppressor gene, but also as oncogene that could be promoted PC progression.

In a collaborative project with Dr.Ochiya group from the National Cancer Center (NCC) in Tokyo, Japan, we found that PC-3M cells secreted exosomes in culture media that contained higher miR-210 expression levels than obtained for PC-3 cells and PNT-2, a prostate normal cell line. Since PC-3M has been described as more aggressive cell line than the others and previous studies shown that cancer cells grow in hypoxic conditions can communicate and enhance tube formation in endothelial cells via exosomes excreting miR-210 (200), its exosomal miR-210 content could be related to PC progression, even angiogenesis.

MiR-28-5p was showed as tumour suppressor gene in several cancers, but nothing is yet known about its function in PC. MiR-28-5p has been seen inhibited cancer cells proliferation, clonogenicity, migration, invasion, whereas increase apoptosis by targeting pro-apoptotic genes (201–203). Furthermore, it is related with chromosome changes in VHL-associated cancers and cervical carcinogenesis (204,205). *In vivo*, colorectal cancer cells over-expression miR-28-5p developed tumours more slowly in mice compared to control cells (201). Here, in addition to obtaining a reduction in LNCaP cells proliferation and viability after miR-28-5p over-expression, it was also observed a decreased in their migration capacity. Protein levels and bioinformatics analysis revealed that MAPK/Erk signalling pathway could be the mechanism responsible of effects on cell proliferation, viability and migration. Furthermore, the fact that in the PC signalling pathway, Erk1/2 induces proliferation and survival by AR-dependent signalling could

explain why we only observed effects on AR positive cell line.

Briefly, MAPK/Erk signalling pathway is triggered by the binding of soluble peptides to a tyrosine-kinase receptor, and initiates a cascade of events that terminates in the appropriated cellular response. It is related to various fundamental cellular processes, such as proliferation, cellular differentiation, survival, migration, and angiogenesis (206)**(Fig.55)**.

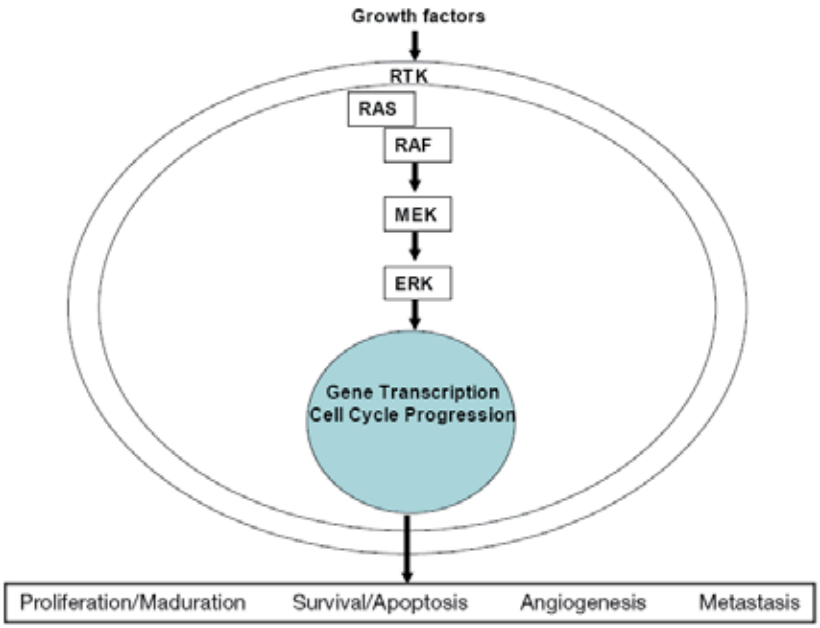

Figure 55. ERK1/2 signalling pathway (Image obtained from http://www.tlcr.org/article/viewFile/1102/1817/6414)

In conclusion, our results showed that miR-210 and mir-28-5p are not just novel promising candidates as diagnostic biomarkers for the early detection of PC, but also they control essential checkpoints involved in prostate carcinogenesis. Therefore, they may help to elucidate the mechanisms of tumour initiation and progression, which may eventually provide a basis for novel therapeutic strategies.

CONCLUSIONS

1-Existing tools for miRNAs isolation (QIAamp Viral RNA mini and miRNAeasy mini kit) and their relative quantification (TaqMan RT-qPCR system) in urine sediment are efficient enough to identify miRNAs differentially expressed between prostate cancer patients and benign prostate disorders

2-AIthough PSA is proposed to be the most stable RG for miRNA expression studies in urine sediments, whereas U44 is the most suitable for FFPE tissues, in the miRNAs field there is no RG that presents all the requirements to be an appropriate endogenous gene. Thus, further studies need to be carried out in order to find the best way to normalise data mainly from biofluids such as urine

3-The pilot study in urine, in which expression levels of miRNAs previously described in the literature were analysed, resulted in 3 candidates differentially expressed between PC patients and benign controls, indicating that the urine content of miRNAs may reflect alterations in prostate

4-MiRNAs high throughput profiling by RT-PCR techniques allowed us to identify a list of differentially expressed miRNAs in urine samples that was subsequently validated in a new cohort of patients. These analyses resulted in a profile of miRNAs closely related to the presence of PC

5-The cross-validation analysis of data led us to obtain a miRNA panel consisting of 3 urinary miRNAs (miR-648, miR-147b and miR-193a-5p) with an AUC value of 0.74, higher than predictive value of each one individually. This result suggests that this miRNAs profile could be a good candidate as a biomarker for the early diagnosis of PC

6-The next step will be to move on towards the validation of these urinary miRNAs profile using a much larger cohort of samples. Then it should be possible to translate these findings to a much easier format for incorporation into diagnostic kits or tests that will be more accessible and applicable in clinical practice

7-A high miR-210 expression in androgen-independent PC cells such as PC3 inhibited their tumorigenic properties in terms of proliferation, viability and colonogenic capacity, whereas enhanced its migration ability. These results suggest that miR-210 may play a role in tumour development but, due to the dual effect, more analysis would be needed to assess its potential as a therapeutic target

8-The aggressive cell line PC-3M presented enriched levels of miR-210 in their exosomes compared to less aggressive cell lines, indicating again that this miRNA could be involved in tumour progression through intercellular communication

9-MiR-28 overexpression decreased proliferation and viability in LNCaP cells. Furthermore, the migration capacity was also impaired. These findings indicate its role as tumour suppressor gene in androgen-dependent prostate cancer cell lines

10-Bioinformatics analysis and protein levels of miR-28 targets led us to think that their anti-tumorigenic properties could be related to the regulation of MAPK/ERK signalling pathway

11-All together analyses constitute an important step towards the accurate diagnosis of PC by non-invasive methods. Thus, miRNA-based biomarkers should have a rapid application in the clinics and, together with serum PSA and DRE, potentially influence decisions that could improve the health system, while reducing the number of unnecessary biopsies

12-On the other hand, both miRNAs studied *in vitro* seem to be involved in PC progression suggesting that themselves or their regulating mRNAs could become future therapeutic targets for the PC treatment

BIBLIOGRAPHY

1. Rönnau CGH, Verhaegh GW, Luna-Velez MV, Schalken JA. Noncoding RNAs as novel biomarkers in prostate cancer. BioMed Res Int. 2014;2014:591703.

2. Dunn MW, Kazer MW. Prostate cancer overview. Semin Oncol Nurs. 2011 Nov;27(4):241–50.

3. Tewari A, editor. Prostate Cancer: A Comprehensive Perspective [Internet]. London: Springer London; 2013 [cited 2015 Sep 13]. Available from: http://link.springer.com/10.1007/978-1-4471-2864-9

4. Selman SH. The McNeal prostate: a review. Urology. 2011 Dec;78(6):1224–8.

5. Myers RP. Structure of the adult prostate from a clinician's standpoint. Clin Anat N Y N. 2000;13(3):214–5.

6. Schrecengost R, Knudsen KE. Molecular pathogenesis and progression of prostate cancer. Semin Oncol. 2013 Jun;40(3):244–58.

7. Frank SB, Miranti CK. Disruption of prostate epithelial differentiation pathways and prostate cancer development. Front Oncol. 2013;3:273.

8. Siegel RL, Miller KD, Jemal A. Cancer statistics, 2015. CA Cancer J Clin. 2015 Feb;65(1):5–29.

9. Jemal A, Bray F, Center MM, Ferlay J, Ward E, Forman D. Global cancer statistics. CA Cancer J Clin. 2011 Apr;61(2):69–90.

10. Parkin DM. Global cancer statistics in the year 2000. Lancet Oncol. 2001 Sep;2(9):533–43.

11. Catalona WJ, Smith DS, Ratliff TL, Dodds KM, Coplen DE, Yuan JJ, et al. Measurement of prostate-specific antigen in serum as a screening test for prostate cancer. N Engl J Med. 1991 Apr 25;324(17):1156–61.

12. Potosky AL, Miller BA, Albertsen PC, Kramer BS. The role of increasing detection in the rising incidence of prostate cancer. JAMA. 1995 Feb 15;273(7):548–52.

13. Wever EM, Draisma G, Heijnsdijk EAM, de Koning HJ. How does early detection by screening affect disease progression? Modeling estimated benefits in prostate cancer screening. Med Decis Mak Int J Soc Med Decis Mak. 2011 Aug;31(4):550–8.

14. Ito K. Prostate cancer in Asian men. Nat Rev Urol. 2014 Apr;11(4):197–212.

15. Obort AS, Ajadi MB, Akinloye O. Prostate-specific antigen: any successor in sight? Rev Urol. 2013;15(3):97–107.

16. Oesterling JE. Prostate specific antigen: a critical assessment of the most useful tumor marker for adenocarcinoma of the prostate. J Urol. 1991 May;145(5):907–23.

17. Klotz L. Active surveillance for prostate cancer: overview and update. Curr Treat Options Oncol. 2013 Mar;14(1):97–108.

18. Velonas VM, Woo HH, dos Remedios CG, Assinder SJ. Current status of biomarkers for prostate cancer. Int J Mol Sci. 2013;14(6):11034–60.

19. Artibani W. Landmarks in prostate cancer diagnosis: the biomarkers. BJU Int. 2012 Oct;110 Suppl 1:8–13.

20. Roobol MJ, Kerkhof M, Schröder FH, Cuzick J, Sasieni P, Hakama M, et al. Prostate cancer mortality reduction by prostate-specific antigen-based screening adjusted for nonattendance and contamination in the European Randomised Study of Screening for Prostate Cancer (ERSPC). Eur Urol. 2009 Oct;56(4):584–91.

21. Stattin P, Carlsson S, Holmström B, Vickers A, Hugosson J, Lilja H, et al. Prostate cancer mortality in areas with high and low prostate cancer incidence. J Natl Cancer Inst. 2014 Mar;106(3):dju007.

22. Ferlay J, Parkin DM, Steliarova-Foucher E. Estimates of cancer incidence and mortality in Europe in 2008. Eur J Cancer Oxf Engl 1990. 2010 Mar;46(4):765–81.

23. Sutton MA, Gibbons RP, Correa RJ. Is deleting the digital rectal examination a good idea? West J Med. 1991 Jul;155(1):43–6.

24. Flanigan RC, Catalona WJ, Richie JP, Ahmann FR, Hudson MA, Scardino PT, et al. Accuracy of digital rectal examination and transrectal ultrasonography in localizing prostate cancer. J Urol. 1994 Nov;152(5 Pt 1):1506–9.

25. Gosselaar C, Kranse R, Roobol MJ, Roemeling S, Schröder FH. The interobserver variability of digital rectal examination in a large randomized trial for the screening of prostate cancer. The Prostate. 2008 Jun 15;68(9):985–93.

26. Smith DS, Catalona WJ. Interexaminer variability of digital rectal examination in detecting prostate cancer. Urology. 1995 Jan;45(1):70–4.

27. Ismail MT, Gomella LG. Transrectal prostate biopsy. Urol Clin North Am. 2013 Nov;40(4):457–72.

28. Scattoni V, Maccagnano C, Zanni G, Angiolilli D, Raber M, Roscigno M, et al. Is extended and saturation biopsy necessary? Int J Urol Off J Jpn Urol Assoc. 2010 May;17(5):432–47.

29. Ukimura O, Coleman JA, de la Taille A, Emberton M, Epstein JI, Freedland SJ, et al. Contemporary role of systematic prostate biopsies: indications, techniques, and implications for patient care. Eur Urol. 2013 Feb;63(2):214–30.

30. Scattoni V, Zlotta A, Montironi R, Schulman C, Rigatti P, Montorsi F. Extended and saturation prostatic biopsy in the diagnosis and characterisation of prostate cancer: a critical analysis of the literature. Eur Urol. 2007 Nov;52(5):1309–22.

31. Gleason DF, Mellinger GT. Prediction of prognosis for prostatic adenocarcinoma by combined histological grading and clinical staging. J Urol. 1974 Jan;111(1):58–64.

32. Humphrey PA. Gleason grading and prognostic factors in carcinoma of the prostate. Mod Pathol Off J U S Can Acad Pathol Inc. 2004 Mar;17(3):292–306.

33. Berg KD, Toft BG, Røder MA, Brasso K, Vainer B, Iversen P. Prostate needle biopsies: interobserver variation and clinical consequences of histopathological re-evaluation. APMIS Acta Pathol Microbiol Immunol Scand. 2011 Apr;119(4-5):239–46.

34. Melia J, Moseley R, Ball RY, Griffiths DFR, Grigor K, Harnden P, et al. A UK-based investigation of inter- and intra-observer reproducibility of Gleason grading of prostatic biopsies. Histopathology. 2006 May;48(6):644–54.

35. Edge SB, Compton CC. The American Joint Committee on Cancer: the 7th edition of the AJCC cancer staging manual and the future of TNM. Ann Surg Oncol. 2010 Jun;17(6):1471–4.

36. Lotan TL, Epstein JI. Clinical implications of changing definitions within the Gleason grading system. Nat Rev Urol. 2010 Mar;7(3):136–42.

37. Joniau S, Tosco L, Briganti A, Vanden Broeck T, Gontero P, Karnes RJ, et al. Results of surgery for high-risk prostate cancer. Curr Opin Urol. 2013 Jul;23(4):342–8.

38. Siegel R, DeSantis C, Virgo K, Stein K, Mariotto A, Smith T, et al. Cancer treatment and survivorship statistics, 2012. CA Cancer J Clin. 2012 Aug;62(4):220–41.

39. Singh J, Trabulsi EJ, Gomella LG. Is there an optimal management for localized prostate cancer? Clin Interv Aging. 2010;5:187–97.

40. Mitin T, Blute M, Lee R, Efstathiou J. Management of lymph node-positive prostate cancer: the role of surgery and radiation therapy. Oncol Williston Park N. 2013 Jul;27(7):647–55.

41. Hong JH, Kim IY. Nonmetastatic castration-resistant prostate cancer. Korean J Urol. 2014 Mar;55(3):153–60.

42. Petrylak DP, Tangen CM, Hussain MHA, Lara PN, Jones JA, Taplin ME, et al. Docetaxel and estramustine compared with mitoxantrone and prednisone for advanced refractory prostate cancer. N Engl J Med. 2004 Oct 7;351(15):1513–20.

43. Tannock IF, de Wit R, Berry WR, Horti J, Pluzanska A, Chi KN, et al. Docetaxel plus prednisone or mitoxantrone plus prednisone for advanced prostate cancer. N Engl J Med. 2004 Oct 7;351(15):1502–12.

44. Botchkina GI, Kim RH, Botchkina IL, Kirshenbaum A, Frischer Z, Adler HL. Noninvasive detection of prostate cancer by quantitative analysis of telomerase activity. Clin Cancer Res Off J Am Assoc Cancer Res. 2005 May 1;11(9):3243–9.

45. Shen MM, Abate-Shen C. Molecular genetics of prostate cancer: new prospects for old challenges. Genes Dev. 2010 Sep 15;24(18):1967–2000.

46. Rigau M, Olivan M, Garcia M, Sequeiros T, Montes M, Colás E, et al. The present and future of prostate cancer urine biomarkers. Int J Mol Sci. 2013;14(6):12620–49.

47. Lapointe J, Li C, Higgins JP, van de Rijn M, Bair E, Montgomery K, et al. Gene expression profiling identifies clinically relevant subtypes of prostate cancer. Proc Natl Acad Sci U S A. 2004 Jan 20;101(3):811–6.

48. Lapointe J, Li C, Giacomini CP, Salari K, Huang S, Wang P, et al. Genomic profiling reveals alternative genetic pathways of prostate tumorigenesis. Cancer Res. 2007 Sep 15;67(18):8504–10.

49. Setlur SR, Mertz KD, Hoshida Y, Demichelis F, Lupien M, Perner S, et al. Estrogen-dependent signaling in a molecularly distinct subclass of aggressive prostate cancer. J Natl Cancer Inst. 2008 Jun 4;100(11):815–25.

50. Taylor BS, Schultz N, Hieronymus H, Gopalan A, Xiao Y, Carver BS, et al. Integrative genomic profiling of human prostate cancer. Cancer Cell. 2010 Jul 13;18(1):11–22.

51. Ludwig JA, Weinstein JN. Biomarkers in cancer staging, prognosis and treatment selection. Nat Rev Cancer. 2005 Nov;5(11):845–56.

52. Becker-Santos DD, Guo Y, Ghaffari M, Vickers ED, Lehman M, Altamirano-Dimas M, et al. Integrin-linked kinase as a target for ERG-mediated invasive properties in prostate cancer models. Carcinogenesis. 2012 Dec;33(12):2558–67.

53. Stephan C, Ralla B, Jung K. Prostate-specific antigen and other serum and urine markers in prostate cancer. Biochim Biophys Acta. 2014 Aug;1846(1):99–112.

54. Stephan C, Rittenhouse H, Cammann H, Lein M, Schrader M, Deger S, et al. New markers and multivariate models for prostate cancer detection. Anticancer Res. 2009 Jul;29(7):2589–600.

55. Casanova-Salas I, Rubio-Briones J, Fernández-Serra A, López-Guerrero JA. miRNAs as biomarkers in prostate cancer. Clin Transl Oncol Off Publ Fed Span Oncol Soc Natl Cancer Inst Mex. 2012 Nov;14(11):803–11.

56. Iorio MV, Croce CM. MicroRNA dysregulation in cancer: diagnostics, monitoring and therapeutics. A comprehensive review. EMBO Mol Med. 2012 Mar;4(3):143–59.

57. Taylor MA, Schiemann WP. Therapeutic Opportunities for Targeting microRNAs in Cancer. Mol Cell Ther. 2014;2(30):1–13.

58. Yun SJ, Jeong P, Kim W-T, Kim TH, Lee Y-S, Song PH, et al. Cell-free microRNAs in urine as diagnostic and prognostic biomarkers of bladder cancer. Int J Oncol. 2012 Nov;41(5):1871–8.

59. Mlcochova H, Hezova R, Stanik M, Slaby O. Urine microRNAs as potential noninvasive biomarkers in urologic cancers. Urol Oncol. 2014 Jan;32(1):41.e1–9.

60. Dijkstra S, Mulders PFA, Schalken JA. Clinical use of novel urine and blood based prostate cancer biomarkers: a review. Clin Biochem. 2014 Jul;47(10-11):889–96.

61. Hessels D, Schalken JA. Urinary biomarkers for prostate cancer: a review. Asian J Androl. 2013 May;15(3):333–9.

62. Bryant RJ, Pawlowski T, Catto JWF, Marsden G, Vessella RL, Rhees B, et al. Changes in circulating microRNA levels associated with prostate cancer. Br J Cancer. 2012 Feb 14;106(4):768–74.

63. Sapre N, Selth LA. Circulating MicroRNAs as Biomarkers of Prostate Cancer: The State of Play. Prostate Cancer. 2013;2013:539680.

64. Srivastava A, Goldberger H, Dimtchev A, Ramalinga M, Chijioke J, Marian C, et al. MicroRNA profiling in prostate cancer--the diagnostic potential of urinary miR-205 and miR-214. PloS One. 2013;8(10):e76994.

65. Stephan C, Jung M, Rabenhorst S, Kilic E, Jung K. Urinary miR-183 and miR-205 do not surpass PCA3 in urine as predictive markers for prostate biopsy outcome despite their highly dysregulated expression in prostate cancer tissue. Clin Chem Lab Med CCLM FESCC. 2015 Jun;53(7):1109–18.

66. Lawrie CH, Gal S, Dunlop HM, Pushkaran B, Liggins AP, Pulford K, et al. Detection of elevated levels of tumour-associated microRNAs in serum of patients with diffuse large B-cell lymphoma. Br J Haematol. 2008 May;141(5):672–5.

67. Rayner KJ, Hennessy EJ. Extracellular communication via microRNA: lipid particles have a new message. J Lipid Res. 2013 May;54(5):1174–81.

68. Ralla B, Stephan C, Meller S, Dietrich D, Kristiansen G, Jung K. Nucleic acid-based biomarkers in body fluids of patients with urologic malignancies. Crit Rev Clin Lab Sci. 2014 Aug;51(4):200–31.

69. Lewis H, Lance R, Troyer D, Beydoun H, Hadley M, Orians J, et al. miR-888 is an expressed prostatic secretions-derived microRNA that promotes prostate cell growth and migration. Cell Cycle Georget Tex. 2014;13(2):227–39.

70. Corcoran C, Rani S, O'Driscoll L. miR-34a is an intracellular and exosomal predictive biomarker for response to docetaxel with clinical relevance to prostate cancer progression. The Prostate. 2014 Sep;74(13):1320–34.

71. Korzeniewski N, Tosev G, Pahernik S, Hadaschik B, Hohenfellner M, Duensing S. Identification of cell-free microRNAs in the urine of patients with prostate cancer. Urol Oncol. 2015 Jan;33(1):16.e17–22.

72. Jia H, Osak M, Bogu GK, Stanton LW, Johnson R, Lipovich L. Genome-wide computational identification and manual annotation of human long noncoding RNA genes. RNA N Y N. 2010 Aug;16(8):1478–87.

73. Bartel DP. MicroRNAs: genomics, biogenesis, mechanism, and function. Cell. 2004 Jan 23;116(2):281–97.

74. Krol J, Loedige I, Filipowicz W. The widespread regulation of microRNA biogenesis, function and decay. Nat Rev Genet. 2010 Sep;11(9):597–610.

75. Hata A, Lieberman J. Dysregulation of microRNA biogenesis and gene silencing in cancer. Sci Signal. 2015 Mar 17;8(368):re3.

76. Lages E, Ipas H, Guttin A, Nesr H, Berger F, Issartel J-P. MicroRNAs: molecular features and role in cancer. Front Biosci Landmark Ed. 2012;17:2508–40.

77. Guo F, Parker Kerrigan BC, Yang D, Hu L, Shmulevich I, Sood AK, et al. Post-transcriptional regulatory network of epithelial-to-mesenchymal and mesenchymal-to-epithelial transitions. J Hematol OncolJ Hematol Oncol. 2014;7:19.

78. Rodriguez A, Griffiths-Jones S, Ashurst JL, Bradley A. Identification of mammalian microRNA host genes and transcription units. Genome Res. 2004 Oct;14(10A):1902–10.

79. Wang Y-L, Wu S, Jiang B, Yin F-F, Zheng S-S, Hou S-C. Role of MicroRNAs in Prostate Cancer Pathogenesis. Clin Genitourin Cancer. 2015 Aug;13(4):261–70.

80. Griffiths-Jones S, Grocock RJ, van Dongen S, Bateman A, Enright AJ. miRBase: microRNA sequences, targets and gene nomenclature. Nucleic Acids Res. 2006 Jan 1;34(Database issue):D140–4.

81. Bolton EM, Tuzova AV, Walsh AL, Lynch T, Perry AS. Noncoding RNAs in prostate cancer: the long and the short of it. Clin Cancer Res Off J Am Assoc Cancer Res. 2014 Jan 1;20(1):35–43.

82. Kozomara A, Griffiths-Jones S. miRBase: integrating microRNA annotation and deep-sequencing data. Nucleic Acids Res. 2011 Jan;39(Database issue):D152–7.

83. Lytle JR, Yario TA, Steitz JA. Target mRNAs are repressed as efficiently by microRNA-binding sites in the 5' UTR as in the 3' UTR. Proc Natl Acad Sci U S A. 2007 Jun 5;104(23):9667–72.

84. Kim DH, Saetrom P, Snøve O, Rossi JJ. MicroRNA-directed transcriptional gene silencing in mammalian cells. Proc Natl Acad Sci U S A. 2008 Oct 21;105(42):16230–5.

85. Gonzalez S, Pisano DG, Serrano M. Mechanistic principles of chromatin remodeling guided by siRNAs and miRNAs. Cell Cycle Georget Tex. 2008 Aug 15;7(16):2601–8.

86. Khraiwesh B, Arif MA, Seumel GI, Ossowski S, Weigel D, Reski R, et al. Transcriptional control of gene expression by microRNAs. Cell. 2010 Jan 8;140(1):111–22.

87. Ørom UA, Nielsen FC, Lund AH. MicroRNA-10a binds the 5'UTR of ribosomal protein mRNAs and enhances their translation. Mol Cell. 2008 May 23;30(4):460–71.

88. Ruan K, Fang X, Ouyang G. MicroRNAs: novel regulators in the hallmarks of human cancer. Cancer Lett. 2009 Nov 28;285(2):116–26.

89. Wen X, Deng F-M, Wang J. MicroRNAs as predictive biomarkers and therapeutic targets in prostate cancer. Am J Clin Exp Urol. 2014;2(3):219–30.

90. Peterson SM, Thompson JA, Ufkin ML, Sathyanarayana P, Liaw L, Congdon CB. Common features of microRNA target prediction tools. Front Genet. 2014;5:23.

91. Yang J-H, Li J-H, Shao P, Zhou H, Chen Y-Q, Qu L-H. starBase: a database for exploring microRNA-mRNA interaction maps from Argonaute CLIP-Seq and Degradome-Seq data. Nucleic Acids Res. 2011 Jan;39(Database issue):D202–9.

92. Kelly BD, Miller N, Healy NA, Walsh K, Kerin MJ. A review of expression profiling of circulating microRNAs in men with prostate cancer. BJU Int. 2013 Jan;111(1):17–21.

93. Sun W, Julie Li Y-S, Huang H-D, Shyy JY-J, Chien S. microRNA: a master regulator of cellular processes for bioengineering systems. Annu Rev Biomed Eng. 2010 Aug 15;12:1–27.

94. Meeker AK, Hicks JL, Platz EA, March GE, Bennett CJ, Delannoy MJ, et al. Telomere shortening is an early somatic DNA alteration in human prostate tumorigenesis. Cancer Res. 2002 Nov 15;62(22):6405–9.

95. Kim WT, Kim W-J. MicroRNAs in prostate cancer. Prostate Int. 2013;1(1):3–9.

96. Cannistraci A, Di Pace AL, De Maria R, Bonci D. MicroRNA as new tools for prostate cancer risk assessment and therapeutic intervention: results from clinical data set and patients' samples. BioMed Res Int. 2014;2014:146170.

97. Mishra S, Deng JJ, Gowda PS, Rao MK, Lin C-L, Chen CL, et al. Androgen receptor and microRNA-21 axis downregulates transforming growth factor beta receptor II (TGFBR2) expression in prostate cancer. Oncogene. 2014 Jul 31;33(31):4097–106.

98. Ambs S, Prueitt RL, Yi M, Hudson RS, Howe TM, Petrocca F, et al. Genomic profiling of microRNA and messenger RNA reveals deregulated microRNA expression in prostate cancer. Cancer Res. 2008 Aug 1;68(15):6162–70.

99. Porkka KP, Pfeiffer MJ, Waltering KK, Vessella RL, Tammela TLJ, Visakorpi T. MicroRNA expression profiling in prostate cancer. Cancer Res. 2007 Jul 1;67(13):6130–5.

100. Tong AW, Fulgham P, Jay C, Chen P, Khalil I, Liu S, et al. MicroRNA profile analysis of human prostate cancers. Cancer Gene Ther. 2009 Mar;16(3):206–16.

101. Volinia S, Calin GA, Liu C-G, Ambs S, Cimmino A, Petrocca F, et al. A microRNA expression signature of human solid tumors defines cancer gene targets. Proc Natl Acad Sci U S A. 2006 Feb 14;103(7):2257–61.

102. Musumeci M, Coppola V, Addario A, Patrizii M, Maugeri-Saccà M, Memeo L, et al. Control of tumor and microenvironment cross-talk by miR-15a and miR-16 in prostate cancer. Oncogene. 2011 Oct 13;30(41):4231–42.

103. Hanahan D, Weinberg RA. Hallmarks of cancer: the next generation. Cell. 2011 Mar 4;144(5):646–74.

104. Rane JK, Pellacani D, Maitland NJ. Advanced prostate cancer--a case for adjuvant differentiation therapy. Nat Rev Urol. 2012 Oct;9(10):595–602.

105. Yu C, Yao Z, Jiang Y, Keller ET. Prostate cancer stem cell biology. Minerva Urol E Nefrol Ital J Urol Nephrol. 2012 Mar;64(1):19–33.

106. Rybak AP, Bristow RG, Kapoor A. Prostate cancer stem cells: deciphering the origins and pathways involved in prostate tumorigenesis and aggression. Oncotarget. 2015 Feb 10;6(4):1900–19.

107. Sen CK. MicroRNA in Regenerative Medicine. Elsevier; 2014. 1305 p.

108. Fang Y-X, Gao W-Q. Roles of microRNAs during prostatic tumorigenesis and tumor progression. Oncogene. 2014 Jan 9;33(2):135–47.

109. Liu C, Kelnar K, Liu B, Chen X, Calhoun-Davis T, Li H, et al. Identification of miR-34a as a potent inhibitor of prostate cancer progenitor cells and metastasis by directly repressing CD44. Nat Med. 2011 Feb;17(2):211–5.

110. Bueno MJ, Pérez de Castro I, Malumbres M. Control of cell proliferation pathways by microRNAs. Cell Cycle Georget Tex. 2008 Oct;7(20):3143–8.

111. Fenderico N, Casamichele A, Profumo V, Zaffaroni N, Gandellini P. MicroRNA-mediated control of prostate cancer metastasis: implications for the identification of novel biomarkers and therapeutic targets. Curr Med Chem. 2013;20(12):1566–84.

112. Iczkowski KA. Cell adhesion molecule CD44: its functional roles in prostate cancer. Am J Transl Res. 2010;3(1):1–7.

113. Iorio MV, Croce CM. MicroRNA dysregulation in cancer: diagnostics, monitoring and therapeutics. A comprehensive review. EMBO Mol Med. 2012 Mar;4(3):143–59.

114. Seto AG. The road toward microRNA therapeutics. Int J Biochem Cell Biol. 2010 Aug;42(8):1298–305.

115. Kasinski AL, Slack FJ. Epigenetics and genetics. MicroRNAs en route to the clinic: progress in validating and targeting microRNAs for cancer therapy. Nat Rev Cancer. 2011 Dec;11(12):849–64.

116. Zhang Y, Wang Z, Gemeinhart RA. Progress in microRNA delivery. J Control Release Off J Control Release Soc. 2013 Dec 28;172(3):962–74.

117. Li Z, Rana TM. Therapeutic targeting of microRNAs: current status and future challenges. Nat Rev Drug Discov. 2014 Aug;13(8):622–38.

118. Skog J, Würdinger T, van Rijn S, Meijer DH, Gainche L, Sena-Esteves M, et al. Glioblastoma microvesicles transport RNA and proteins that promote tumour growth and provide diagnostic biomarkers. Nat Cell Biol. 2008 Dec;10(12):1470–6.

119. Akao Y, Iio A, Itoh T, Noguchi S, Itoh Y, Ohtsuki Y, et al. Microvesicle-mediated RNA molecule delivery system using monocytes/macrophages. Mol Ther J Am Soc Gene Ther. 2011 Feb;19(2):395–9.

120. Kosaka N, Iguchi H, Yoshioka Y, Takeshita F, Matsuki Y, Ochiya T. Secretory mechanisms and intercellular transfer of microRNAs in living cells. J Biol Chem. 2010 Jun 4;285(23):17442–52.

121. Kosaka N, Iguchi H, Yoshioka Y, Hagiwara K, Takeshita F, Ochiya T. Competitive interactions of cancer cells and normal cells via secretory microRNAs. J Biol Chem. 2012 Jan 6;287(2):1397–405.

122. Kosaka N, Takeshita F, Yoshioka Y, Hagiwara K, Katsuda T, Ono M, et al. Exosomal tumor-suppressive microRNAs as novel cancer therapy: “exocure” is another choice for cancer treatment. Adv Drug Deliv Rev. 2013 Mar;65(3):376–82.

123. Sobel RE, Sadar MD. Cell lines used in prostate cancer research: a compendium of old and new lines--part 1. J Urol. 2005 Feb;173(2):342–59.

124. Schaefer A, Jung M, Miller K, Lein M, Kristiansen G, Erbersdobler A, et al. Suitable reference genes for relative quantification of miRNA expression in prostate cancer. Exp Mol Med. 2010 Nov 30;42(11):749–58.

125. Moldovan L, Batte KE, Trgovcich J, Wisler J, Marsh CB, Piper M. Methodological challenges in utilizing miRNAs as circulating biomarkers. J Cell Mol Med. 2014 Mar;18(3):371–90.

126. Leite KRM, Canavez JMS, Reis ST, Tomiyama AH, Piantino CB, Sañudo A, et al. miRNA analysis of prostate cancer by quantitative real time PCR: comparison between formalin-fixed paraffin embedded and fresh-frozen tissue. Urol Oncol. 2011 Oct;29(5):533–7.

127. Kuner R, Brase JC, Sültmann H, Wuttig D. microRNA biomarkers in body fluids of prostate cancer patients. Methods San Diego Calif. 2013 Jan;59(1):132–7.

128. Mathieu J, Ruohola-Baker H. Regulation of stem cell populations by microRNAs. Adv Exp Med Biol. 2013;786:329–51.

129. Navon R, Wang H, Steinfeld I, Tsalenko A, Ben-Dor A, Yakhini Z. Novel rank-based statistical methods reveal microRNAs with differential expression in multiple cancer types. PloS One. 2009;4(11):e8003.

130. Ozen M, Creighton CJ, Ozdemir M, Ittmann M. Widespread deregulation of microRNA expression in human prostate cancer. Oncogene. 2008 Mar 13;27(12):1788–93.

131. Szczyrba J, Löprich E, Wach S, Jung V, Unteregger G, Barth S, et al. The microRNA profile of prostate carcinoma obtained by deep sequencing. Mol Cancer Res MCR. 2010 Apr;8(4):529–38.

132. Cao P, Deng Z, Wan M, Huang W, Cramer SD, Xu J, et al. MicroRNA-101 negatively regulates Ezh2 and its expression is modulated by androgen receptor and HIF-1alpha/HIF-1beta. Mol Cancer. 2010;9:108.

133. Hao Y, Zhao Y, Zhao X, He C, Pang X, Wu TC, et al. Improvement of prostate cancer detection by integrating the PSA test with miRNA expression profiling. Cancer Invest. 2011 May;29(4):318–24.

134. Varambally S, Cao Q, Mani R-S, Shankar S, Wang X, Ateeq B, et al. Genomic loss of microRNA-101 leads to overexpression of histone methyltransferase EZH2 in cancer. Science. 2008 Dec 12;322(5908):1695–9.

135. Yaman Agaoglu F, Kovancilar M, Dizdar Y, Darendeliler E, Holdenrieder S, Dalay N, et al. Investigation of miR-21, miR-141, and miR-221 in blood circulation of patients with prostate cancer. Tumour Biol J Int Soc Oncodevelopmental Biol Med. 2011 Jun;32(3):583–8.

136. Gonzales JC, Fink LM, Goodman OB, Symanowski JT, Vogelzang NJ, Ward DC. Comparison of circulating MicroRNA 141 to circulating tumor cells, lactate dehydrogenase, and prostate-specific antigen for determining treatment response in patients with metastatic prostate cancer. Clin Genitourin Cancer. 2011 Sep;9(1):39–45.

137. Mitchell PS, Parkin RK, Kroh EM, Fritz BR, Wyman SK, Pogosova-Agadjanyan EL, et al. Circulating microRNAs as stable blood-based markers for cancer detection. Proc Natl Acad Sci U S A. 2008 Jul 29;105(30):10513–8.

138. Vallejo DM, Caparros E, Dominguez M. Targeting Notch signalling by the conserved miR-8/200 microRNA family in development and cancer cells. EMBO J. 2011 Feb 16;30(4):756–69.

139. Waltering KK, Porkka KP, Jalava SE, Urbanucci A, Kohonen PJ, Latonen LM, et al. Androgen regulation of micro-RNAs in prostate cancer. The Prostate. 2011 May;71(6):604–14.

140. Clapé C, Fritz V, Henriquet C, Apparailly F, Fernandez PL, Iborra F, et al. miR-143 interferes with ERK5 signaling, and abrogates prostate cancer progression in mice. PloS One. 2009;4(10):e7542.

141. Lee CYF, Rennie PS, Jia WWG. MicroRNA regulation of oncolytic herpes simplex virus-1 for selective killing of prostate cancer cells. Clin Cancer Res Off J Am Assoc Cancer Res. 2009 Aug 15;15(16):5126–35.

142. Peng X, Guo W, Liu T, Wang X, Tu X, Xiong D, et al. Identification of miRs-143 and -145 that is associated with bone metastasis of prostate cancer and involved in the regulation of EMT. PloS One. 2011;6(5):e20341.

143. Xu B, Niu X, Zhang X, Tao J, Wu D, Wang Z, et al. miR-143 decreases prostate cancer cells proliferation and migration and enhances their sensitivity to docetaxel through suppression of KRAS. Mol Cell Biochem. 2011 Apr;350(1-2):207–13.

144. Chiyomaru T, Tatarano S, Kawakami K, Enokida H, Yoshino H, Nohata N, et al. SWAP70, actin-binding protein, function as an oncogene targeting tumor-suppressive miR-145 in prostate cancer. The Prostate. 2011 Oct 1;71(14):1559–67.

145. Schaefer A, Jung M, Mollenkopf H-J, Wagner I, Stephan C, Jentzmik F, et al. Diagnostic and prognostic implications of microRNA profiling in prostate carcinoma. Int J Cancer J Int Cancer. 2010 Mar 1;126(5):1166–76.

146. Suh SO, Chen Y, Zaman MS, Hirata H, Yamamura S, Shahryari V, et al. MicroRNA-145 is regulated by DNA methylation and p53 gene mutation in prostate cancer. Carcinogenesis. 2011 May;32(5):772–8.

147. Zaman MS, Chen Y, Deng G, Shahryari V, Suh SO, Saini S, et al. The functional significance of microRNA-145 in prostate cancer. Br J Cancer. 2010 Jul 13;103(2):256–64.

148. Wang L, Tang H, Thayanithy V, Subramanian S, Oberg AL, Cunningham JM, et al. Gene networks and microRNAs implicated in aggressive prostate cancer. Cancer Res. 2009 Dec 15;69(24):9490–7.

149. Lin S-L, Chiang A, Chang D, Ying S-Y. Loss of mir-146a function in hormone-refractory prostate cancer. RNA N Y N. 2008 Mar;14(3):417–24.

150. Kong D, Li Y, Wang Z, Banerjee S, Ahmad A, Kim H-RC, et al. miR-200 regulates PDGF-D-mediated epithelial-mesenchymal transition, adhesion, and invasion of prostate cancer cells. Stem Cells Dayt Ohio. 2009 Aug;27(8):1712–21.

151. Bhatnagar N, Li X, Padi SKR, Zhang Q, Tang M-S, Guo B. Downregulation of miR-205 and miR-31 confers resistance to chemotherapy-induced apoptosis in prostate cancer cells. Cell Death Dis. 2010;1:e105.

152. Majid S, Dar AA, Saini S, Yamamura S, Hirata H, Tanaka Y, et al. MicroRNA-205-directed transcriptional activation of tumor suppressor genes in prostate cancer. Cancer. 2010 Dec 15;116(24):5637–49.

153. Li T, Li D, Sha J, Sun P, Huang Y. MicroRNA-21 directly targets MARCKS and promotes apoptosis resistance and invasion in prostate cancer cells. Biochem Biophys Res Commun. 2009 Jun 5;383(3):280–5.

154. Liu L-Z, Li C, Chen Q, Jing Y, Carpenter R, Jiang Y, et al. MiR-21 induced angiogenesis through AKT and ERK activation and HIF-1α expression. PloS One. 2011;6(4):e19139.

155. Ribas J, Lupold SE. The transcriptional regulation of miR-21, its multiple transcripts, and their implication in prostate cancer. Cell Cycle Georget Tex. 2010 Mar 1;9(5):923–9.

156. Shi G, Ye D, Yao X, Zhang S, Dai B, Zhang H, et al. Involvement of microRNA-21 in mediating chemo-resistance to docetaxel in androgen-independent prostate cancer PC3 cells. Acta Pharmacol Sin. 2010 Jul;31(7):867–73.

157. Siva AC, Nelson LJ, Fleischer CL, Majlessi M, Becker MM, Vessella RL, et al. Molecular assays for the detection of microRNAs in prostate cancer. Mol Cancer. 2009;8:17.

158. Zhang H-L, Yang L-F, Zhu Y, Yao X-D, Zhang S-L, Dai B, et al. Serum miRNA-21: elevated levels in patients with metastatic hormone-refractory prostate cancer and potential predictive factor for the efficacy of docetaxel-based chemotherapy. The Prostate. 2011 Feb 15;71(3):326–31.

159. Galardi S, Mercatelli N, Giorda E, Massalini S, Frajese GV, Ciafrè SA, et al. miR-221 and miR-222 expression affects the proliferation potential of human prostate carcinoma cell lines by targeting p27Kip1. J Biol Chem. 2007 Aug 10;282(32):23716–24.

160. Gordanpour A, Stanimirovic A, Nam RK, Moreno CS, Sherman C, Sugar L, et al. miR-221 Is down-regulated in TMPRSS2:ERG fusion-positive prostate cancer. Anticancer Res. 2011 Feb;31(2):403–10.

161. Mercatelli N, Coppola V, Bonci D, Miele F, Costantini A, Guadagnoli M, et al. The inhibition of the highly expressed miR-221 and miR-222 impairs the growth of prostate carcinoma xenografts in mice. PloS One. 2008;3(12):e4029.

162. Spahn M, Kneitz S, Scholz C-J, Stenger N, Rüdiger T, Ströbel P, et al. Expression of microRNA-221 is progressively reduced in aggressive prostate cancer and metastasis and predicts clinical recurrence. Int J Cancer J Int Cancer. 2010 Jul 15;127(2):394–403.

163. Sun T, Wang Q, Balk S, Brown M, Lee G-SM, Kantoff P. The role of microRNA-221 and microRNA-222 in androgen-independent prostate cancer cell lines. Cancer Res. 2009 Apr 15;69(8):3356–63.

164. Koh CM, Iwata T, Zheng Q, Bethel C, Yegnasubramanian S, De Marzo AM. Myc enforces overexpression of EZH2 in early prostatic neoplasia via transcriptional and post-transcriptional mechanisms. Oncotarget. 2011 Sep;2(9):669–83.

165. Mahn R, Heukamp LC, Rogenhofer S, von Ruecker A, Müller SC, Ellinger J. Circulating microRNAs (miRNA) in serum of patients with prostate cancer. Urology. 2011 May;77(5):1265.e9–16.

166. Hagman Z, Larne O, Edsjö A, Bjartell A, Ehrnström RA, Ulmert D, et al. miR-34c is downregulated in prostate cancer and exerts tumor suppressive functions. Int J Cancer J Int Cancer. 2010 Dec 15;127(12):2768–76.

167. Östling P, Leivonen S-K, Aakula A, Kohonen P, Mäkelä R, Hagman Z, et al. Systematic analysis of microRNAs targeting the androgen receptor in prostate cancer cells. Cancer Res. 2011 Mar 1;71(5):1956–67.

168. Rokhlin OW, Scheinker VS, Taghiyev AF, Bumcrot D, Glover RA, Cohen MB. MicroRNA-34 mediates AR-dependent p53-induced apoptosis in prostate cancer. Cancer Biol Ther. 2008 Aug;7(8):1288–96.

169. Carlsson J, Helenius G, Karlsson M, Lubovac Z, Andrén O, Olsson B, et al. Validation of suitable endogenous control genes for expression studies of miRNA in prostate cancer tissues. Cancer Genet Cytogenet. 2010 Oct 15;202(2):71–5.

170. Gee HE, Buffa FM, Camps C, Ramachandran A, Leek R, Taylor M, et al. The small-nucleolar RNAs commonly used for microRNA normalisation correlate with tumour pathology and prognosis. Br J Cancer. 2011 Mar 29;104(7):1168–77.

171. Gordanpour A, Nam RK, Sugar L, Bacopulos S, Seth A. MicroRNA detection in prostate tumors by quantitative real-time PCR (qPCR). J Vis Exp JoVE. 2012;(63):e3874.

172. Mateo F, Fernandez PL, Thomson TM. Stem cells in prostate cancer. Arch Esp Urol. 2013 Jun;66(5):475–86.

173. Huang C, Jacobson K, Schaller MD. MAP kinases and cell migration. J Cell Sci. 2004 Sep 15;117(Pt 20):4619–28.

174. Iglesias-Gato D, Chuan Y-C, Jiang N, Svensson C, Bao J, Paul I, et al. OTUB1 de-ubiquitinating enzyme promotes prostate cancer cell invasion in vitro and tumorigenesis in vivo. Mol Cancer. 2015;14:8.

175. Shiraishi T, Getzenberg RH, Kulkarni P. Cancer/testis antigens: novel tools for discerning aggressive and non-aggressive prostate cancer. Asian J Androl. 2012 May;14(3):400–4.

176. Makovey I, Stephenson AJ, Haywood S. Response to the U.S. Preventative Services Task Force decision on prostate cancer screening. Curr Urol Rep. 2013 Jun;14(3):168–73.

177. Hessels D, Schalken JA. The use of PCA3 in the diagnosis of prostate cancer. Nat Rev Urol. 2009 May;6(5):255–61.

178. Rittenhouse H, Blase A, Shamel B, Schalken J, Groskopf J. The long and winding road to FDA approval of a novel prostate cancer test: our story. Clin Chem. 2013 Jan;59(1):32–4.

179. Gittelman MC, Hertzman B, Bailen J, Williams T, Koziol I, Henderson RJ, et al. PCA3 molecular urine test as a predictor of repeat prostate biopsy outcome in men with previous negative biopsies: a prospective multicenter clinical study. J Urol. 2013 Jul;190(1):64–9.

180. Redshaw N, Wilkes T, Whale A, Cowen S, Huggett J, Foy CA. A comparison of miRNA isolation and RT-qPCR technologies and their effects on quantification accuracy and repeatability. BioTechniques. 2013 Mar;54(3):155–64.

181. Peltier HJ, Latham GJ. Normalization of microRNA expression levels in quantitative RT-PCR assays: identification of suitable reference RNA targets in normal and cancerous human solid tissues. RNA N Y N. 2008 May;14(5):844–52.

182. Dieci G, Preti M, Montanini B. Eukaryotic snoRNAs: a paradigm for gene expression flexibility. Genomics. 2009 Aug;94(2):83–8.

183. Mattick JS, Makunin IV. Small regulatory RNAs in mammals. Hum Mol Genet. 2005 Apr 15;14 Spec No 1:R121–32.

184. Benes V, Castoldi M. Expression profiling of microRNA using real-time quantitative PCR, how to use it and what is available. Methods San Diego Calif. 2010 Apr;50(4):244–9.

185. Mannoor K, Liao J, Jiang F. Small nucleolar RNAs in cancer. Biochim Biophys Acta. 2012 Aug;1826(1):121–8.

186. Hansen CN, Ketabi Z, Rosenstierne MW, Palle C, Boesen HC, Norrild B. Expression of CPEB, GAPDH and U6snRNA in cervical and ovarian tissue during cancer development. APMIS Acta Pathol Microbiol Immunol Scand. 2009 Jan;117(1):53–9.

187. Chen Q, Zhao X, Zhang H, Yuan H, Zhu M, Sun Q, et al. MiR-130b suppresses prostate cancer metastasis through down-regulation of MMP2. Mol Carcinog. 2014 Aug 23;

188. Hessels D, Klein Gunnewiek JMT, van Oort I, Karthaus HFM, van Leenders GJL, van Balken B, et al. DD3(PCA3)-based molecular urine analysis for the diagnosis of prostate cancer. Eur Urol. 2003 Jul;44(1):8–15; discussion 15–6.

189. Rigau M, Ortega I, Mir MC, Ballesteros C, Garcia M, Llauradó M, et al. A three-gene panel on urine increases PSA specificity in the detection of prostate cancer. The Prostate. 2011 Dec;71(16):1736–45.

190. Härmä V, Virtanen J, Mäkelä R, Happonen A, Mpindi J-P, Knuuttila M, et al. A comprehensive panel of three-dimensional models for studies of prostate cancer growth, invasion and drug responses. PloS One. 2010;5(5):e10431.

191. Larne O, Östling P, Haflidadóttir BS, Hagman Z, Aakula A, Kohonen P, et al. miR-183 in Prostate Cancer Cells Positively Regulates Synthesis and Serum Levels of Prostate-specific Antigen. Eur Urol. 2015 Oct;68(4):581–8.

192. Barfeld SJ, East P, Zuber V, Mills IG. Meta-analysis of prostate cancer gene expression data identifies a novel discriminatory signature enriched for glycosylating enzymes. BMC Med Genomics. 2014;7:513.

193. Gelmini S, Tricarico C, Petrone L, Forti G, Amorosi A, Dedola GL, et al. Real-time RT-PCR for the measurement of prostate-specific antigen mRNA expression in benign hyperplasia and adenocarcinoma of prostate. Clin Chem Lab Med CCLM FESCC. 2003 Mar;41(3):261–5.

194. Andersson E, Steven K, Guldberg P. Size-based enrichment of exfoliated tumor cells in urine increases the sensitivity for DNA-based detection of bladder cancer. PloS One. 2014;9(4):e94023.

195. Rondinelli RH, Epner DE, Tricoli JV. Increased glyceraldehyde-3-phosphate dehydrogenase gene expression in late pathological stage human prostate cancer. Prostate Cancer Prostatic Dis. 1997 Dec;1(2):66–72.

196. Hanke M, Hoefig K, Merz H, Feller AC, Kausch I, Jocham D, et al. A robust methodology to study urine microRNA as tumor marker: microRNA-126 and microRNA-182 are related to urinary bladder cancer. Urol Oncol. 2010 Dec;28(6):655–61.

197. Huang X, Ding L, Bennewith KL, Tong RT, Welford SM, Ang KK, et al. Hypoxia-inducible mir-210 regulates normoxic gene expression involved in tumor initiation. Mol Cell. 2009 Sep 24;35(6):856–67.

198. Qin Q, Furong W, Baosheng L. Multiple functions of hypoxia-regulated miR-210 in cancer. J Exp Clin Cancer Res CR. 2014;33:50.

199. Choi YH, Lee WH, Park KY, Zhang L. p53-independent induction of p21 (WAF1/CIP1), reduction of cyclin B1 and G2/M arrest by the isoflavone genistein in human prostate carcinoma cells. Jpn J Cancer Res Gann. 2000 Feb;91(2):164–73.

200. Tadokoro H, Umezu T, Ohyashiki K, Hirano T, Ohyashiki JH. Exosomes derived from hypoxic leukemia cells enhance tube formation in endothelial cells. J Biol Chem. 2013 Nov 29;288(48):34343–51.

201. Almeida MI, Nicoloso MS, Zeng L, Ivan C, Spizzo R, Gafà R, et al. Strand-specific miR-28-5p and miR-28-3p have distinct effects in colorectal cancer cells. Gastroenterology. 2012 Apr;142(4):886–96.e9.

202. Shi X, Teng F. Down-regulated miR-28-5p in human hepatocellular carcinoma correlated with tumor proliferation and migration by targeting insulin-like growth factor-1 (IGF-1). Mol Cell Biochem. 2015 Jul 10;

203. Schneider C, Setty M, Holmes AB, Maute RL, Leslie CS, Mussolin L, et al. MicroRNA 28 controls cell proliferation and is down-regulated in B-cell lymphomas. Proc Natl Acad Sci U S A. 2014 Jun 3;111(22):8185–90.

204. Hell MP, Thoma CR, Fankhauser N, Christinat Y, Weber TC, Krek W. miR-28-5p promotes chromosomal instability in VHL-associated cancers by inhibiting Mad2 translation. Cancer Res. 2014 May 1;74(9):2432–43.

205. Wilting SM, Snijders PJF, Verlaat W, Jaspers A, van de Wiel MA, van Wieringen WN, et al. Altered microRNA expression associated with chromosomal changes contributes to cervical carcinogenesis. Oncogene. 2013 Jan 3;32(1):106–16.

206. Rodríguez-Berriguete G, Fraile B, Martínez-Onsurbe P, Olmedilla G, Paniagua R, Royuela M. MAP Kinases and Prostate Cancer. J Signal Transduct. 2012;2012:169170.

207. Guidelines EAoU. European Association of Urology; 2010.